MECHANISMS OF SYNOVIAL FLUID LUBRICATION AT THE MOLECULAR AND TISSUE SCALE

A Dissertation

Presented to the Faculty of the Graduate School

of Cornell University

In Partial Fulfillment of the Requirements for the Degree of

Doctor of Philosophy

by

Sierra Grace Cook

August 2019

© 2019 Sierra Grace Cook

MECHANISMS OF SYNOVIAL FLUID LUBRICATION AT THE MOLECULAR AND TISSUE SCALE

Sierra Grace Cook, Ph. D.

Cornell University 2019

Articular joints are one of the most robust bearing systems found in the natural world. Healthy joints can withstand over 100 million shearing and compressive cycles without wear. This phenomenal lubrication is due to both the cartilage that forms the bearing surface and the synovial fluid that lubricates the joint.

However, in cases of joint disease such as osteoarthritis, chemical and mechanical changes in the cartilage and synovial fluid compromise the lubrication of the entire joint. Understanding the lubrication mechanisms of synovial fluid and how they are altered in disease and under various therapeutic interventions is critical for developing osteoarthritis therapies that restore joint functionality. This thesis presents studies on synovial fluid lubrication at both the molecular and tissue scale.

Under shear, aggregates form within the synovial fluid that lubricates articular joints. This dissertation investigates the composition and lubricating role of these aggregates (Chapter 2). Our results reveal that the globular protein albumin is the primary molecule involved in aggregate formation. This finding is relevant for artificial joint lubrication because protein aggregates have been attributed with improving wear protection between metal surfaces in-vitro.

Lubricin is a molecule in synovial fluid that shows therapeutic potential as a

treatment for osteoarthritis but is challenging to produce in large volumes. Synthetic lubricin-mimetics that imitate both the lubrication and surface attachment of natural lubricin offer a promising alternative. In this dissertation, the interaction between fibronectin (a cartilage surface protein that interacts with lubricin) and a lubricin-mimetic was characterized and their combined tribological behavior was monitored (Chapter 3). The mimetic lubricin was found to interact with fibronectin to provide lubrication and wear protection comparable to natural lubricin.

Hyaluronic acid viscosupplementation is a prevalent treatment for osteoarthritis. However, while high viscosity is associated with improved lubrication in vitro, hyaluronic acid viscosity and clinical efficacy are uncorrelated. This may be because traditional viscosity measurements capture only bulk viscosity, while on cartilage, hyaluronic acid is localized at the surface forming a highly viscous boundary layer. Our results demonstrate that functionalizing rheometer fixtures with cartilage surfaces significantly increases the effective viscosity of hyaluronic solutions (Chapter 4). This modification allows the localization of hyaluronic acid on cartilage to be captured in a commercial rheometer, thus providing a viscosity measurement that is more relevant to lubrication and therefore likely more predictive of clinical efficacy.

Altogether, the studies in the following thesis unveil molecular interactions that occur during joint lubrication and examine their measurable macroscale effects in order to inform the development of improved therapeutic strategies for joint disease.

The results emphasize the critical importance of interactions between synovial fluid molecules and the substrate they lubricate (either cartilage, or joint implant materials) on lubrication and wear protection mechanisms.

BIOGRAPHICAL SKETCH

Sierra grew up in Simi Valley, a sunny suburb of Los Angeles. She was homeschooled along with her four rambunctious siblings by her intrepid and long-suffering parents. Throughout her teenage years her education was supplemented by and eventually completely outsourced to the local community college. In 2011 she graduated from Moorpark College with Associate's degrees in Liberal Arts, Chemistry, and Physics and transferred to the University of California, Berkeley to earn her Bachelor's degree in Physics. During her junior year at Berkeley, Sierra participated in an undergraduate research program at Cornell University and fell in love with the gorges, waterfalls, and fireflies that are critical elements of Summer in Ithaca.

After graduating from UC Berkeley, Sierra entered the Applied Physics PhD Program at Cornell University. She joined the lab of Professor Delphine Gourdon in the department of Materials Science and Engineering and began her research on the molecular mechanisms of joint lubrication. When the Gourdon Lab relocated to the University of Ottawa she had the opportunity to continue her studies on joint lubrication in the Bonassar lab in the department of Biomedical Engineering. Despite being truly shocked by the winter climate, Sierra is grateful to have spent the last six years in the vibrant Ithaca community. When she is not in lab, she enjoys swing dancing, biking, taking classes at the local circus school, and hiking around the famous Ithaca gorges.

Following the completion of her PhD, Sierra has accepted a position as a Science Fellow for the California Council on Science and Technology. In this role, she will act as a science policy advisor for the California state legislature.

To Noah, Sophia, and Brynn

ACKNOWLEDGMENTS

Firstly, I would like to thank my advisors Delphine Gourdon and Larry Bonassar for their critical support and guidance throughout my PhD. Delphine's mentorship and academic expertise were instrumental to me in the early stages of my PhD program as I began my career as a researcher, and it has been a privilege to spend the last years of my PhD in Larry's lab. His patience and support have been invaluable to my progress. I would also like to thank Lena Kourkoutis for always being available when I needed support or guidance in my PhD career.

Some say that the PhD is a marathon, not a sprint. I think it is more like a relay—if you try to do it alone you've missed the point, you won't win, and you might get hurt. I have been incredibly lucky to have so many supportive friends and colleagues on my team. I am deeply grateful to Roberto Carlos Andresen Equiluz, who was my first mentor in graduate school. His patience, kindness, intellect, and generosity with his time and expertise made all the difference to me as I started my PhD.

As part of "Team Lube" in the Bonassar Lab, I have had the privilege to work with a group of intelligent, collaborative, talented and supportive researchers. The Man Cave has been a welcoming work home for me, thanks to Liz Feeney, Becka Irwin, and Sarah Snyder. I will be lucky to find another workplace filled with so much laughter and support. The other members of the Bonassar Lab, past and present, have been a fantastic team of people to work with. Marrianne Lintz, Stephen Sloan, Alex Boys, Nicole Diamantides, Jill Middendorf, Jongkil Kim, Steven Ayala, Sean Kim, Leigh Slyker, Hau Zhou as well as Zhexun Sun and Hania Koziol in the Putnam Lab have all contributed positively to my experience and I am grateful to them for always taking the

time to give insightful feedback on my work.

The friendships I have formed during my PhD have filled the last six years with laughter, joy, and small adventures. I am grateful to my “physics gang” who have been an amazing group of friends from our very first week in the program. I’m glad we did this thing together. Thanks also to my ever-changing family at 314 University who have made this home a place of comfort that can diffuse any amount of stress. Noah, I will always be grateful for your patience and loving support. Thank you for believing in me even when I did not.

Finally and most importantly, I must thank those who have been my strongest advocates and supports from day one. My parents Susanne and Randy, and my siblings Kyla, Shea, Tess and Brynn. You are my foundation; I could not have done this without you.

TABLE OF CONTENTS

APPENDIX A

Effect of Shearing Parameters on the Formation of a Shear-Induced Protein AggregateFilm in Synovial Fluid

CHAPTER 1

Introduction: Synovial Fluid and Cartilage Lubrication

Introduction to Cartilage and Osteoarthritis

Articular cartilage is the soft tissue that lines the ends of our long bones and forms the bearing surface in articular joints such as the knee and hip. The cartilage is lubricated by synovial fluid which fills the joint capsule, and together they form one of the most impressive lubricating systems found in nature. The friction coefficient for cartilage sliding against cartilage is more than five times lower than that of ice sliding against ice.[1] In addition to exhibiting extraordinary lubricity, the cartilage-synovial fluid tribosystem is remarkably robust. A healthy joint can withstand over 100 million shearing and loading cycles over a person's lifetime without damage, a feat that surpasses the performance of most engineered bearings.

Unfortunately, many individuals do not experience a full lifetime of healthy joint function. More than 30 million Americans suffer from osteoarthritis, making this condition the leading cause of disability in the US.[2,3] Osteoarthritis can result in severe pain, loss of joint function, and limited mobility, and it is associated with comorbidities such as obesity and hypertension, which further impact quality of life.[4] There is no cure for osteoarthritis, and the target of current therapies is to delay the progression of the disease and extend the functional lifetime of the joint before arthroplasty may become necessary. Current therapeutic interventions for the treatment of osteoarthritis symptoms include physical therapy, NSAIDs, corticosteroid injections, viscosupplementation, and arthroplasty, depending on the severity and stage of the

disease.[5,6]

Understanding the molecular mechanisms that facilitate the excellent lubrication of healthy joints is critical for the development of improved osteoarthritis treatments. Restoring the native lubricating function of synovial fluid and cartilage in cases of disease or after joint replacement, which both significantly change the chemistry and mechanics of the joint, is only possible if the molecular mechanisms of healthy joint lubrication are fully understood.

Articular Cartilage: Composition and Structure

The hyaline cartilage found in articular joints is a heterogeneous, aneural, avascular tissue that exhibits anisotropic mechanical properties. It is highly hydrated, comprising 85% water by weight.[7] The primary structural components of the cartilage are collagen II and proteoglycans, though non-collagenous proteins, glycoproteins, lipids, and other collagens are present in smaller amounts.[8,7] The chemical composition and orientation of collagen II fibers vary with depth into the cartilage tissue. The cartilage structure is typically categorized into three zones: superficial, transitional, and deep, corresponding to increasing depths from the cartilage surface down to the subchondral bone.

In the deep zone of cartilage, bundles of collagen fibers are oriented radially outwards from the surface of the subchondral bone and are attributed with providing resistance to compressive forces.[9] The transitional or middle zone provides an anatomical and functional bridge between the deep and superficial zones. The collagen fibers in this region are less organized but follow a generally oblique orientation. The

superficial or surface zone of cartilage is of the greatest relevance to joint tribology as it is the sliding surface during joint motion. In this zone, thin collagen fibrils are oriented parallel to the surface of the tissue, forming a dense "mesh" that is attributed with enhancing toughness and resistance to shear and tensile forces[9,10,11]. Furthermore, the superficial zone is compositionally distinct from the underlying tissue. The proteoglycan content is lowest and hydration is highest in this region, making it more compliant under shear and compressive forces than the deeper zones under. The structural protein fibronectin is present in the superficial zone in the form of laterally-oriented fibers but it is notably absent from the deeper zones of cartilage. The lubricating glycoprotein lubricin is also concentrated only at the surface of cartilage. This localized presence near the bearing surface implicates these proteins in a lubricating role, and indeed the critical contribution of lubricin to joint lubrication is well documented.[12,13,14,15] A non-collagenous, non-fibrous layer termed the "lamina splendens" has been reported to exist on top of the superficial zone of cartilage,[16,17,18,19] and other reports suggest adsorbed layers of synovial fluid constituents may form at the surface. [17,20,21,22]

The proteoglycans within the cartilage have negatively charged sites that, in aqueous solution, result in osmotic swelling of the tissue. This swelling is confined by the collagen structure of the tissue. Under compression, the negative sites on the proteoglycans are brought into closer proximity, which increases their mutual repulsive force and increases the compressive stiffness of the tissue.[8,9,10] The unique combination of collagen and proteoglycan is largely responsible for the mechanical response of cartilage to load and shear; however, the flow of the interstitial fluid through the tissue

also has a profound effect on mechanics. In fact, the mechanics of cartilage are well-described by modeling it as a biphasic material comprising the solid-like collagen-proteoglycan network and a fluid phase which flows through this network.[8,9,10,23] These unique structural and mechanical properties are responsible for the excellent lubricating and load-supporting properties of cartilage tissue.

Synovial Fluid

While the mechanical properties of cartilage tissue are a critical element of healthy joint function, cartilage does not work alone to provide the ultra-low friction that is characteristic of articular joints. Synovial fluid is a viscous, heterogeneous fluid that fills the joint cavity and acts in conjunction with cartilage to form a highly adaptive, robust, and lubricious tribological system. The Swiss renaissance physician Paracelsus (1493-1540) made the first recorded observation of the viscous fluid within the joint capsule of articulating joints.[8,24] Due to its viscid, stringy consistency and yellowish-clear color, he termed the fluid "synovia", from the Greek "syn" and Latin "ovum" (literally, "with egg")[1]. The synovial fluid exhibits complex rheological, tribological, and mechanical properties due to the behaviors and interactions of its multiple components during shear.

The viscoelastic properties of the synovial fluid are attributed to hyaluronic acid (HA), a long-chain unsulfated glycosaminoglycan comprised of D-glucuronic acid and N-acetyl-D-glucosamine monomers.[25,26,27,28] HA is a non-Newtonian shear-thinning

[1] The etymology of synovia is a matter of some debate, as some sources report that Paracelsus used the spelling "synophia" which is not clearly derived from the Latin.[91]

fluid with a time-dependent elastic modulus[29,30]. These rheological properties allow it to function as an elastic shock absorber under impact, and also facilitate viscous lubrication under continuous or prolonged load. While the molecular weight and concentration of HA in the synovial fluid varies depending on age, species, and health, 1-7MDa at circa 3.5mg/mL is typical for healthy human knee joints.[31,32,33] In cases of joint disease such as rheumatoid- or osteoarthritis however, the viscosity of the synovial fluid decreases due to a decrease in the molecular weight and, in some reports, the concentration of HA.[34,35,36,37,38]

Interestingly, the first commercial use of HA occurred in 1942, when Endre Balazs filed a patent to use HA as a supplement for egg in bakery products: apparently Balazs, like Paracelsus, was struck by the egg-like consistency of HA-based fluids.[39] HA is ubiquitous in human and animal tissues and biological fluids, and patents for its medical use soon followed in the 1950s.[40] In recent decades, HA has been used in an array of cosmetic procedures, and for the last thirty years, HA injections have been used clinically as a treatment for osteoarthritis. This procedure, called viscosupplementation, restores the viscosity of the synovial fluid, which is depleted in disease.

Although HA was one of the first molecules in the synovial fluid identified as a lubricant,[25] experiments conducted as early as 1968 demonstrated that while degradation of HA with enzymes reduced the viscosity of the synovial fluid, it did not disrupt its lubricating ability. Linn hypothesized that the primary lubricating component of the synovial fluid was instead a mucin.[27] This theory was later supported by the

identification of proteoglycan 4 (PRG4), which was later determined to be the same molecule as the lubricating mucin lubricin. [12,38,41]

Lubricin comprises distinct lubricating and binding domains: the central glycosylated region is negatively charged, highly hydrated, and lubricous, while the end domains are non-glycosylated, positively charged, and facilitate surface attachment and self-aggregation. Strong surface attachment is a critical for lubricin to function successfully as a lubricating molecule. Some studies indicate that lubricin attaches to collagen II via its N-terminus, while it binds to fibronectin, another protein present in the superficial zone of cartilage, through its C-terminus.[42,43] Other reports hypothesize that the C-terminus is responsible for cartilage attachment and that the N-terminus facilitates self-aggregation of lubricin molecules into loop-like dimers on the cartilage surface.[44] The lubricious, highly hydrated central domain of lubricin, paired with its ability to anchor to the cartilage surface results in the formation of a robust lubricating boundary layer on cartilage.[21,42,44] Lubricin significantly reduces friction between model surfaces[13,45] and cartilage surfaces in-vitro[12,46] and has been shown to mitigate cartilage damage in-vivo in animal studies.[47,48,49] These results make tribosupplementation with lubricin a promising future direction for the development of osteoarthritis therapies. However, despite recent progress,[50] producing significant volumes of lubricin (via recombinant production or purification from synovial fluid) remains a serious challenge that limits research into lubricin tribosupplementation. Therefore, significant work has been conducted in the development of biocompatible lubricin-mimetic molecules.[51,52,53]

While most studies of synovial fluid lubrication have focused on the roles of HA and lubricin due to their high viscosity and lubricity, respectively, other molecules of the synovial fluid warrant further investigation. The globular protein albumin represents 90% of the protein content of synovial fluid, but it has been largely overlooked in studies of synovial fluid lubrication. However, some recent studies of high concentration protein solutions under shear indicate that globular proteins may play a wear-protecting role in model systems.[54,55,56] Under shear between rigid surfaces, globular proteins formed dense aggregates which were proposed to function as protein "pillows", cushioning the contacting surfaces and mitigating wear. While these studies were done in protein solutions between rigid, non-porous model surfaces, they pose an interesting theory of lubrication that could be relevant for artificial joints, which have similar mechanical properties. A study by Banquy in 2015 reported the formation of aggregates in synovial fluid; however, the composition of the aggregates was not determined, so whether this phenomenon was related to the protein-mediated lubrication observed in high-concentration protein solutions was not established.[57]

Some molecules in the synovial fluid have been individually associated with lubricating roles, but several synergistic mechanisms of synovial fluid lubrication have also been proposed. Many studies report a synergistic interaction between lubricin and HA that enhances lubrication on both model surfaces and cartilage.[58,59,60,61] Lubricin has been reported to entangle HA near the cartilage surface, thereby enhancing the local viscosity at the surface and improving viscous lubrication.[21] Phospholipids at the cartilage surface have also been reported to interact synergistically with HA, forming a gel-like, ultra-low-friction boundary layer.[17,62,63] A recent study showed that

interactions between lubricin and the structural protein fibronectin synergistically improved lubrication by significantly mitigating wear.[64] Similar studies with HA confirm that for both lubricin and HA, surface localization is critical for effective lubrication.[21,64]

Synovial fluid is a complex, heterogeneous fluid. The initial perspective that there may exist a single lubricating molecule that was responsible for its excellent tribological properties has been replaced with an understanding that several molecules play important roles. Some synovial fluid constituents, including globular proteins, may exhibit shear-induced lubricating behaviors that are not observed statically. Furthermore, synergistic interactions between various synovial fluid molecules, or between synovial fluid molecules and the cartilage surface (via collagen, fibronectin or other surface constituents) may be critical components of the remarkable lubricating properties observed in healthy joints.

Theories of Cartilage Lubrication

Together, cartilage and SF provide extreme low friction and remarkable wear resistance under a vast array of loading and shearing conditions. Providing successful lubrication during activities like walking, running, or jumping require different lubricating strategies. The cartilage-SF tribosystem adaptively changes its lubrication mechanism in response to external stimulus, thereby protecting and lubricating the joint over a lifetime of activities. While the lubrication mechanisms are complex and

nuanced, we can turn to classical engineering frameworks for lubrication theory to understand some of the lubricating behaviors of joints.

Engineered bearing systems, such as journal bearings, are comprised of rigid sliding surfaces that also shift between lubricating mechanisms in response to changing shearing parameters. The framework used to characterize these changes is the Stribeck Curve (Figure 1.1), which describes the frictional response to changes in sliding speed, lubricant viscosity, normal load, and contact width. Changes in these external parameters cause the bearing system to shift between three distinct lubricating mechanisms: boundary mode lubrication, mixed mode lubrication, and hydrodynamic lubrication.

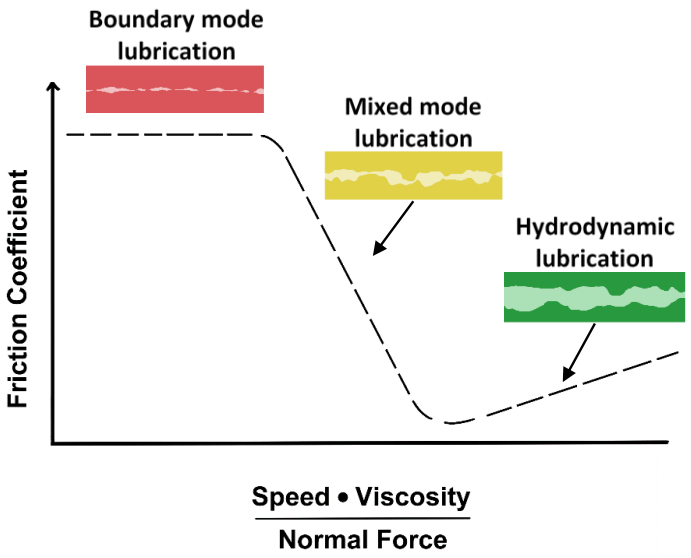

Figure 1.1[2]. The classical Stribeck curve describes lubrication modes that occur in response to changes in shearing parameters. In boundary mode lubrication, friction is mediated by the solid-solid contact of asperites on the opposing surfaces resulting in

[2] The artwork for this figure was created by Marianne Lintz

high friction that is dependent on surface properties. In mixed mode lubrication, interfacial fluid supports part of the load, and the friction response is due to both fluid and solid properties. Hydrodynamic lubrication occurs when the interfacial film fully separates the opposing surfaces and friction is determined by the viscous properties of the fluid.

In boundary mode lubrication, the sliding surfaces are in contact and friction is mediated by surface properties such as surface chemistry, roughness, and hardness.[65] Because friction in boundary mode lubrication is primarily due to solid asperities on the opposing surfaces sliding against each other, the friction coefficient obeys Amonton's Law, and is relatively insensitive to sliding speed and normal load.

As the sliding speed increases or the normal load decreases, a pressurized lubricant film is formed between the surfaces. In mixed mode lubrication, this pressurized film partially separates surfaces, reducing the total area in contact. The applied load is distributed between the pressurized interfacial fluid and the contacting asperities, reducing the pressure on the contacting regions and lowering the friction coefficient. Friction in mixed mode lubrication depends partially on the viscous properties of the lubricating fluid and partially on the surface chemistry and roughness of the contacting asperities.

Under increasing sliding speed or decreasing normal load, the pressurized film can eventually fully separate the surfaces so that there are no areas in contact. This type of lubrication, in which the load is fully supported by a pressurized film, is termed hydrodynamic lubrication. Once full separation has been achieved, the thickness of the

pressurized fluid film increases with increasing sliding speed and decreasing load. This leads to rising friction coefficients in response to increasing stresses across the sheared film. Hydrodynamic friction is mediated almost entirely by the viscous properties of the fluid rather than properties of the bearing surfaces themselves.

The Stribeck framework was developed to describe the lubrication of hard, rigid, impermeable bearings. The soft, deformable, permeable, porous nature of cartilage has led many researchers to question the applicability of the Stribeck framework and terminology to cartilage lubrication.[66,67,68] However, despite some significant differences, which will be discussed, cartilage does demonstrate a Stribeck-like response to changes in shearing parameters which is striking enough to make a strong argument against discarding the Stribeck framework entirely[21,23].

Cartilage is a highly hydrated, soft, and porous tissue that is more easily compared to a hydrogel than to a classical engineered bearing surface. Recent studies on hydrogel lubrication have indicated that hydrogels do not experience true boundary mode friction, as the high hydration at the surface and deformability of the surfaces prevents true "dry friction" from occurring. Instead, factors such as porosity and effective mesh size may affect the friction coefficient more than surface roughness.[66,67,68] However, surface chemistry is still a critical factor and cartilage surfaces exhibit a "boundary-like" lubrication regime under high loads and/or slow sliding speeds, so the term boundary mode friction will be used for the predominantly surface-mediated lubrication regime in cartilage.

The classical transition from boundary lubrication to low-friction, fluid-supported hydrodynamic lubrication is inhibited in cartilage due to its porosity and permeability.[23] Unlike an engineered bearing surface, the cartilage surface can intake fluid and rehydrate during shearing if the pressure in the interfacial film is greater than the interstitial fluid pressure within the tissue. The combination of interstitial and interfacial pressure in cartilage under fast sliding speeds and/or low loads, supports the applied load and results in a Stribeck-like decrease in the friction coefficient. However, the formation of an uninterrupted fluid film that fully supports the load is extremely unlikely, so there is no true hydrodynamic lubrication regime in cartilage. This alteration in the classical Stribeck framework has recently been termed the "elastoviscous" transition and is consistent with experimental observation of cartilage lubrication under an array of sliding speeds and contact pressures.[21,69,70] This elastoviscous lubrication mechanism depends primarily on the viscous properties of the lubricant.

Some molecules in synovial fluid are associated with specific lubricating regimes. Lubricin's lubricious central domain, paired with its ability to anchor to the cartilage surface, makes it an exceptional boundary lubricant.[12,46] Lubricin films reduce surface adhesion and friction under high loads and slow shearing speeds, i.e. under boundary mode conditions when the cartilage surfaces are in contact. On the other hand, HA is highly viscous and contributes to elastoviscous lubrication. The synergistic interaction between lubricin and HA reportedly entangles HA near the cartilage surface. The formation of a dense HA layer boosts the viscosity near the cartilage surface and facilitates the transition from boundary to elastoviscous lubrication.[21,58]

Current Therapies for Osteoarthritis

Osteoarthritis is a collection of degenerative joint diseases that affect over 30 million people in the United States. Osteoarthritis is a multifactorial disease with diverse causes and manifestations, but it results in cartilage degradation and chemical changes in both the cartilage and synovial fluid that result in compromised lubrication.[32,33,71,72] This disruption of normal joint lubrication can cause extreme pain and loss of mobility, resulting in significant negative effects on the quality of life of patients.

While there is no cure for osteoarthritis, symptomatic interventions exist for various stages of disease progression. Oral NSAIDS are a first line of defense due to the low risk of use; they result in a small but statistically significant reduction in pain.[73,74] Injection of corticosteroids to reduce pain and inflammation is another pain-mitigating treatment measure used in the clinic, although their efficacy has recently been called into question.[75] Over the last several decades, tribosupplementation has emerged as a therapeutic strategy for osteoarthritis treatment. Tribosupplements involves the intra-articular injection of lubricants to restore cartilage lubrication and slow the progression of tissue degradation.

Viscosupplementation with HA to restore the viscosity of arthritic joints has been used clinically for over thirty years.[76] The mechanism of action of HA viscosupplements is not fully understood, but the high viscosity of the injections is attributed with improving viscous lubrication. As such, various HA derivatives that are cross-linked or modified to enhance viscosity are clinically available.[77] However, despite this hypothesis, the viscosity of HA viscosupplements is not well correlated with

clinical efficacy.[69] Futhermore, numerous studies report that on cartilage a dense HA layer is localized at the surface with a viscosity higher than that of the bulk fluid.[21,78] Together, these findings raises questions about the clinical relevance of traditional in-vitro measurements of HA viscosity, which do not capture this critical surface interaction.[69]

Lubricin is a critically important boundary lubricating component of the synovial fluid. In small animal models, intra-articular injection of lubricin slowed the degeneration of cartilage tissue more effectively than saline or HA injections.[47,79,80] While these studies are promising, there is so far no data on their performance in large animal models or humans. While significant progress has been made recently towards the efficient production of recombinant lubricin,[50] the production of sufficient volumes of recombinant lubricin for large animal or human studies remains challenging and expensive. Because of this, significant effort has been directed towards the development of lubricin-mimetic molecules for osteoarthritis therapy.[51,52,81,82] The bottle-brush structure of this polymers mimic the lubricous, highly hydrated lubricating domain of lubricin. Equally important to the efficacy of native lubricin is its ability to anchor to the cartilage surface,[43,44,64] and successful biomimetic lubricins must also be capable of robust surface attachment.

If patients do not experience satisfactory pain reduction from less intrusive interventions, total joint replacement is a cost-effective long-term solution. Because the materials used for joint implants (metal alloys, ceramics, or ultra-high molecular weight polyethylene (UHMWPE)) are solid, rigid, and non-porous, the lubricating mechanisms

are distinct from those in native cartilage. The development of artificial joint surfaces has focused on reducing wear and improving the tribological properties of the implant material.[83] However, as for cartilage lubrication, the entrapment of native synovial fluid lubricants at the surface may also be important for successful lubrication. Some recent studies have focused on the role of synovial fluid globular proteins in the lubrication of artificial joints. It has been proposed that proteins adsorb onto implant surfaces and aggregate under shear to form protein "cushions" that protect the implant surface.[55,56,84] These studies have primarily been conducted in high-concentration protein solutions rather than synovial fluid, so the roles played by other synovial fluid components in this mechanism are poorly understood.

Strategies for Assessing Synovial Fluid Lubrication at the Nano- and Macro-Scale

The work presented in this dissertation probes the dynamics of molecular interactions that occur within in the synovial fluid and between synovial fluid and proteins at the cartilage surface. Furthermore, the measurable, macroscale effects of these interactions and their implications for osteoarthritis therapies are investigated. This view of synovial fluid lubrication over multiple length scales facilitates a deeper understanding of the molecular origins of tissue-scale phenomena.

A primary tool used for assessing the molecular-scale lubrication mechanisms of synovial fluid is the Surface Forces Apparatus (SFA). Developed in the 1970s by Tabor and Israelachvilli,[85,86,87] the SFA combines optical interferometry with tribometry to form a sophisticated shearing system that allows for precise force measurements and

direct visualization of the shearing junction. The SFA predates the invention of atomic force microscopy by a decade, so at the time of its development it was the only technique available for making force measurements at the molecular scale. Even today, the SFA offers some unique advantages over other imaging and force-measuring systems. The foremost of these is the ability to visualize the shearing junction in real time during shearing using interferometry. Furthermore, the SFA is uniquely adapted for making high precision measurements of force and film thickness for aqueous films, making it a natural choice for studying the dynamics of biological molecules which are in aqueous environments physiologically. However, one limitation of using the SFA is that the sample is confined between mica surfaces, which are smooth, non-porous, and rigid. While this reduces the complexity of the system, it limits the extrapolations that can be made between SFA experiments and lubrication of native cartilage, which is porous, permeable, and compliant. In this dissertation, the SFA is used (1) to determine the dynamics and molecular origins of aggregate formation that occur in synovial fluid under shear, which has been proposed as an adaptive, self-replenishing lubricating mechanism[57] and (2) to investigate the interactions between a mimetic lubricin polymer and the cartilage surface protein fibronectin, and the effect of this interaction on lubrication and wear protection.

In this dissertation, a commercial DHR3 rheometer was used to assess the macro-scale effects of molecular interactions between hyaluronic acid and the cartilage surfaces. Rheometers measure the viscous and viscoelastic response of fluids under external forces, and are useful for characterizing the behavior of non-newtonian fluids such as HA, which has a non-linear response to shear. Despite the association between

high viscosity and successful viscous lubrication, no correlation exists between the viscosity of HA viscosupplements and their clinical efficacy. Rather, frictional characterization of viscosupplements provides a better predictor of efficacy. Tribometer systems capable of characterizing the frictional behavior of cartilage lubricated by HA viscsupplements are costly, rare, and typically custom produced, leading to challenges in making direct quantitative comparisons between results acquired from different tribometers. Rheometers, on the other hand, are commercially available, easy to use, and yield reproducible results across machines. Therefore, the advantages of using rheology as a heuristic for lubrication data in assessing the efficacy of HA viscosuplements are significant. In this dissertation, the rheological effect of functionalizing commercial rheometer fixtures to facilitate surface localization of HA (which has been reported on cartilage) is investigated.

The SFA has been used widely to study the molecular mechanisms of synovial fluid lubricatoin.[58,60,88,63] While these experiments provide high precision measurements of molecular adsorption, friction, and wear, the potential differences between the behavior of molecules in the idealized and highly controlled SFA system and their behavior on cartilage tissue is often overlooked. Conversely, macro-scale friction experiments performed using custom tribometers provide information on cartilage friction at the tissue-scale,[21,89,90] but do not probe the molecular origins of lubrication. There is a shortage of research that spans both length scales and connects molecular interactions to their macroscopic outcomes at the tissue scale. The work presented in this dissertation identifies molecular-scale interactions that contribute to lubrication in

the SFA and measures the tissue-scale effects of molecular interactions on the viscosity of synovial fluid lubricants using a commercial rheometer.

REFERENCES

1. Mow, V. C. & Huiskes, R. *Basic Orthopaedic Biomechanics and Mechanobiology*. (Lippincott Williams and Wilkins, 2005).

2. Cisternas, M. G. *et al.* Alternative Methods for Defining Osteoarthritis and the Impact on Estimating Prevalence in a US Population-Based Survey. *Arthritis Care Res. (Hoboken).* **68**, 574–580 (2016).

3. Lawrence, R. C. *et al.* Estimates of the prevalence of arthritis and other rheumatic conditions in the United States: Part II. *Arthritis Rheum.* **58**, 26–35 (2008).

4. Hunter, D. J., Neogi, T. & Hochberg, M. C. Quality of osteoarthritis management and the need for reform in the US. *Arthritis Care Res. (Hoboken).* **63**, 31–38 (2011).

5. Anandacoomarasamy, A. & March, L. Current evidence for osteoarthritis treatments. *Ther. Adv. Musculoskelet. Dis.* **2**, 17–28 (2010).

6. Mora, J. C., Przkora, R. & Cruz-Almeida, Y. Knee osteoarthritis: pathophysiology and current treatment modalities. *J. Pain Res.* **11**, 2189–2196 (2018).

7. Cohen, N. P., Foster, R., Mow, V. C. & Foster, R. J. Composition and dynamics of articular cartilage: structure, function, and maintaining healthy state. *J. Orthop. Sport. Phys. Ther.* **28**, 203–215 (1998).

8. Mansour, J. Biomechanics of Cartilage. in *Kinesiology: The Mechanics and Pathomechanics of Human Movement* (ed. Otis, C.) 68–77 (2013).

9. Sophia, A., Bedi, A. & Rodeo, S. The basic science of articular cartilage: structure, composition, and function. *Sport. Heal. Orthop.* **1**, 461–468 (2009).

10. Camarero-Espinosa, S., Weder, C., Rothen-Rutishauser, B. & Foster, E. J. Articular cartilage: from formation to tissue engineering. *Biomater. Sci* **4**, (2016).

11. Kaab, M. J., Gwynn, I. A. & Notzli, H. Collagen fibre arrangement in the tibial plateau articular cartilage of man and other mammalian species. *J. Anat* **193**, 23–34 (1998).

12. Gleghorn, J. P., Jones, A. R. C., Flannery, C. R. & Bonassar, L. J. Boundary mode lubrication of articular cartilage by recombinant human lubricin. *J. Orthop. Res.* **27**, 771–777 (2009).

13. Zappone, B., Ruths, M., Greene, G. W., Jay, G. D. & Israelachvili, J. N. Adsorption, lubrication, and wear of lubricin on model surfaces: polymer brush-like behavior of a glycoprotein. *Biophys. J.* **92**, 1693–708 (2007).

14. Jay, G. D. *et al.* Association between friction and wear in diarthrodial joints lacking lubricin. *Arthritis Rheum.* **56**, 3662–9 (2007).

15. Waller, K. a *et al.* Role of lubricin and boundary lubrication in the prevention of chondrocyte apoptosis. *Proc. Natl. Acad. Sci. U. S. A.* **110**, 5852–5857 (2013).

16. Fujioka, R., Aoyama, T. & Takakuwa, T. The layered structure of the articular surface. *Osteoarthr. Cartil.* **21**, 1092–1098 (2013).

17. Crockett, R. *et al.* Biochemical composition of the superficial layer of articular cartilage. *J. Biomed. Mater. Res. Part A* **82**, 958–964 (2007).

18. Jeffery, A. K., Blunn, G. W., Archer, C. W. & Bentley, G. Three-dimensional collagen architecture in bovine articular cartilage. *J. bone Jt. surgery, Br. Addit.* **73**, 795–801 (1991).

19. Kobayashiv, S. & Kurogouchf, Y. Cryoscanning electron microscopic study of the surface amorphous layer of articular cartilage. *J. Anat* **187**, 429–444 (1995).

20. Noyori, K., Takagi, T. & Jasin, H. E. Characterization of the macromolecular components of the articular cartilage surface. *Rheumatol. Int.* **18**, 71–77 (1998).

21. Bonnevie, E. D., Galesso, D., Secchieri, C., Cohen, I. & Bonassar, L. J. Elastoviscous transitions of articular cartilage reveal a mechanism of synergy between lubricin and hyaluronic acid. *PLoS One* **10**, (2015).

22. Gispert, M. P., Serro, A. P., Colaço, R. & Saramago, B. Friction and wear mechanisms in hip prosthesis: Comparison of joint materials behaviour in several lubricants. *Wear* **260**, 149–158 (2006).

23. Gleghorn, J. P. & Bonassar, L. J. Lubrication mode analysis of articular cartilage using Stribeck surfaces. *J. Biomech.* **41**, 1910–1918 (2008).

24. Bronzino, J. *The Biomedical Engineering Handbook 1*. (CRC Press, 2000).

25. Ogston, A. G. & Stanier, J. E. The physiological function of hyaluronic acid in synovial fluid; viscous, elastic and lubricant properties. *J. Physiol.* **4**, 244–252 (1952).

26. Linn, F. C. Lubrication of animal joints. *J. Biomech.* **1**, 193–205 (1968).

27. Linn, F. C. Lubrication of animal joints II: the mechanism. *J. Biomech.* **1**, 193–205 (1968).

28. Gibbs, D. A., Merrill, E. W., Smith, K. A. & Balazs, E. A. Rheology of hyaluronic acid. *Biopolymers* **6**, 777–791 (1968).

29. Zhang, Z. & Christopher, G. F. The nonlinear viscoelasticity of hyaluronic acid and its role in joint lubrication Soft Matter. *Soft Matter* **11**, 2596–2603 (2015).

30. Cowman, M. K., Schmidt, T. A., Raghavan, P. & Stecco, A. Viscoelastic properties of hyaluronan in physiological conditions. *F1000Research* **4**, 622–625 (2015).

31. Mazzucco, D., Scott, R. & Spector, M. Composition of joint fluid in patients undergoing total knee replacement and revision arthroplasty: correlation with flow properties. *Biomaterials* **25**, 4433–4445 (2004).

32. Balazs, E. A., Watson, D., Duff, I. F. & Roseman, S. Hyaluronic acid in synovial fluid: Molecular parameters of hyaluronic acid in normal and arthritic human fluids. *Arthritis Rheum.* **10**, 357–376 (1967).

33. Dahl, L. B. *et al.* Concentration and molecular weight of sodium hyaluronate in synovial fluid from patients with rheumatoid arthritis and other arthropathies. *Ann. Rheum. Dis.* **44**, 817–822 (1985).

34. Henrietta Jebens, E. & Eileen Monk-jones, M. On the viscosity and pH of synovial fluid and the pH of blood. *J. Bone Jt. Surgery*- **41B**, 388–400 (1959).

35. Stafford, C. T., Niedermeier, W., Holley, H. L. & Pigmant, W. Studies on the concentration and intrinsic viscosity of hyaluronic acid in synovial fluids of patients with rheumatic diseases. *Ann. rheum. Dis* **23**, 152–157 (1964).

36. Ludwig, T. E., Hunter, M. M. & Schmidt, T. A. Cartilage boundary lubrication synergism is mediated by hyaluronan concentration and PRG4 concentration and structure. *BMC Musculoskelet. Disord.* **16**, (2015).

37. Decker, B., Mcguckin, W. F., Mckenzie, B. F. & Slocumb, C. H. Concentration of Hyaluronic Acid in Synovial Fluid. *Clin. Chem.* **5**, 465–469 (1959).

38. Swann, D. A., Silver, F. H., Slayter, H. S., Stafford, W. & Shore, E. The molecular structure and lubricating activity of lubricin isolated from bovine and human synovial fluids. *Biochem. J.* **225**, 195–201 (1985).

39. Necas, J., Bartosikova, L., Brauner, P. & Kolar, J. Hyaluronic acid (hyaluronan): a review. *Vet. Med. (Praha).* **53**, 397–411 (2008).

40. Nečas, D., Vrbka, M., Urban, F., Křupka, I. & Hartl, M. The effect of lubricant constituents on lubrication mechanisms in hip joint replacements. *J. Mech. Behav. Biomed. Mater.* **55**, 295–307 (2016).

41. Schmid, T. *et al.* Superficial zone protein (SZP) is an abundant glycoprotein in human synovial fluid and serum. in *Transactions of the Orthopoedic Research Society* (2001).

42. Flowers, S. A. *et al.* Lubricin binds cartilage proteins, cartilage oligomeric matrix protein, fibronectin and collagen II at the cartilage surface. *Sci. Rep.* **7**, (2017).

43. Chang, D. P., Guilak, F., Jay, G. D. & Zauscher, S. Interaction of lubricin with type II collagen surfaces: Adsorption, friction, and normal forces. *J. Biomech.* **47**, 659–666 (2014).

44. Jones, A. R. C. *et al.* Binding and localization of recombinant lubricin to articular cartilage surfaces. *J. Orthop. Res.* **25**, 283–292 (2007).

45. Coles, J. M., Chang, D. P. & Zauscher, S. Molecular mechanisms of aqueous boundary lubrication by mucinous glycoproteins. *Curr. Opin. Colloid Interface Sci.* **15**, 406–416 (2010).

46. Schmidt, T. A., Gastelum, N. S., Nguyen, Q. T., Schumacher, B. L. & Sah, R. L. Boundary lubrication of articular cartilage: Role of synovial fluid constituents. *Arthritis Rheum.* **56**, 882–891 (2007).

47. Waller, K. A. *et al.* Intra-articular recombinant human proteoglycan 4 mitigates cartilage damage after destabilization of the medial meniscus in the yucatan minipig. *AJSM* **45**, (2017).

48. Jay, G. & Waller, K. The Biology of Lubricin: Near Frictionless Joint Motion. *Matrix Biol.* **39**, 17–24 (2014).

49. Jay, G. D. *et al.* Prevention of cartilage degeneration and restoration of chondroprotection by lubricin tribosupplementation in the rat following anterior cruciate ligament transection. *Arthritis Rheum.* **62**, 2382–2391 (2010).

50. Shurer, C. *et al.* Stable recombinant production of codon-scrambled lubricin and mucin in human cells. *Biotechnol. Bioeng.* **116**, 1292–1303 (2019).

51. Samaroo, K. J., Tan, M., Putnam, D. & Bonassar, L. J. Binding and lubrication of biomimetic boundary lubricants on articular cartilage. *J. Orthop. Res.* **35**, 548–557 (2016).

52. Banquy, X., Burdyńska, J., Lee, D. W., Matyjaszewski, K. & Israelachvili, J. Bioinspired bottle-brush polymer exhibits low friction and Amontons-like behavior. *J. Am. Chem. Soc.* **136**, 6199–202 (2014).

53. Faivre, J. *et al.* Intermolecular Interactions between Bottlebrush Polymers Boost the Protection of Surfaces against Frictional Wear. *Chem. Mater.* **30**, 4140–4149 (2018).

54. Mavraki, A. & Cann, P. M. Lubricating film thickness measurements with bovine serum. *Tribol. Int.* **44**, 550–556 (2011).

55. Fan, J., Myant, C. W., Underwood, R., Cann, P. M. & Hart, A. Inlet protein aggregation: a new mechanism for lubricating film formation with model synovial fluids. *Proc. Inst. Mech. Eng. Part H.* **225**, 696–709 (2011).

56. Myant, C. & Cann, P. In contact observation of model synovial fluid lubricating mechanisms. *Tribiology Int.* **63**, 97–104 (2013).

57. Banquy, X., Lee, D. W., Das, S., Hogan, J. & Israelachvili, J. N. Shear-induced aggregation of mammalian synovial fluid components under boundary lubrication conditions. *Adv. Funct. Mater.* **24**, 3152–3161 (2014).

58. Greene, G. W. *et al.* Adaptive mechanically controlled lubrication mechanism found in articular joints. *Proc. Natl. Acad. Sci. U. S. A.* **108**, 5255–5259 (2011).

59. Ye, H. *et al.* The Interactions between Lubricin and Hyaluronic Acid Synergistically Enhance Anti-Adhesive Properties. *ACSApplied Mater. Interfaces* **11**, (2019).

60. Das, S. *et al.* Synergistic interactions between grafted hyaluronic acid and lubricin provide enhanced wear protection and lubrication. *Biomacromolecules* **14**, 1669–1677 (2013).

61. Ludwig, T. E., Hunter, M. M. & Schmidt, T. A. Cartilage boundary lubrication synergism is mediated by hyaluronan concentration and PRG4 concentration and structure. *BMC Musculoskelet. Disord.* **16**, (2015).

62. Seror, J., Zhu, L., Goldberg, R., Day, A. J. & Klein, J. Supramolecular synergy in the boundary lubrication of synovial joints. *Nat. Commun.* **6**, (2015).

63. Zhu, L., Seror, J., Day, A. J., Kampf, N. & Klein, J. Ultra-low friction between boundary layers of Hyaluronan-phosphatidylcholine Complexes. *Acta Biomater.* **59**, 283–292 (2017).

64. Eguiluz, R. C. A. *et al.* Fibronectin mediates enhanced wear protection of lubricin during shear. *Biomacromolecules* **16**, 2884–2894 (2015).

65. Bowden, F. P. & Tabor, D. *The friction and lubrication of solids*. (Clarendon Press, 2001).

66. Briscoe, W. H. Aqueous boundary lubrication: Molecular mechanisms, design strategy, and terra incognita. *Curr. Opin. Colloid Interface Sci.* **27**, 1–8 (2017).

67. Pitenis, A. A. *et al*. Polymer fluctuation lubrication in hydrogel gemini interfaces. *Soft Matter* **10**, 8955–8962 (2014).

68. Urueña, J. M. *et al.* Mesh size control of polymer fluctuation lubrication in gemini hydrogels. *Biotribology* **1**, 24–29 (2015).

69. Bonnevie, E. D., Galesso, D., Secchieri, C. & Bonassar, L. J. Frictional characterization of injectable hyaluronic acids is more predictive of clinical outcomes than traditional rheological or viscoelastic characterization. *PLoS One* **14**, (2019).

70. Feeney, E. *et al.* Temporal changes in synovial fluid composition and elastoviscous lubrication in the equine carpal fracture model. *J. Orthop. Res.* **37**, (2019).

71. Temple-Wong, M. M. *et al.* Hyaluronan concentration and size distribution in human knee synovial fluid: variations with age and cartilage degeneration. *Arthritis Res. Ther.* **18**, 18 (2016).

72. Belcher, C., Yaqub, R., Fawthrop, F., Bayliss, M. & Doherty, M. Synovial fluid chondroitin and keratan sulphate epitopes, glycosaminoglycans, and hyaluronan in arthritic and normal knees. *Ann Rheum Dis* **56**, 299–307 (1997).

73. Zhang, W., Jones, A. & Doherty, M. Does paracetamol (acetaminophen) reduce the pain of osteoarthritis? A meta-analysis of randomised controlled trials. *Ann. Rheum. Dis.* **63**, 901–7 (2004).

74. Zhang, W. *et al.* OARSI recommendations for the management of hip and knee osteoarthritis, Part II: OARSI evidence-based, expert consensus guidelines. *Osteoarthr. Cartil.* **16**, 137–62 (2008).

75. Jüni, P. *et al.* Intra-articular corticosteroid for knee osteoarthritis. *Cochrane Database Syst. Rev.* (2015). doi:10.1002/14651858.CD005328.pub3

76. Bellamy, N. *et al.* Viscosupplementation for the treatment of osteoarthritis of the knee. *Cochrane Database Syst. Rev.* (2006). doi:10.1002/14651858.CD005321.pub2

77. Nicholls, M., Manjoo, A., Shaw, P., Niazi, F. & Rosen, J. Rheological properties of commercially available hyaluronic acid products in the United States for the treatment of osteoarthritis knee pain. *Clin. Med. Insights. Arthritis Musculoskelet. Disord.* **11**, (2018).

78. Crockett, R. Boundary lubrication in natural articular joints. *Tribology Letters* **35**, 77–84 (2009).

79. Flannery, C. R. *et al.* Prevention of cartilage degeneration in a rat model of osteoarthritis by intraarticular treatment with recombinant lubricin. *Arthritis Rheum.* **60**, 840–847 (2009).

80. Teeple, E. *et al.* Effects of supplemental intra-articular lubricin and hyaluronic acid on the progression of posttraumatic arthritis in the anterior cruciate ligament–deficient rat knee. *Am. J. Sports Med.* **39**, 164–172 (2011).

81. Lawrence, A. *et al.* Synthesis and characterization of a lubricin mimic (mLub) to reduce friction and adhesion on the articular cartilage surface. *Biomaterials* **73**, 42–50 (2015).

82. Sun, Z. *et al.* Boundary mode lubrication of articular cartilage with a biomimetic diblock copolymer. *Proc. Natl. Acad. Sci.* **116**, 12437–12441 (2019).

83. Wang, W., Ouyang, Y. & Khoon Poh, C. Orthopaedic implant technology: biomaterials from past to future. *Ann. Acad. Med.* **40**, 237–244 (2011).

84. Fan, J., Myant, C., Underwood, R. & Cann, P. Synovial fluid lubrication of artificial joints: protein film formation and composition. *R. Soc. Chem.* **156**, 69–85 (2012).

85. Israelachvili, J. N. Thin film studies using multiple-beam interferometry. *J. Colloid Interface Sci.* **44**, 259–272 (1973).

86. Heuberger, M., Luengo, G. & Israelachvili, J. Topographic information from multiple beam interferometry in the surface forces apparatus. *Langmuir* **13**, 3839–3848 (1997).

87. Israelachvili, J. *et al.* Recent advances in the surface forces apparatus (SFA) technique. *Reports Prog. Phys.* **73**, (2010).

88. Tadmor, R., Chen, N. & Israelachvili, J. N. Thin film rheology and lubricity of hyaluronic acid solutions at a normal physiological concentration. *J Biomed Mater Res* **61**, 514–523 (2002).

89. Bonnevie, E., Galesso, D., Secchieri, C. & Bonassar, L. Stribeck analysis of articular cartilage lubrication: roles of different injectable hyaluronic acids and endogenous lubricin. *Orthop. Proc.* **96-B**, (2014).

90. Gleghorn, J. P., Jones, A. R. C., Flannery, C. R. & Bonassar, L. J. Boundary mode lubrication of articular cartilage by recombinant human lubricin. *J. Orthop. Res.* **27**, 771–777 (2009).

91. Synovia | Definition of Synovia by Merriam-Webster. Available at: https://www.merriam-webster.com/dictionary/synovia. (Accessed: 13th July 2019)

CHAPTER 2

Dynamics of Synovial Fluid Aggregation under Shear[3]

Abstract

The synovial fluid (SF) that lubricates articular joints exhibits complex rheological and tribological properties due the interactions and behaviors of its various molecular components. Under shear, SF films abruptly thicken by more than 300% and large, dense aggregates form within the fluid. In this study, we used the Surface Force Apparatus to elucidate which SF components are involved in this shear-induced transformation by (i) determining which (if any) of all major SF components replicate the behavior of SF under shear and (ii) observing the effect of removing implicated components from SF by enzymatic digestion. While most previous studies of SF have focused on the tribological roles of lubricin or hyaluronic acid, our results indicate that albumin is a key contributor to the formation of aggregates in SF under shear. Our results also suggest that SF aggregation is associated with efficient surface protection against wear. As our findings are based on experiments involving rigid, nonporous surfaces, they may be used to investigate shear-mediated aggregation mechanisms occurring during the lubrication of artificial joints, ultimately advancing our current vision of implant design.

[3]This chapter has been submitted for publication: Cook, SG; Guan, Y; Pacifici, NJ; Brown, CN; Czako, E; Samak, MS; Bonassar, LJ; Gourdon, D. Dynamics of Synovial Fluid Aggregation under Shear. *Langmuir*, 2019

Introduction

Healthy articular joints exhibit remarkable lubrication, providing extremely low friction while withstanding over 100 million shearing cycles without wear.[1] This efficient lubrication is attributed to the composition and structure of both cartilage and the synovial fluid (SF) that together lubricate the joint. SF is a complex, multi-component system comprising protein (90% serum albumin (SA) by weight),[2] glycosaminoglycans, glycoproteins, and phospholipids (PL). Individually, several SF components have been implicated in specific lubricating roles in the joint. Hyaluronic acid (HA) is a large glycosaminoglycan that was one of the first SF components to be identified as a key lubricating component of SF. Its high viscosity promotes a transition from boundary to elasto-hydrodynamic lubrication during shearing resulting in decreased friction, and it has also been implicated in the reduction of boundary-mode friction.[3,4,5] Impressive boundary lubricating capabilities have also been reported for lubricin (LUB), a major mucinous glycoprotein found in mammalian SF.[6,7,8] More recently, PL have been associated with boundary lubrication, especially in conjunction with HA.[9] Various synergistic interactions between SF components have recently been proposed as mechanisms of lubrication: LUB-HA interactions promote a transition from boundary to elastoviscous lubrication by boosting viscosity at the cartilage surface,[10] HA-PL mixtures provide extreme low-friction boundary lubrication,[11,12] and FN-LUB interactions delay the onset of wear in model systems,[13] to name a few. However, the role of interactions between SF components in lubrication is generally less well characterized than that of individual SF components. Unraveling the molecular interactions between SF components, in particular their dynamics under shear, is critical

for our understanding of the complex mechanisms that contribute to the extraordinary lubrication of articular joints.

SF undergoes significant mechanical changes under shear, evolving from a thin, homogenous fluid layer to a thicker, heterogeneous mixture of fluid and SF aggregates, referred to as an "aggregate gel layer".[14] These shear-induced changes in SF have been identified in a variety of mammalian synovial fluids under a wide range of shearing conditions using the surface forces apparatus (SFA).[14] However, the roles of individual SF components in the formation of SF aggregates have not been determined. The formation of a thick shear-induced "protein aggregate gel" has been reported in *in-vitro* tests of artificial hip joints sheared in fetal bovine serum (FBS) and recently observed in arthritic SF samples.[15,16,17,18] This aggregate gel was identified as a transient protective layer made of globular proteins including albumin and γ-globulin formed at the surface of the artificial implant. However, both the FBS and the diseased SF (from patients with osteo- or rheumatoid arthritis) used in these experiments contained globular proteins in higher concentrations than those found in healthy SF, and the involvement of other SF components in aggregate formation was not investigated in detail.[15,19] HA and LUB have both been long implicated in joint lubrication, and they are known to be localized at the bearing surface of joints during shear. They have also been reported to interact synergistically to form a gel-like layer that has distinct mechanical properties from the surrounding SF, which facilitates lubrication and wear protection at the cartilage surface.[5,10,20,21] Other studies have implicated HA-PL[2,11,12] or SA-HA[22] complexes in the formation of a distinct lubricating layer that is localized at the shearing surface. Thus, while there are multiple reports examining the lubrication

by pairs of SF components, a systematic study of how all these components interact to produce a thick SF aggregate film under shear has not previously been conducted.

In this paper, we used a two-pronged approach to determine the SF components involved in the shear-induced film thickening and aggregation of SF. First, we monitored the effect of shear on film thickness, aggregation, and friction of SF components both individually and in combination to identify which (if any) demonstrated a shearing behavior similar to that of SF. Second, we eliminated individual components from SF by enzymatic digestion and measured how this affected its shearing and aggregating behavior. We specifically focused on the roles of SA, HA, and LUB. Interactions of HA with SA, LUB, and PL were also investigated, as they were previously reported to interact synergistically to form a lubricating boundary layer.

Methods

Our experiments were performed using a Surface Forces Apparatus (SFA), which enables concurrent measurements of film thickness, normal forces and friction forces while simultaneously monitoring film aggregation, shape of the shearing junction, and onset of wear. Unless otherwise noted, the SFA surfaces were first coated with a layer of fibronectin (FN), a structural protein present in the superficial zone of cartilage that has been shown to ensure good attachment of SF components to the shearing surfaces, even under high applied load.[13]

Consecutive incubations are denoted with a "+" (e.g. FN+SF indicates that SF was incubated on top of a previously deposited FN layer) while solutions that were mixed together and incubated simultaneously are denoted with "/" (e.g. FN+HA/SA

indicates a mixture of HA and SA was prepared and then injected onto a previously deposited layer of FN). A summary of all films tested in this study is shown in Table 1.

Table 1. Materials and Concentrations Tested

Film	Experimental Concentration (mg/mL in PBS)	Physiological Concentration in SF (mg/mL)
FN+SF	N/A	N/A
FN+SA	8.0	8-11[23]
SA	8.0	8-11[23]
FN+LUB	0.02	0.05-0.35[6,24]
FN+HA	3.0 (1 MDa)	1-4 (1-6 MDa)[25,26]
FN+HA+LUB	3.0 (HA), 0.02 (LUB)	1-4 (HA), 0.05-0.35 (LUB)
FN+HA-PL	3.0 (HA), 0.2 (PL)	1-4 (HA), 0.1-0.2 (PL)[25]
FN+HA-SA	3.0 (HA), 8.0 (SA)	1-4 (HA), 8-11 (SA)
FN+tryp-SF	0.05mg per mL SF	N/A
FN+hy-SF	0.05 mg per mL SF	N/A

*All FN solutions were prepared at 0.3mg/mL in PBS[13]

Surface Forces Apparatus:

An SFA Mark III (SurForce, Santa Barbara CA) was used to measure film thickness and friction coefficient of sheared SF films while simultaneously monitoring average size, distribution and index of refraction of aggregates formed in the contact junction. The SFA method has been thoroughly described elsewhere[27,28] and the SFA surface preparation protocol used here has been previously published.[13] Briefly, thin homogeneous sections of back-silvered mica were glued onto semi-cylindrical silica

disks. These disks were mounted in a crossed-cylindrical configuration in the SFA chamber to form an optical interferometer. Light passing through the interferometer forms fringes of equal chromatic order (FECO). The even-ordered fringes are sensitive to the optical properties of the material confined between the SFA surfaces and are used for monitoring film aggregation and quantification of their index of refraction, whereas odd-ordered fringes are insensitive to optical properties and are used to make precise film thickness measurements. The lower SFA surface was mounted on a piezo-electric bimorph to actuate shear, and a horizontal double-cantilever spring (k=1650 N/m) to measure normal forces. The upper surface was mounted on a strain gauged lateral double spring to detect friction forces. In our experiments, surfaces were sheared at 3μm/s under normal loads of 1-2mN (3.5-5.5MPa).

Preparation of samples for SFA experiments:

Mica surfaces were mounted in the SFA and separated by several millimeters. 50 μL of soluble human plasma fibronectin (FN) (Sigma Aldrich, St. Louis MO) diluted to 0.3mg/mL in phosphate buffered saline (PBS) was injected between the surfaces to form a meniscus and coat both opposing mica surfaces. The FN was incubated for 1 hour to allow appropriate adsorption onto the mica surfaces, and then rinsed with PBS. A 50 μL droplet of dilute (0.02 mg/mL in PBS) bovine SA was then incubated between the FN-coated surfaces for 30 minutes to block non-specific interactions of SF with the FN layer, and rinsed with PBS. Finally, a 50 μL droplet of our sample (SF, isolated SF component(s), or enzyme-treated SF) was injected between the surfaces and incubated for at least 1 hour before starting experiments. The incubated sample was left in the

junction after incubation and used as the shearing medium. Equine SF samples were acquired from the Cornell College of Veterinary Medicine.[29] The SF component(s) used were: bovine SA (Sigma Aldrich, St Louis MO), HA (1 MDa, Lifecore Biomedical, Chaska, MN), PL (1,2-Dipalmitoyl-sn-glycero-3-phosphocholine, Sigma Aldrich, St. Louis MO), LUB,[7] and mixtures of the above. The enzymes used were TCPK trypsin and hyaluronidase (Sigma Aldrich, St. Louis MO).

For FN+SF, FN+HA, FN+HA/SA, FN+HA/PL, FN+tryp-SF, and FN+hy-SF films, the procedure outlined above was followed: 1-hour incubation with FN, 30 min passivation with dilute SA, and 1-hour incubation with sample prior to testing. Three tests were exceptions to this protocol. (1) One test was performed with SA (8 mg/mL) between bare mica surfaces, omitting both FN incubation and passivation steps. (2) For FN+LUB tests, LUB (0.02 mg/mL) was incubated for at least 4 hours and up to overnight—long enough to ensure good surface coverage using this subphysiological concentration.[7,30] Before starting the experiment, the LUB droplet was removed and replaced with an additional 50 μL of LUB at 0.02 mg/mL to avoid any effects due to dehydration. (3) FN+LUB+HA tests involved an extra incubation step. After the incubation of LUB, a droplet of HA was incubated between the surfaces for at least 1 hour before testing and was left in the junction for shearing.

Tryp-SF was prepared following an established protocol[31] at a concentration of 5 mg per 100 mL of SF. The tryp-SF solution was heated to 37 ºC and shaken for at least 2 hours, after which it was injected between the surfaces and incubated for 1 hour before testing to allow adsorption onto the surfaces. Hyaluronidase-SF (hy-SF) was prepared similarly.[32] Hyaluronidase was added to SF at a concentration of 5mg/100mL,

left at room temperature for 2 hours, and then injected between the FN-coated surfaces and incubated for 1 hour before testing. Hyaluronidase activity was confirmed by a noticeable decrease in the SF viscosity to a water-like consistency.

HA-PL solutions were sonicated for 15 min before use. All samples were stored frozen and thawed immediately before use. All film preparation and incubation steps were performed in a laminar flow hood to prevent contamination, and the SFA was closed and sealed during incubation. Experiments were conducted at room temperature.

Friction data was acquired using LabVIEW software (National Instruments, Austin TX). FECO were visualized and recorded using LightField software (Princeton Instruments, Trenton NJ). Data was analyzed using a custom MATLAB code (MathWorks, Natick MA) and Excel.

Statistical Analysis

One-way ANOVA with Tukey's posttest and Student's t-test were used to determine statistical significance between conditions in GraphPad Prism (GraphPad Software, California USA); $p < 0.05$ is indicated by a single star (*).

Results

2.1 Behavior of Synovial Fluid (SF) Films under Shear

Under shear, FN+SF films abruptly thicken and form aggregates (Figure 2.1). In our tests, SF films were anchored to confining mica surfaces via an FN layer, subjected to normal loads of circa 1-2 mN and sheared at 3μm/s. Under these conditions, film

thickness (D) increased sharply as soon as shear was applied, from D=21.4 ± 3.8 nm before shearing to D=69.3 ± 13.1 nm within one 20-second shearing cycle (an increase of over 300%, n=4). This initial film thickening was followed by a prolonged monotonic increase in film thickness, eventually ending in a plateau (Figure 2.1A). The friction force and associated friction coefficient of FN+SF films were relatively stable throughout the entire shearing test (Figure 2.1B). Both the increase in film thickness and the formation of aggregates were quantified via FECO images acquired in real time during shear (Figure 2.1C) while aggregates distribution and location were later visualized via Newton rings images of the contact junction acquired after shearing using a top-view optical microscope (Figure 2.1D). These results are similar to those reported by Banquy *et al.* in their seminal work characterizing SF aggregation using an SFA.[14] The index of refraction of the aggregates (IR=1.52 ± 0.069) was significantly higher than that of the surrounding FN+SF film (IR=1.45 ± 0.06, n=14, p=0.0146) (Figure 2.1E), indicating local variations in film density likely associated with molecular structural/conformational and/or orientational changes within the sheared film. IR measurements of several aggregates were made during each shearing test and the results shown represent the overall average IR for the aggregates and for the surrounding "non-aggregate" media, respectively (n=14). As a comparison, an index of refraction IR=1.34 was reported by Banquy et al. for bulk (uncompressed) SF, which is predictably lower than that measured for aggregated and non-aggregated SF under compression.[14] Indexes of refraction were calculated from FECO wavelengths using equations 1 and 2

$$IR = IR_{mica}\sqrt{\frac{(n-1)F_{n-1}}{nF_n}\cdot\frac{\lambda_{n-1}^{D}-\lambda_{n-1}^{0}}{\lambda_{n}^{D}-\lambda_{n}^{0}}}, \text{ for odd } n \quad (1)$$

$$F_n = \frac{\lambda_{n-1}^0}{\lambda_{n-1}^0 - \lambda_n^0} \qquad (2)$$

where λ_n^0 is the wavelength of the nth interference fringe when the mica surfaces are in direct contact (before incubating samples) and λ_n^D is the wavelength of the nth interference fringe when the mica surfaces are separated by a film of thickness D.

Following the characterization of SF under shear, we next analyzed the behavior of individual SF components subjected to the same shearing conditions. We specifically focused on HA, SA, and LUB, as well as on combinations of HA with LUB, SA, and PL that have been implicated in the formation of a lubricating film, and we systematically compared their behavior with that of SF.[2,5,9,10,11,12,16,17,18]

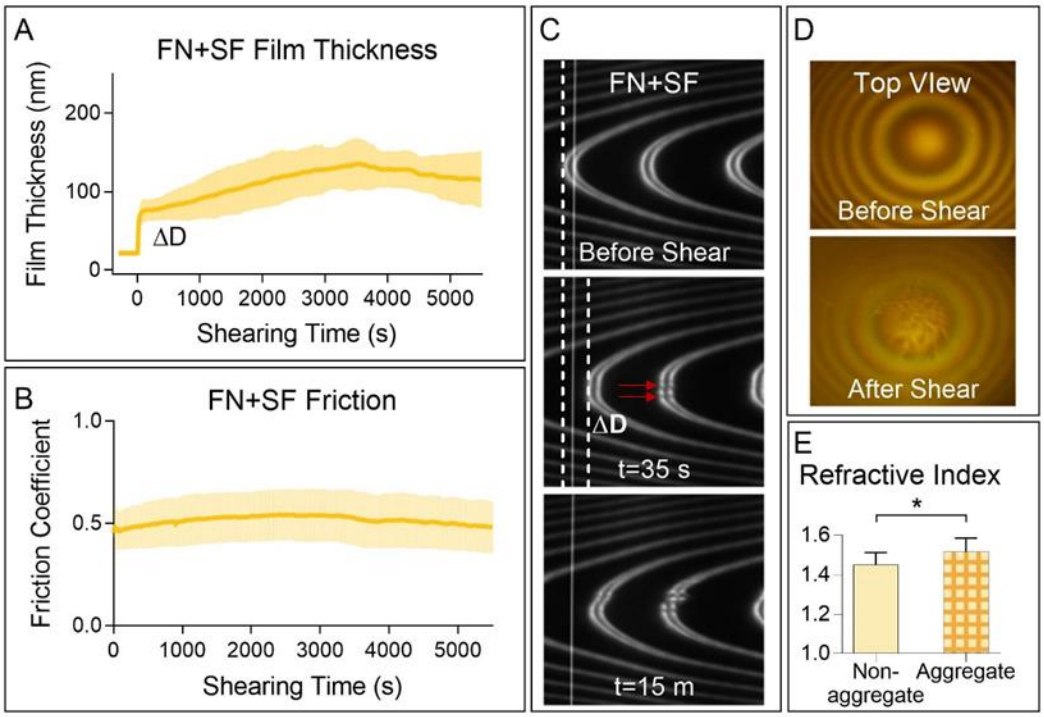

Figure 2.1 (A) Thickness of FN+SF films increased abruptly under shear and was sustained under prolonged shearing (n=4). (B) Friction of FN+SF films was stable under prolonged shearing. (C) FECO images of FN+SF films show aggregates (red arrows)

which began to form simultaneously with the onset of shear and ocntinued to develop under prlonged shearing. (D) SF aggregates were visible in top-view images of the contact junction after shearing. (E) The index of refractoin of SF aggregates was significantly higher than that of the surrounding confined synovial fluid (n=14, p=0.015)

2.2 Behavior of Hyaluronic Acid (HA) Films under Shear

HA is responsible for the high viscosity of SF, which facilitates the "elastoviscous transition" from boundary mode lubrication to elasto-hydrodynamic lubrication, resulting in reduced friction.[10] HA has also been implicated in the formation of a localized lubricating boundary layer at the surface of cartilage via synergistic interactions with LUB[5,10,21] and/or PL.[11,12] Due to its various reported roles in joint lubrication, we next assessed the potential involvement of HA in SF aggregation and film thickening.

Under shear, FN+HA films formed aggregates that were similar in size and distribution to those formed in FN+SF films (Figure 2.2A). Over time, however, aggregates within the FN+HA film tended to migrate towards the edges of the shearing junction whereas no new aggregates would form in the center of the contact. Despite the apparent similarities between FN+HA and FN+SF aggregates, FN+HA films exhibited a different film thickening behavior from that of FN+SF films (Figure 2.2B). While the magnitude of the initial film thickness increase was similar (ΔD_{FN+HA}=52.9 ± 21.6 nm and ΔD_{FN+SF}=48.0 ± 12.3 nm, inset of Figure 2.2B, n=7), the thickening observed in FN+HA films occurred more gradually. For FN+HA the initial increase occurred over ~2-3 minutes (6-9 shearing cycles), compared to under ~10-20 seconds (<1 shearing cycle) for FN+SF, which suggests that the underlying mechanisms of

aggregation/film thickening are likely different. Following the initial increase, FN+HA film thickness immediately began to decrease until the entire film was expelled from the shearing junction. In most tests, film depletion resulted in eventual damage of the underlying mica surfaces (detected via FECO images, not shown), which was never observed for FN+SF. FN+HA films exhibited high initial friction that rapidly decreased over several shearing cycles, which may be due to the shear-thinning nature of HA.[33] After this transient initial behavior, the friction of FN+HA was very similar to that of FN+SF (Figure 2.2C).

HA/PL mixtures were also tested since HA and PL have been reported to interact synergistically to form a gel-like protective lubricating layer on mica surfaces.[2,11,12] However, the aggregation (FECO not shown here), film thickness evolution, and friction of FN+HA/PL films were indistinguishable from those observed for FN+HA (Figure 2.2, n=2). Some reports of HA/PL gels have used concentrations that greatly exceed the physiological concentrations used here, which could explain why we did not notice any additional effect due to the presence of PL.[2] Furthermore, HA/PL films have been demonstrated to develop from PL vesicles that rupture upon interaction with HA to form a boundary lubricating film, and the initial presence and stability of those vesicles may be critical.[11,12]

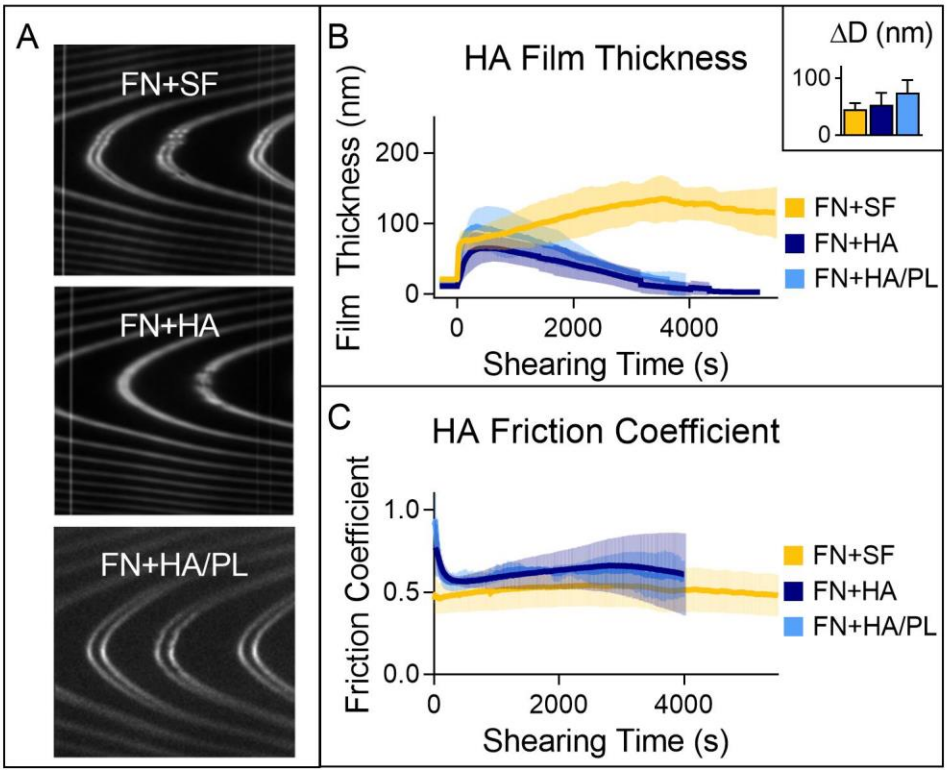

Figure 2.2. (A) FN+HA aggregates were similar in size and number to those formed in FN+SF films. (B) FN+HA and FN+HA/PL films thickened more gradually than FN+SF films and depleted after an initial increase. (C) Other than a transient initial behavior, FN+HA and FN+HA/PL friction were similar to FN+SF.

2.3 *Behavior of Serum Albumin (SA) Films under Shear*

The aggregation of globular proteins under shear has been reported in various model systems,[15,16,22,23,34] making SA a key component of interest in our study of SF aggregation. Our data reveal that, under shear, FN+SA films abruptly thickened and formed aggregates; however, both the magnitude of thickening and the size of aggregates were greater than those in FN+SF films (Figure 2.3). The aggregates formed in FN+SA films were denser and larger than those observed in FN+SF, as monitored by the FECO, which show alterations in shape and intensity of both even fringes (indicative

of changes in refractive index) and odd fringes (indicative of aggregates large enough to deform confining surfaces and obstruct the light path) (Figure 2.3A). Furthermore, FN+SA films thickened by ΔD_{FN+SA}=140.0 ± 18.3 nm, nearly three times more than FN+SF films (Inset of Figure 2.3B). Nevertheless, the long-term behavior of FN+SA under shear was similar to that of FN+SF: after an initial abrupt film thickening, both films reached a steady film thickness, with no sign of depletion during the course of the ~1.5 hr shearing test (Figure 2.3B). The larger magnitude of the film thickening and aggregation in FN+SA films (compared to FN+SF films) could be due to strong interactions between SA and the underlying FN layer that could lead to the formation of aggregates composed of entangled FN and SA, a phenomenon that has previously been reported in similar tests[13] (see Discussion section). To better assess the role of SA *within* SF, where other molecules (with larger size and higher affinity for FN) may eventually adsorb onto the FN layer, hence exchanging with SA and preventing FN-SA interactions, we also tested SA without an underlying layer of FN.

SA films deposited directly onto mica surfaces (in absence of FN) exhibited a shear behavior very similar to that of FN+SF films (Figure 2.3A and 3B). Under shear, SA film thickness increased by ΔD_{SA}=53.3 ± 3.6 nm (n=3) for SA compared to ΔD_{FN+SF}=48.0 ± 12.3 nm (n=4) for FN+SF, and their long-term film thickness reached a similar plateau with no sign of depletion, even after prolonged shear. The rate of aggregation was also identical in SA, FN+SA, and FN+SF films with aggregates measurable circa 10s after shear started—another strong indicator that SA plays a prominent role in the overall shear response of SF.

The friction coefficients of both SA and FN+SA films were identical, suggesting that SA molecules (in similar amount and conformation) were localized at the shearing interface and controlled the friction, independently of the presence of FN (Figure 2.3C). In both films, friction increased moderately with shearing time/number of shearing cycles. In contrast, the friction of FN+SF films remained nearly constant, likely due to the additional contribution of other lubricating components in SF. Even though SA and FN+SA films exhibited increasing friction over time, they demonstrated remarkable surface protection against wear, as no sign of damage was visible on the FECO, even after shearing overnight (data not shown).

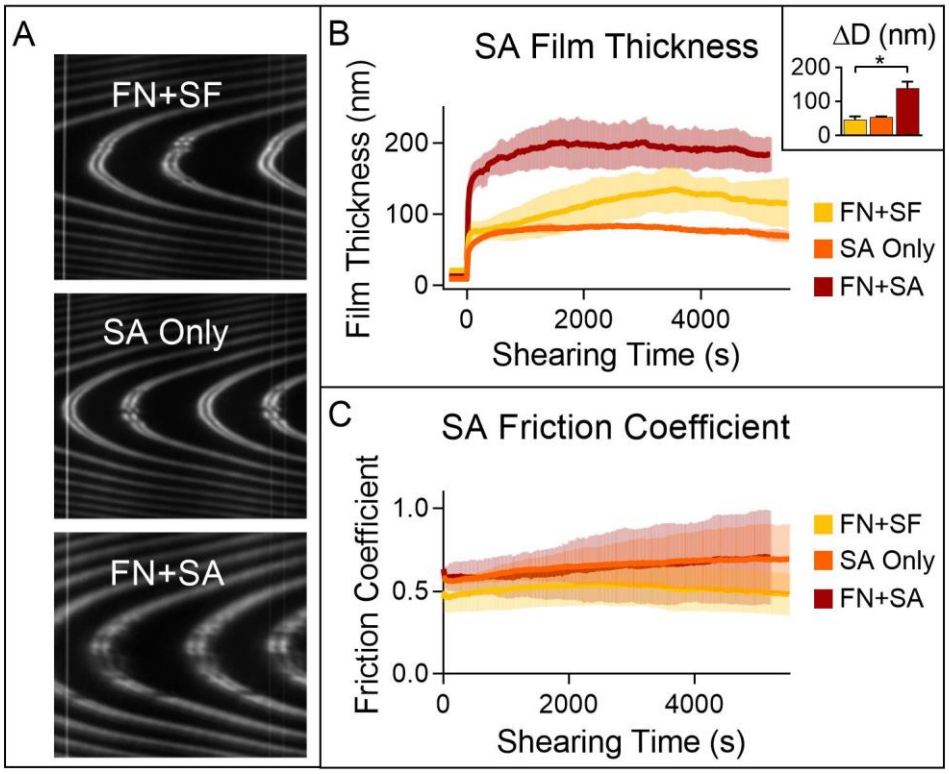

Figure 2.3. (A) SA and FN+SF films exhibited similar aggregation, while FN+SA films formed larger and more numerous aggregates which were visible in both even and odd fringes. (B) The initial thickness (ΔD) was significantly greater for FN+SA films than

for SA or FN+SF films ($p<.0001$, n=2-4). All samples exhibited abrupt initial thickening, which was sustained throughout the entire shearing test. (C) Friction between SA films (with or without FN) increased with prolonged shear while friction between FN+SF films remained stable.

2.4 Behavior of Hyaluronic Acid/Serum Albumin (HA/SA) Mixture under Shear

Although both HA and SA films formed aggregates under shear, only SA exhibited long-lasting film thickening. To determine whether HA and SA interact with each other and replicate the aggregation and film thickening observed in FN+SF films, we next tested a mixture of HA and SA at physiological concentrations. Interestingly, aggregation occurred shortly upon shearing and was visible in both odd and even FECO, indicative of large light-obstructing aggregates, as observed for FN+SA films (Figure 2.4A). This was accompanied by an abrupt film thickening that was much greater in magnitude than for FN+SF, similar to that measured for FN+SA (($\Delta D_{FN+HA/SA}$=150.2 ± 10.2 nm, and ΔD_{FN+SA}=140.0 ± 18.3 nm, while ΔD_{FN+SF}=48.0 ± 12.3 nm) (Figure 2.4B and 2.3B). However, after this initial FN+SA-like behavior, the aggregates migrated towards the edges of the junction and no new aggregates were formed at the center of the junction, similar to FN+HA films. Simultaneously, the film thickness depleted at a rate (acquired from linear fits, not shown) that was similar to the depletion of FN+HA films ($m_{FN+HA/SA}$=0.0168 nm/s and m_{FN+HA}=0.0189 nm/s, respectively; R^2 >0.99 in both cases) (Figure 2.4B). The friction of the HA/SA mixture increased significantly with shearing time (Figure 2.4C). Overall, these data suggest that SA is responsible for the initial film thickening occurring at the onset of shear while HA becomes predominant at later time points when shear is prolonged.

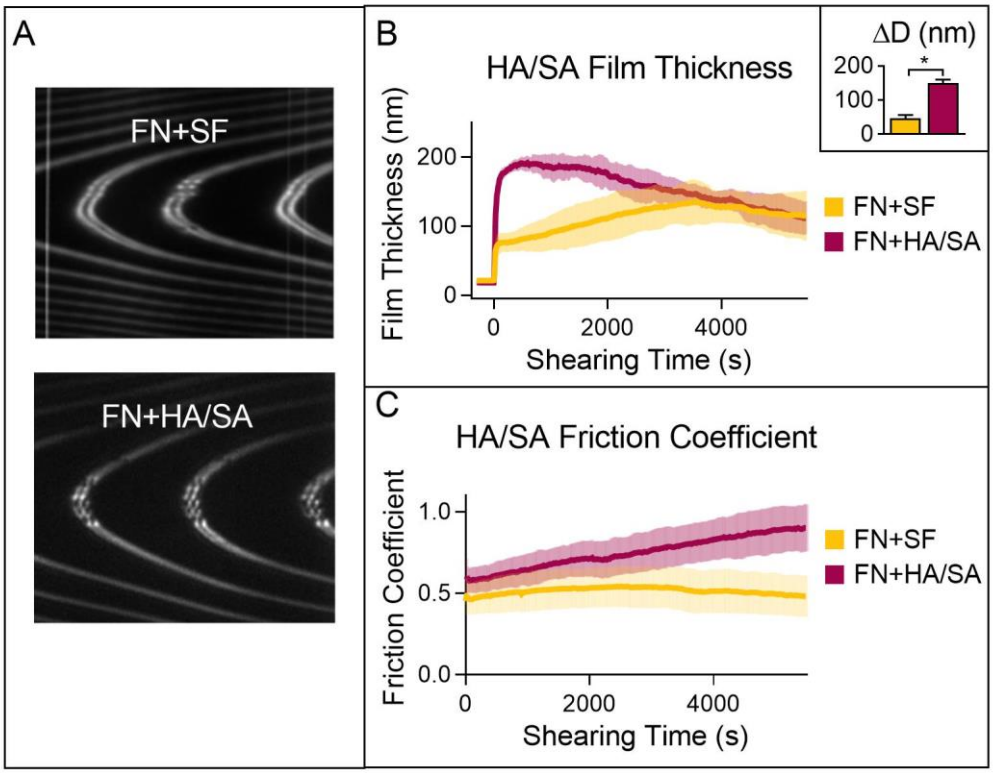

Figure 2.4. (A) Initial aggregation was greater for FN+HA/SA than for FN+SF films, with aggregates visible in both odd and even fringes. (B) The initial FN+SF films ($p=.0001$, $n=3$). However, after reaching a maximum, FN+HA/SA films depleted in thickness. (C) Initially, friction coefficients were similar between FN+SF and FN+HA/SA films; however, under prolonged shearing friction increased in FN+HA/SA films.

2.5 Behavior of Lubricin (LUB) Films under Shear

LUB is a glycoprotein in SF that exhibits excellent boundary lubrication due to its highly hydrated bottlebrush structure and its ability to attach to the cartilage surface, thereby ensuring low friction at the shearing interface. LUB has also been shown to interact synergistically with HA to promote elasto-hydrodynamic lubrication by anchoring HA to the cartilage surface and thereby increasing the local viscosity at the

surface.[10] We therefore tested whether LUB could be involved in the shear-induced thickening and aggregation of SF. Our data indicate that only minimal aggregation occurred in FN+LUB films under shear, and that film thickness barely increased at the onset of shear (Figure 2.5A and B). Although the friction coefficient of FN+LUB films was initially lower than that of SF, it increased significantly with prolonged shearing (Figure 2.5C). This increase in friction was simultaneous to a gradual decrease in film thickness, suggesting that LUB plays an essential role in lowering friction but can easily be expelled from the shearing junction.

We next evaluated whether the reported synergistic interactions between LUB and HA would lead to SF-like behavior under shear by testing FN+LUB+HA layered films.[5,10,21] We found that film thickness, aggregation, and friction traces of FN+LUB+HA films were unchanged with respect to those observed for FN+LUB films (Figure 2.5). This result is likely due to weak interactions between HA and LUB, which prevent retention of HA within the shearing junction under the pressures used in our experiments (up to ~5.5 MPa).

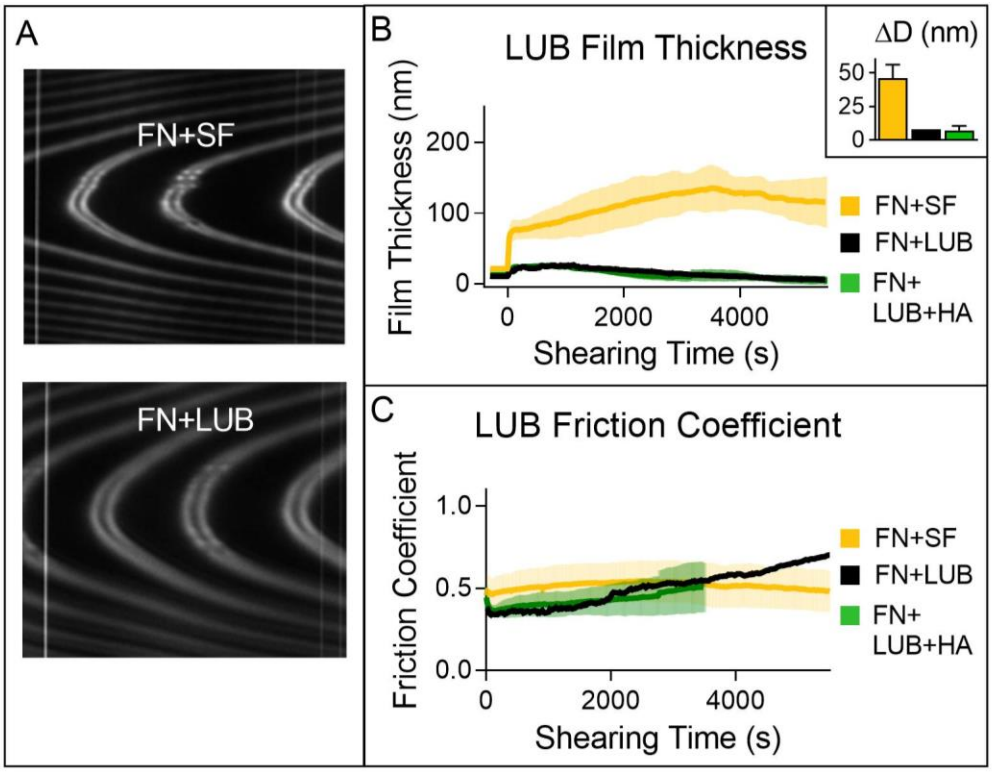

Figure 2.5. (A) Compared to FN+SF, FN+LUB exhibited only minimal aggregation. (B) FN+LUB and FN+LUB+HA films thickened significantly less upon shearing than FN+SF films ($p<.01$) and depleted under prolonged shearing. (C) FN+LUB and FN+LUB+HA friction increased over time, while FN+SF friction remained stable.

2.6 Effect of Hyaluronidase Treatment on Synovial Fluid (hy-SF) Behavior under Shear

While the thickness of FN+HA and FN+SF films evolved differently over shearing time, both their aggregation and their friction behaviors were similar. To assess whether HA (possibly interacting with other SF components) contributes to the SF response under shear, we treated SF films with hyaluronidase and found that HA digestion had no significant effect on aggregation, film thickness, or friction of the treated FN+SF films (Figure 2.6). Although the amount/distribution of aggregates varied between FN+hy-SF experiments (n=7), the overall aggregation behavior was

similar to those observed for untreated FN-SF films (Figure 2.6A). Both the initial increase in film thickness and the long-term film thickness behavior under continued shearing were indistinguishable between hyaluronidase-treated and untreated FN+SF films (Figure 2.6B). The friction data were also unchanged by hyaluronidase treatment (Figure 2.6C). These data demonstrate that HA is not involved in the shear-induced transformation of SF.

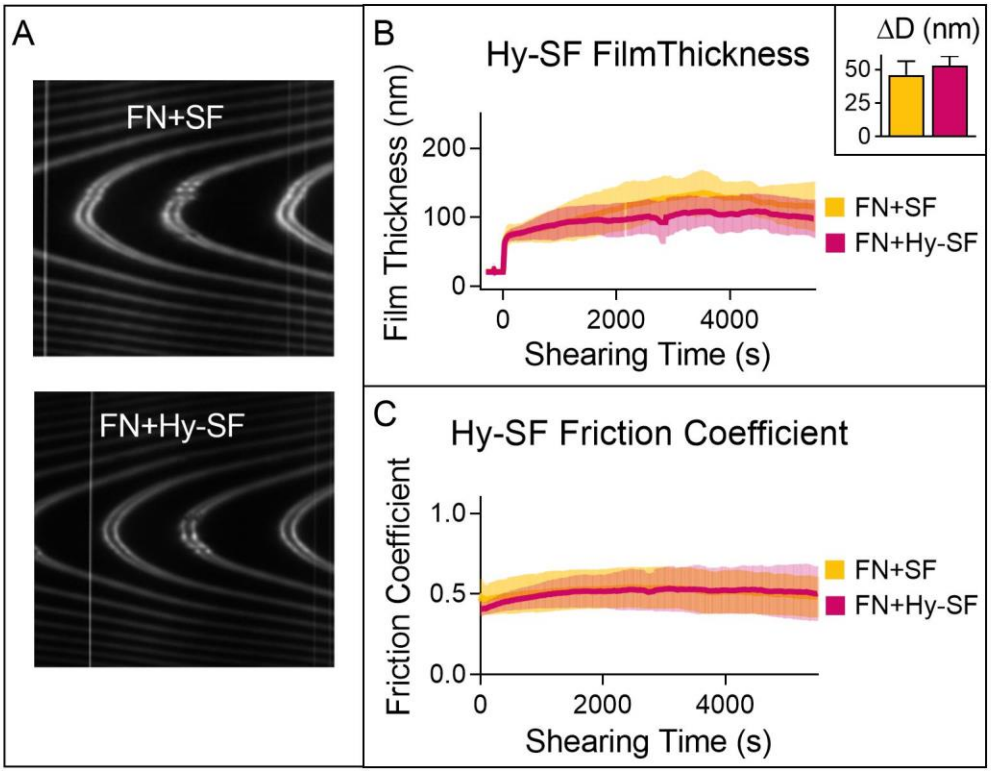

Figure 2.6. (A) Aggregation was similar between FN+hy-SF films and normal FN+SF films. (B) The initial thickening and the evolution of film thickness under prolonged shearing was unaffected by hyaluronicase treatment. (C) Friction was not affected by hyaluronidase treatment.

2.7 Effect of Trypsin Treatment on Synovial Fluid (tryp-SF) Behavior under Shear

After we established that both FN+SA and isolated SA films formed aggregates and exhibited stable, long-term thickening under shear, we next evaluated the specific role of SA in governing the behavior of SF under shear by treating SF with trypsin to digest its protein content. Although the size and the amount of aggregates varied between FN+tryp-SF experiments (n=5), on average, overall aggregation behavior of FN+tryp-SF films did not differ significantly from that of FN+SF films (Figure 2.7A). However, while both aggregate formation and *initial* increase in film thickness were similar between FN+tryp-SF and FN+SF films, *long-term* evolution of film thickness was noticeably different. Trypsin-treated SF film thickness reached a plateau faster and at significantly lower value than that of untreated SF (Figure 2.7B). This difference indicates that without SA, the long-term shear-induced behavior of SF is disrupted. We measured an initial film thickness increase of ΔD_{tryp}=39.9 ± 9.1 nm and ΔD_{FN+SF}=48.0 ± 12.3 nm for FN+tryp-SF and FN+SF films, respectively. After this initial increase, trypsin-treated SF films abruptly reached constant thickness whereas untreated SF films continued thickening over time (Figure 2.7B). It is known that trypsin hydrolyzes most proteins present in SF, which includes not only SA but also LUB; however, the lack of aggregate formation and film thickening observed in FN+LUB films (Figure 2.5) suggets that the effect of trypsin on the long-term film thicknening reported here can be attributed to its role in SA digestion. While both FN+tryp-SF and FN+SF films initially exhibited similar friction coefficients, the friction of FN+tryp-SF films gradually increased after circa one hour, wheras it remained constant for untreated SF films (Figure 2.7C). This relative friction increase in FN+tryp-SF could be the result of the tryptic digestion of LUB, an effect that has been previously reported.[35,36]

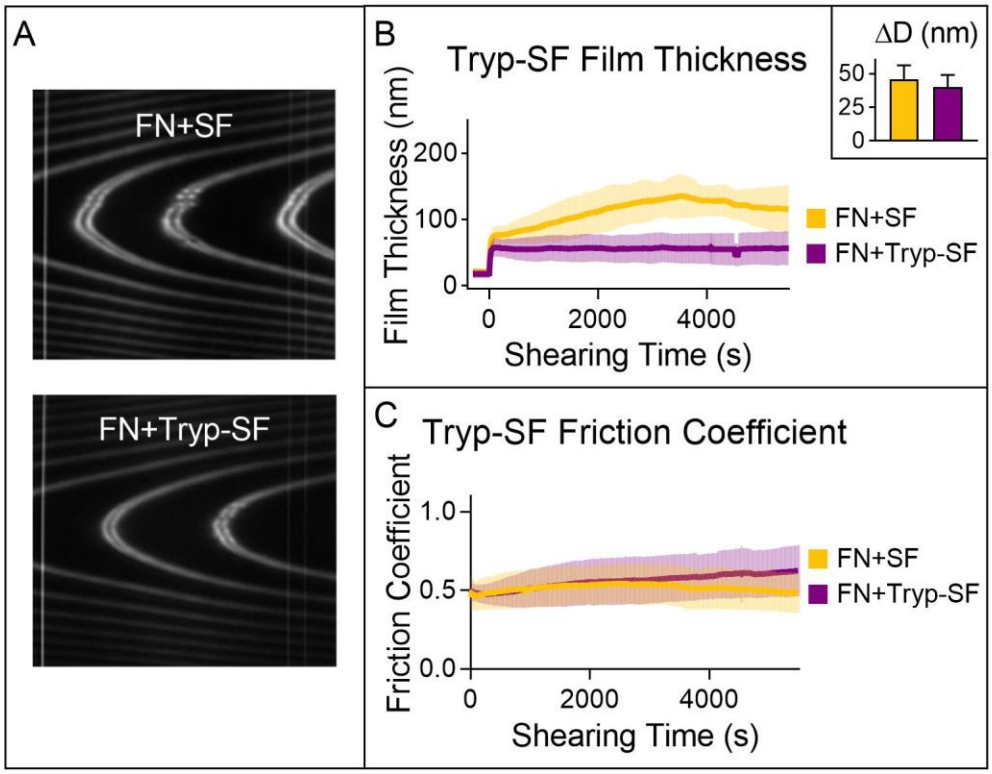

Figure 2.7. (A) The aggregates that formed in trypsin-treated and untreated SF were similar. (B) Film thickness of trypsin-treated and normal FN+SF films were similar at the onset of shearing but evolved differently under prolonged shearing. (C) Friction between trypsin-treated FN+SF and untreated FN+SF films reached a plateau.

Discussion

In this study, we used the SFA to measure the tribological properties of various SF components and determine which of them could replicate (individually or synergistically) the shear-induced transformation of SF, i.e., a sustainable film thickening accompanied by the formation of large and dense aggregates. The SF components tested in our experiments were chosen because of their reported role either in lubrication or in the formation of an aggregate film at the shearing interface. Overall

our results show that, among all SF components tested, SA governs the shear-induced transformation of SF over time. The key role of SA in SF behavior was indicated (i) by similar dynamics of aggregate formation and similar size/distribution of aggregates between FN+SF and FN+SA films, and (ii) by an alteration of SF behavior when SF was treated with trypsin, which digests SA and LUB. Because LUB demonstrates minimal aggregation and thickening under shear, the effect of trypsin on SF can be reasonably attributed to the digestion of SA. While our data do not rule out the possibility that other SF components may also contribute to SF transformation under shear, they clearly establish a prominent role for SA. For example, despite the ability of HA to form aggregates similar to those observed in SF, the drastically different behavior of FN+HA film thickness over time combined with the observation that hyaluronidase treatment (which digests HA) had no effect on SF evolution confirm that HA is not a critical mediator of the shear-induced transformation of SF.

Our results show striking similarities in the response of SA, FN+SA and FN+SF films to shear: all films undergo initial, abrupt thickening associated with nearly instantaneous formation of aggregates, and then maintain constant thickness (no film depletion) over time under prolonged shearing. Interestingly, although the initial thickening measured in SA alone (without FN) and FN+SF films were similar, FN+SA thickening was significantly larger. This difference may be due to strong interactions between SA molecules and the underlying FN layer. Previous work has reported that the concentration of SA used in our study is able to partially unfolds FN,[13] which could lead to the formation of large aggregates composed of entangled, unfolded FN and SA. However, in the case of FN+SF films, a layer of LUB attaches to FN via its C-

terminus,[37] which prevents most SA from interacting with the FN layer and thereby mitigates FN unfolding.[13] Thus, the results we obtained for SA *without* underlying FN may be more representative of the actual behavior of SA present within SF.

Shear-induced aggregation of globular proteins, such as BSA, has been widely reported in the literature.[15,16,23,34] The formation of a proteinaceous "gel layer" in vitro has been observed under various shearing conditions between a CoCrMo femoral head implant and a glass plate when sheared in either FBS[16-18] or in arthritic SF.[15] Comparable protein deposits have also been found on the bearing surfaces of recovered artificial joints.[38] The formation of such a protein gel has been proposed as a mechanism of surface protection against wear in artificial joints, termed "protein aggregation lubrication".[16] Our results provide experimental evidence of similar aggregation phenomena in healthy equine SF and SA solutions when sheared between model surfaces. Furthermore, our experimental setup allowed us to monitor the dynamics of aggregate formation in real-time while simultaneously measuring film thickness with extremely high accuracy (nanometer resolution) via interferometry. Importantly, SA aggregate films (as well as FN+SF films) also exhibited remarkable resistance to wear and protected the underlying mica surfaces from damage even after several hours of shear, whereas HA and LUB films revealed damage typically in under two hours. These results support the idea that SA aggregates could mediate wearless friction in artificial joints by providing a gel-like "cushion" that protects shearing surfaces. Although multiple mechanisms might be simultaneously responsible for aggregation, pressure and/or shear stress mediated protein denaturation seems consistent with the abrupt formation of aggregates observed in our study.[39] Additionally, the nature of the

aggregates, as measured in both our SA and FN-SA experiments reinforces the idea of irreversibly entangled structures composed either of denatured SA or denatured SA and FN, respectively, and stabilized by strong hydrophobic interactions consequent to the exposure of the proteins' cores. Denatured/decomposed protein deposits have also been previously identified on the bearing surfaces of recovered metal-on-metal implants, and local shear stresses were proposed as the mechanism of this protein decomposition, either via a direct 'mechanical' effect on protein structure or via an indirect 'thermal' effect associated with shear-induced temperature increase within the shearing junction.[38,40]

Protein adsorption on artificial joints depends on the chemistry and the material properties of the implant surface. Different amounts of adsorbed proteins were found (under the same testing conditions) on stainless steel, alumina, and UHMWPE surfaces with and without plasma treatment.[39,41] Hydrophobicity and surface charge were also identified as factors that affect both the amount and the adsorption mechanisms of albumin onto Ti and CoCrMo implant surfaces.[42,43] In some cases, such protein adsorption was reported to promote enhanced lubrication and wear protection via the "protein aggregation lubrication" mechanism discussed above.[16,18] Here we present a framework that allows in situ simultaneous measurement of film thickness, protein aggregation, friction, and presence of surface damage (if any). Therefore, our technique could be used for systematic characterization of adsorption, aggregate formation, and lubrication of protein films on a variety of implant materials with different surface properties not only to advance our understanding of the structure-function relationship

of protein films but also to improve the design and the materials properties of artificial joints.

Although our findings establish a prominent role of SA in SF structural changes under shear, we cannot exclude a supporting role (either individual or combined) of other SF constituents. For example, while HA films also undergo shear-induced film thickening and aggregate formation these phenomena do not occur as quickly as in the case of SF but rather gradually over time, suggesting that different mechanisms may be involved. Shear-induced HA-protein aggregation in SF has been previously reported but no mechanism of aggregation was proposed.[22] In fact, the response of HA to shear is complex and not yet fully understood despite numerous existing rheological and tribological studies. Additionally, in our experiments, HA behavior results from the combined effects of confinement, shear thinning (a characteristic behavior of HA under shear,[33] although viscosity was not directly measured here), and molecular interactions with FN, which make the identification of aggregation mechanisms quite challenging. Further studies are needed to deconvolute the individual and/or cooperative roles of these parameters in the HA response to shear.

We also evaluated the shear response of combined SF components previously shown to act synergistically in boundary lubrication: LUB+HA,[5,10,21] HA/PL,[2,11,12] and HA/SA.[22] However, no significant difference was observed between the behavior of LUB+HA and HA/PL films compared to that of LUB and HA, respectively. This absence of synergy could be due to differences in solution concentration, surface binding, and applied load between our experiments and previous studies. The reported synergy between LUB and HA is dependent on the immobilization of HA[5,21] or LUB[10]

at the surface. LUB has been shown to anchor HA to the surface of cartilage via molecular entanglement.[10] Therefore, the lack of LUB/HA synergy in our study could be attributed to the inability of HA to entangle properly with LUB when it is attached to FN-coated mica surfaces compared to native cartilage.[5,10,21] In fact, recent work indicates that LUB binds to collagen II (the dominant structural protein at the cartilage surface) via the N-terminus whereas it interacts with FN (present both in SF and at the cartilage surface) via the C-terminus.[13,37] Additionally, a previous report of HA/LUB synergy measured in SFA studies involves HA that was directly grafted to the underlying mica surface[21] while our experiments relied on physisorption of LUB onto FN. These results highlight the importance of the balance of interactions within the various SF components *vs.* interactions between SF components and the confining surfaces for optimized lubrication and surface protection during shear. While HA/PL films have been reported to form a low friction boundary-lubricating complex, in our experiments HA/PL films exhibited identical behavior to HA films without PL, with no difference in film thickness, aggregation, or friction. This could be because reports of a lubricating HA/PL gel have used concentrations of PL that greatly exceeded the physiological concentration used in our experiments,[2] or because reports of a boundary lubricating HA/PL synergy have used PL vesicles that would complex with HA to form mono- or bilayers along HA chains.[11,12] The initial presence of vesicles may be critical for the eventual stability of PL layers attached to HA, which may be unstable or unable to form from free-floating PL. Although both HA and SA films individually exhibited some SF-like characteristics during shear, HA/SA mixtures did not combine these behaviors to replicate those of SF. Instead, the behavior of HA/SA mixtures was

predominantly mediated (i) by SA at the onset of shearing, as indicated by an abrupt initial film thickening and formation of large/dense aggregates (characteristic of SA) and (ii) by HA under prolonged shearing, as indicated by a gradual depletion of the film from the shearing junction.

The friction coefficients measured in our FN+SF, FN+HA, FN+SA, and FN+LUB experiments are notably higher than the values reported in previous SFA experiments on isolated SF components.[13] One key difference is that the data presented here are *instantaneous* measurements calculated for each shearing cycle under constant load while previous studies have typically reported *average* friction coefficients measured over a range of incrementally increasing loads.[13] It should also be noted that in the case of FN+HA and FN+SA, the pressures applied in our experiments exceeded the pressures at which damage occurred in previously reported experiments[13] performed under incrementally increasing loads, which may explain the incongruity in friction coefficient. Regardless, for the purposes of this paper the comparative friction behaviors of the various SF components, not the absolute friction values, give meaningful insights into the lubricating mechanisms involved.

Finally, we should point out that the SFA surfaces used in all our experiments are made of freshly cleaved mica, which is atomically smooth, rigid, and non-porous. These surface properties are therefore structurally and mechanically different from those of cartilage, which is heterogeneous, comparatively rough, compliant, and porous. Because of these differences, caution must be used in generalizing our findings beyond rigid surfaces. Nevertheless, using these model surfaces allows us to evaluate accurately the structure-tribology relationship of thin lubricating films by ensuring that all shear-

induced events measured can be attributed to changes in the interfacial lubricant, i.e., to phenomena occurring at the junction *between* surfaces rather than *within* surfaces. Additionally, our results are applicable to numerous tribosystems involving rigid surfaces, in particular most artificial joints.

Conclusions

Current approaches that seek to elucidate the remarkable lubrication of SF usually focus on the roles of HA and LUB and frequently overlook the role SA although it represents 90% of the protein content of SF. In this study, we used the SFA to measure the shear response of all major SF components and determine which of them could replicate the structural transformations of SF under shear, i.e., the formation of large, dense, long-lived aggregates associated with efficient surface protection against damage. Collectively, our data provide evidence that SA is a key contributor to the formation of wear-protective aggregates in SF films under shear. While the formation of aggregates in SF and the development of wear-protecting "protein gels" in FBS have been previously observed in separate studies, our findings correlate both phenomena by revealing the prominent role of globular proteins in SF aggregation and its connection to surface protection. Our results are likely applicable to other rigid systems such as artificial joints, in which the dynamic aggregation of SF may play a pivotal lubricating role by providing an 'on demand' wear protecting protein cushion in response to shear stresses. Although it will be of future interest to investigate SF aggregation between cartilage surfaces to elucidate its role (if any) in natural joints, the identification of a self-replenishing, shear-induced lubricating mechanism of SF mediated by the

aggregation of globular proteins advances our current understanding of the lubrication of joint implants with implications for future design and therapeutic interventions.

REFERENCES

1. Silva, M., Shepherd, E. F., Jackson, W. O., Dorey, F. J. & Schmalzried, T. P. Average patient walking activity approaches 2 million cycles per year: Pedometers under-record walking activity. *J. Arthroplasty* **17**, 693–697 (2002).

2. Crockett, R. *et al.* Biochemical composition of the superficial layer of articular cartilage. *J. Biomed. Mater. Res. Part A* **82**, 958–964 (2007).

3. Ogston, A. G. & Stanier, J. E. The physiological function of hyaluronic acid in synovial fluid; viscous, elastic and lubricant properties. *J. Physiol.* **4**, 244–252 (1952).

4. Schmidt, T. A., Gastelum, N. S., Nguyen, Q. T., Schumacher, B. L. & Sah, R. L. Boundary lubrication of articular cartilage: Role of synovial fluid constituents. *Arthritis Rheum.* **56**, 882–891 (2007).

5. Greene, G. W. *et al.* Adaptive mechanically controlled lubrication mechanism found in articular joints. *Proc. Natl. Acad. Sci. U. S. A.* **108**, 5255–5259 (2011).

6. Swann, D. A., Silver, F. H., Slayter, H. S., Stafford, W. & Shore, E. The molecular structure and lubricating activity of lubricin isolated from bovine and human synovial fluids. *Biochem. J.* **225**, 195–201 (1985).

7. Gleghorn, J. P., Jones, A. R. C., Flannery, C. R. & Bonassar, L. J. Boundary mode lubrication of articular cartilage by recombinant human lubricin. *J. Orthop. Res.* **27**, 771–777 (2009).

8. Chan, S. M., Neu, C. P., Duraine, G., Komvopoulos, K. & Reddi, A. H. Atomic force microscope investigation of the boundary-lubricant layer in articular cartilage. *Osteoarthr. Cartil.* **18**, 956–963 (2010).

9. Hills, B. A. & Crawford, R. W. Normal and prosthetic synovial joints are lubricated by surface-active phospholipid: a hypothesis. *J. Arthroplasty* **18**, 499–505 (2003).

10. Bonnevie, E. D., Galesso, D., Secchieri, C., Cohen, I. & Bonassar, L. J. Elastoviscous transitions of articular cartilage reveal a mechanism of synergy between lubricin and hyaluronic acid. *PLoS One* **10**, (2015).

11. Seror, J., Zhu, L., Goldberg, R., Day, A. J. & Klein, J. Supramolecular synergy in the boundary lubrication of synovial joints. *Nat. Commun.* **6**, (2015).

12. Zhu, L., Seror, J., Day, A. J., Kampf, N. & Klein, J. Ultra-low friction between boundary layers of Hyaluronan-phosphatidylcholine Complexes. *Acta Biomater.* **59**, 283–292 (2017).

13. Eguiluz, R. C. A. *et al.* Fibronectin mediates enhanced wear protection of lubricin during shear. *Biomacromolecules* **16**, 2884–2894 (2015).

14. Banquy, X., Lee, D. W., Das, S., Hogan, J. & Israelachvili, J. N. Shear-induced aggregation of mammalian synovial fluid components under boundary lubrication conditions. *Adv. Funct. Mater.* **24**, 3152–3161 (2014).

15. Stevenson, H. *et al.* The development of a small-scale wear test for CoCrMo specimens with human synovial fluid. *Biotribology* **14**, 1–10 (2018).

16. Fan, J., Myant, C. W., Underwood, R., Cann, P. M. & Hart, A. Inlet protein aggregation: a new mechanism for lubricating film formation with model synovial fluids. *Proc. Inst. Mech. Eng. Part H.* **225**, 696–709 (2011).

17. Mavraki, A. & Cann, P. M. Lubricating film thickness measurements with bovine serum. *Tribol. Int.* **44**, 550–556 (2011).

18. Myant, C. & Cann, P. In contact observation of model synovial fluid lubricating mechanisms. *Tribiology Int.* **63**, 97–104 (2013).

19. Zheng, X. *et al.* Proteomic analysis for the assessment of different lots of fetal bovine serum as a raw material for cell culture. part IV: Application of proteomics to the manufacture of biological drugs. *Biotechnol. Prog.* **22**, 1294–1300 (2006).

20. Chang, D. P. *et al.* Conformational mechanics, adsorption, and normal force interactions of lubricin and hyaluronic acid on model surfaces. *Langmuir* **24**, 1183–1193 (2007).

21. Das, S. *et al.* Synergistic interactions between grafted hyaluronic acid and lubricin provide enhanced wear protection and lubrication. *Biomacromolecules* **14**, 1669–1677 (2013).

22. Walker, P. S., Unsworth, A., Dowson, D., Sikorski, J. & Wright, V. Mode of aggregation of hyaluronic acid protein complex on the surface of articular cartilage. *Ann. Rheum. Dis* **29**, 591–602 (1970).

23. Oates, K. M. N., Krause, W. E., Jones, R. L. & Colby, R. H. Rheopexy of synovial fluid and protein aggregation. *J. R. Soc. Interface* **3**, 167–74 (2006).

24. Schmid, T. *et al.* Superficial zone protein (SZP) is an abundant glycoprotein in human synovial fluid and serum. in *Transactions of the Orthopoedic Research Society* (2001).

25. Mazzucco, D., Scott, R. & Spector, M. Composition of joint fluid in patients undergoing total knee replacement and revision arthroplasty: correlation with flow properties. *Biomaterials* **25**, 4433–4445 (2004).

26. Balazs, E. A., Watson, D., Duff, I. F. & Roseman, S. Hyaluronic acid in synovial fluid: Molecular parameters of hyaluronic acid in normal and arthritic human fluids. *Arthritis Rheum.* **10**, 357–376 (1967).

27. Israelachvili, J. *et al.* Recent advances in the surface forces apparatus (SFA) technique. *Reports Prog. Phys.* **73**, (2010).

28. Israelachvili, J. N. Thin film studies using multiple-beam interferometry. *J. Colloid Interface Sci.* **44**, 259–272 (1973).

29. Gleghorn, J. P. & Bonassar, L. J. Lubrication mode analysis of articular cartilage using Stribeck surfaces. *J. Biomech.* **41**, 1910–8 (2008).

30. Zappone, B., Ruths, M., Greene, G. W., Jay, G. D. & Israelachvili, J. N. Adsorption, lubrication, and wear of lubricin on model surfaces: polymer brush-like behavior of a glycoprotein. *Biophys. J.* **92**, 1693–708 (2007).

31. Jay, G. D., Torres, J. R., Warman, M. L., Laderer, M. C. & Breuer, K. S. The role of lubricin in the mechanical behavior of synovial fluid. *Proc. Natl. Acad. Sci. U. S. A.* **104**, 6194–6199 (2007).

32. Linn, F. C. Lubrication of animal joints II: the mechanism. *J. Biomech.* **1**, 193–205 (1968).

33. Gibbs, D. A., Merrill, E. W., Smith, K. A. & Balazs, E. A. Rheology of hyaluronic acid. *Biopolymers* **6**, 777–791 (1968).

34. Myant, C. W. & Cann, P. The effect of transient conditions on synovial fluid protein aggregation lubrication. *J. Mech. Behav. Biomed. Mater.* **34**, 349–357 (2014).

35. Sun, Y., Chen, M., Zhao, C., An, K. & Amadio, P. C. The effect of hyaluronidase, phospholipase, lipid solvent and trypsin on the lubrication of canine flexor digitorum profundus tendon. *J. Orthop. Res.* **26**, 1225–9 (2008).

36. Jay, G. The effect of phospholipase digestion upon the boundary lubricating ability of synovial fluid. *J. Rheumatol.* **26**, 2454–2457 (1999).

37. Flowers, S. A. *et al.* Lubricin binds cartilage proteins, cartilage oligomeric matrix protein, fibronectin and collagen II at the cartilage surface. *Sci. Rep.* **7**, (2017).

38. Wimmer, M. A., Sprecher, C., Hauert, R., Täger, G. & Fischer, A. Tribochemical reaction on metal-on-metal hip joint bearings A comparison between in-vitro and in-vivo results. *Wear* **255**, 1007–1014 (2003).

39. Heuberger, M. P., Widmer, M. R., Zobeley, E., Glockshuber, R. & Spencer, N. D. Protein-mediated boundary lubrication in arthroplasty. *Biomaterials* **26**, 1165–1173 (2005).

40. Mathew, M. T. *et al.* Tribolayer formation in a metal-on-metal (MoM) hip joint: an electrochemical investigation. *J. Mech. Behav. Biomed. Mater.* **29**, 199–212 (2014).

41. Serro, A. P., Colaço, R. & Saramago, B. Effect of Albumin Adsorption on Biotribological Properties of Artificial Joint Materials. in *Proteins and Interfaces III State of the Art* 497–523 (American Chemical Society, 2012).

42. Yan, Y., Yang, H., Su, Y. & Qiao, L. Albumin adsorption on CoCrMo alloy surfaces. *Sci. Rep.* **5**, (2015).

43. Escudeiro, A., Polcar, T. & Cavaleiro, A. Adsorption of bovine serum albumin on Zr co-sputtered a-C(:H) films: Implication on wear behaviour. *J. Mech. Behav. Biomed. Mater.* **39**, 316–327 (2014).

CHAPTER 3

Synergistic Interactions of a Synthetic Lubricin-Mimetic with Fibronectin for Enhanced Wear Protection[4]

Abstract

Lubricin is a major mucinous glycoprotein of mammalian synovial fluids providing excellent lubrication to cartilage surfaces. Here, we report the design and characterization of a multiblock bottle-brush polymer whose architecture was inspired by lubricin, and we investigate the role of fibronectin (FN), a glycoprotein found in the superficial zone of cartilage, in mediating the structural and tribological properties of the polymer upon shear between mica surfaces. While atomic force microscopy (AFM) imaging revealed a polymer average contour length and diameter of 72 nm and 10 nm, respectively, surface force apparatus (SFA) normal force measurements demonstrated that it was firmly bound to mica (in a brush-like configuration) in the presence of an intermediate layer of FN. Additional SFA lateral forces characterization indicated that FN could extend the wearless friction regime of the polymer up to pressures of 3.4 MPa while ensuring stable friction coefficients ($\mu \approx 0.28$). These results demonstrate synergistic interactions between our lubricin-mimetic and fibronectin in assisting the lubrication and wear protection of ideal (mica) substrates upon shearing. Collectively, these findings also suggest that our proposed lubricin-mimetic might be a promising

[4] This chapter has been published: Andresen Eguiluz, RC*; Cook, SG*; Tan, M; Brown, CN; Pacifici, NJ; Samak, MS; Bonassar, LJ; Putnam, D; Gourdon, D. "Synergistic Interactions of a Synthetic Lubricin-Mimetic with Fibronectin for Enhanced Wear Protection". *Frontiers in Bioengineering and Biotechnology.* 2017
*Equally contributing authors

affordable alternative to lubricin, as similar mechanisms could potentially also facilitate the interaction between the polymer and cartilage surfaces in articular joints and prosthetic implants in vivo.

Introduction

Successful biomimetic lubricants should prevent wear and reduce friction between contacting surfaces when subjected to (i) high loading pressures, (ii) a wide range of sliding speeds, and (iii) large shearing distances (with respect to the contact area between surfaces): conditions that are all found in synovial joints. Another notable characteristic of synovial joints is their ability to rapidly switch between biolubrication modes, which include boundary and elasto-hydrodynamic lubrication mechanisms.[1–3] Nature has developed a solution to overcome fast changing sliding speeds with efficient lubrication, anti-adhesion, and robust wear protection: a mucinous glycoprotein known as lubricin (LUB). It is found in mammalian synovial fluids,[4,5] and is reported to be a key contributor to the exceptional tribological properties of synovial joints, not only in reducing the friction between cartilage surfaces, but also in protecting them against potential damage during shear.[6] Cartilage-bound lubricin sheared against glass exhibits very low friction coefficients ($\mu = 0.1$) in boundary lubrication mode, the lubrication mode investigated in this report.[7] This remarkable lubrication is believed to arise from the bottle-brush structure of LUB combined with its ability to self-associate into dimers or multimers that anchor robustly to the cartilage surface.[8] LUB has been reported to bind to cartilage through its carboxyl-terminus,[7] building a brush-like layer of dimers forming an arc-like (loop) architecture.[9–11] Importantly, LUB is able to bind to various extracellular matrix components, including collagen[12] (COL), hyaluronan[13] (HA), though its highest affinity is for fibronectin[14] (FN), a prominent glycoprotein found in the superficial zone of cartilage,[15] *that is,* at the interface between cartilage and synovial fluid.

Inspired by natural lubricants with bottle-brush architecture, various mimetic analogues have been explored.[16–23] Overall, these studies suggest that bottle-brush architecture provides efficient lubrication in aqueous environments because it prevents interdigitation between brushes bound to opposing surfaces. Both the steric repulsion between protruding molecular chains and the presence of a hydration layer likely contribute to the swelling and stretching of the brushes, which then provide low friction. However, the inability of brushes to efficiently lubricate junctions under high pressures[24,25] suggests that hydration itself is insufficient to guarantee good lubrication and that the polymers must also be strongly anchored to the surfaces either via their central backbone[16,18] or via their terminal moieties.[21] Strong attachment can be achieved by covalent bonding[18] or by electrostatic interactions.[21,26] In the particular case of bottle-brush copolymers decorated with poly(ethylene glycol) (PEG) side chains, both grafting density[19] and length of side chains[16] in the interfacial regions were also shown to be key mediators of lubrication, and friction coefficients as low as $\mu = 0.06$ were reported.[25] Yet, despite these low friction coefficients, PEG-based brushes have not been commonly utilized as water-based lubricants but rather as protective and/or anti-fouling coatings.[27–29]

While the interactions of LUB with COL[12] and HA[13,30,31] have been widely investigated, the role of FN in enhancing LUB-mediated low friction and wear protection at the superficial zone of cartilage has only recently been proposed.[11] In this study, we report the design of a LUB-inspired bottle-brush polymer (mimLUB) and we combine AFM and SFA characterization to assess both structural and tribological properties (adhesion, friction, and wear) of the polymer upon shearing between model

(mica) surfaces in presence/absence of FN. MimLUB consists of a long and flexible poly(acrylic acid) (pAA) backbone grafted with PEG side chains. It possesses a thiol terminus on one end to mimic the LUB carboxyl-terminus tethering moiety while the other end is not functionalized. Our choice of pAA and PEG polymers is predominantly based on the excellent biocompatibility reported for those two polymers.[32] To assess the tribological properties of mimLUB and determine the role of FN in mediating these properties, we sheared mimLUB between either bare or FN-coated mica surfaces. Our main findings indicate that the presence of FN strengthens the binding of mimLUB to mica surfaces, which significantly extends its wearless friction regime up to physiologically relevant pressures, while maintaining friction coefficients similar to those measured across native lubricin under identical experimental conditions.[11] Collectively, our findings suggest that, when combined to FN, our proposed lubricin-mimetic provides enhanced wear protection and might be a promising affordable alternative to lubricin in articular joints and prosthetic implants in vivo.

Materials and Methods

Synthesis of mimLUB

Acrylic acid (AA, 99.5%) stabilized with 200 ppm 4-methoxyphenol, methanol (99.8%) and sodium borate buffer were obtained from VWR (Radnor, PA, USA). 4,4'-azobis-(4-cyanopentanoic acid) (A-CPA) and 4-cyano-4-(phenylcarbonothioylthio)pentanoic acid (CPA-DB) (>97% HPLC) was obtained from Sigma-Aldrich (St. Louis, MO, USA). Methoxy-poly(ethylene glycol)-amine powder

(PEG-NH_2) was obtained from Jenkem Technologies (Beijing, PRC) and 4-(4,6-dimethoxy-1,3,5-triazin-2-yl)-4-methylmorpholinium chloride (DMTMM) was obtained from TCI America (Portland, OR, USA). All chemicals were used as received unless otherwise specified.

Synthesis and characterization of poly(acrylic acid) backbone (pAA)

Synthesis: Poly(acrylic acid) was synthesized by RAFT polymerization using acrylic acid (AA), A-CPA as initiator (I) and CPA-DB as chain transfer agent (CTA) under anhydrous, airtight and dark conditions in methanol. AA concentration was maintained at ~3.8 mM, while [AA]:[I]:[CTA] was 762:0.25:1. The general reaction scheme is as follows: AA was added to a flame dried 5 ml brown ampule with one magnetic stir bar, to which CPA-DB dissolved in 2.9 ml of nitrogen-purged methanol was added, followed by A-CPA dissolved in 0.7 ml of nitrogen-purged methanol. Nitrogen gas was bubbled through the reaction mixture after addition of each reagent for several minutes to prevent oxygen gas influx. After the last nitrogen purge the reaction ampule was flame sealed, placed in a 60 ^{o}C oil bath to initiate polymerization, and allowed to stir for 48 hours. Upon reaction completion the ampule neck was broken to expose the reactants to air and the reaction was cooled in ice to stop the polymerization. The solution was diluted with water, dialyzed against deionized water for 3 days, and then lyophilized to obtain a white, waxy powder.

Characterization: Poly(acrylic acid) was dissolved in D_2O and characterized using ^{1}H NMR (INOVA 400 MHz). The methylene and methine chemical shifts are at

1.5-2 and 2.25-2.75 ppm respectively. Molecular weight was determined by Waters gel permeation chromatography (GPC) system (Waters 1515 Isocratic HPLC Pump, Waters 2414 Refractive Index Detector) using poly(methacrylic acid) standards and phosphate buffered saline (pH 7.4) as the mobile phase at 30 ^{o}C.

Synthesis of the pAA-g-PEG bottle-brush polymer

The pAA-*graft*-PEG (pAA-*g*-PEG) copolymer was synthesized by polymer analogous conjugation of monoamine-functionalized PEG to the pAA backbone using DMTMM as the coupling agent. pAA was dissolved in 0.1 M borate buffer (pH 8.5) at 3.3 mg/ml, with reactant mole ratios of [AA]:[DMTMM]:[PEG] set at 1:2:2. The general reaction is as follows: pAA (M_w 60,000) and M_n PEG-amine (M_w 2000) were dissolved in 3 ml borate buffer in a 10 ml flask with magnetic stir bar. DMTMM was dissolved in 0.6 ml borate buffer and added drop-wise into the reaction flask with the final pH adjusted to 6-7 using 1 M HCl. The conjugation reaction was conducted for 24 hours at room temperature, dialyzed against deionized water for 3 days and lyophilized to obtain a white powder. The tail end of pAA has a thiolcarbionylthio group that is cleaved during the PEG conjugation step exposing a free thiol group. The assigned nomenclature for the polymer brushes are given as pAA(*a*)-*g*-PEG(*b*), where *a* and *b* are molecular weights of pAA and PEG respectively, and *g* is the grafting ratio defined by the moles of PEG over the moles of AA monomers in the pAA backbone used during the reaction. pAA(60)-2-PEG(2) and PEG calibrations standards were sent to the Biophysics Resource of Keck Laboratory at the Yale School of Medicine to be

analyzed by the DAWN Helios multi-angle laser light scattering size exclusion chromatography system (MALLS/SEC). A Superpose 6 column was used to fractionate the samples at ambient temperatures. pAA(60)-2-PEG(2) was dissolved at 3mg/ml in phosphate buffered saline (PBS) solution containing 120 mM NaCl, 10 mM phosphate salt, and 2.7 mM KCl (pH 7.4), and sonicated for 15 minutes before injection into the SEC using a dn/dc value of 0.135 ml/g. COOH groups on pAA are the potential conjugation sites for PEG. With this premise, the percent conjugation of PEG onto pAA was calculated from the molecular weight (Mw) of pAA(60)-2-PEG(2).

Preparation of mimLub and FN solutions

The synthesis of our LUB-inspired synthetic polymer mimLUB has been recently described in detail by our collaborators.[22] The polymer, with average molecular weight of 1400 kDa, was dissolved in PBS (PBS from EMD, Billerica, USA) with a final concentration of 3 mg/ml. The solution was sonicated for 30 minutes using 18 MΩ Milli-Q water (Millipore Corporation, Billerica, MA, USA) to completely dissolve the mimLUB. A FN solution of 1 mg/ml in PBS was purchased from Sigma-Aldrich (St. Louis, Missouri, USA). Low concentration FN aliquots at 0.3 mg/ml in PBS were prepared and stored at -80 ^{o}C, and thawed when needed. All glassware used in the preparation was cleaned with ethanol and rinsed with DI.

Atomic force microscopy (AFM)

Atomic force microscopy (AFM) measurements were performed in air using a commercial AFM (MFP-3D, Asylum, Sta. Barbara, CA, USA) to assess the nanostructure of mimLUB adsorbed onto mica. Conical SiO_2 probes with nominal radius of curvature of 9 nm mounted on compliant (k = 42 N/m) levers (AC160TS, Olympus, USA) were used for intermittent contact mode imaging. Images were taken over a range of 500 x 500 nm, at a frequency of 1 Hz and 1536 x 1536 pixels for maximal resolution. Image analysis was performed in Gwyddion (Czech Metrology Institute) and ImageJ (NIH). AFM samples consisted of freshly cleaved mica substrates, spin-coated at 2000 rpm for one minute with 100 µl of a dilute mimLub solution in DI water (0.3 mg/ml) and left 4-5 hours for complete drying.

Surface forces apparatus (SFA)

Normal and friction forces between two mimLUB-coated mica surfaces were measured using the surface forces apparatus (SFA) Mark III (SurForce, LLC, Sta. Barbara, CA, USA) using well-established procedures.[33] Briefly, two freshly cleaved back-silvered mica sections (S&J Trading, Glen Oaks, NY, USA) were glued onto semi-cylindrical silica discs (R ≈ 1 cm) with UV curing glue (Norland 61, Cranbury, NJ, USA). The discs were mounted in a cross-cylindrical configuration and the absolute separation distance between them, *D*, was measured in real time by multiple beam interferometry (MBI). Additionally, MBI was used to monitor the onset of damage of the shearing surfaces: both shape and intensity of interference fringes were used as

indicators of shape (and size) of the contacting junction and presence of shear-induced wear debris.[11,34,35] Before functionalizing the mica surfaces with either mimLUB or FN+mimLUB, mica-mica contact in air was measured to determine the reference distance, $D = 0$. To quantify normal forces, the lower surface was mounted onto a compliant horizontal double cantilever spring ($k_{\perp}$ = 590 N/m) and displaced at a constant approach speed of circa 5 nm/s. For tribological characterization requiring higher applied pressures, the lower surface was mounted onto a stiffer horizontal spring ($k_{\perp}$ = 1650 N/m), whereas the upper surface was mounted onto a vertical double cantilever spring ($k_{\parallel}$ = 700 N/m) holding strain gauges to measure friction forces. Shearing was achieved via a ceramic bimorph slider, and shearing velocities of $V \approx 0.3$ µm/s, 3 µm/s, and 30 µm/s were used in our experiments, corresponding to the range of boundary lubrication modes present during physical activity such as walking. MBI fringes of equal chromatic order were collected using a SP2300 photospectrometer (Princeton Instruments, NJ, USA) with a 600 g/mm grating and 500 nm blaze, digitalized with a ProEM CCD camera (Princeton Instruments, NJ, USA), and visualized using Lightfield v4.0 (Princeton Instruments, NJ, USA). Friction forces were acquired and quantified with a NI USB-6210 and LabView v8.6 (National Instruments, Austin, TX, USA), respectively.

Surface functionalization with mimLUB

Two protocols were carried out for surface functionalization: mimLUB was adsorbed either (i) directly onto bare mica or (ii) onto mica previously coated with FN.

For protocol (i), freshly prepared mica surfaces were incubated with 50 µl mimLUB solutions at 3 mg/ml in PBS for one hour and rinsed with PBS. For protocol (ii), freshly prepared mica surfaces were first incubated with 50 µl of FN solution (0.3 mg/ml in PBS) for one hour and rinsed with PBS. 50 µl of bovine serum albumin (BSA) at 0.02 mg/ml in PBS were then added for 30 minutes to block non-specific interactions, and rinsed with PBS. Finally, these FN-bound mica surfaces were incubated with 50 µl mLUB solutions at 3 mg/ml in PBS for one hour and rinsed with PBS. In addition, we used two different experimental conditions: surfaces were sheared either in PBS or in mimLUB (3 mg/ml) solution. All surface functionalization steps were carried out by injecting liquid drops between mica surfaces that were previously mounted in the SFA chamber to ensure similar protein adsorption on both upper and lower surfaces. All steps were performed in a laminar flow cabinet to prevent particle contamination.

Results

Molecular design and characterization of mimLUB

We designed a pAA-g-PEG based lubricin-mimetic polymer, named mimLUB, as depicted in Figure 3.1A. It possesses a long region with bottle-brush architecture composed of a flexible pAA backbone decorated with PEG side-chains. To determine the dimensions of single molecules, we spin-coated freshly cleaved mica surfaces with low concentrations of mimLUB solutions (0.3 mg/ml in DI) and imaged individual polymer chains in air (intermittent contact) using atomic force microscopy (AFM). As shown in Figure 3.1B, the molecules exhibit worm-like morphology; their average

contour length l_N and average diameter d_N were 72 ± 18 nm and 10 ± 2.6 nm, respectively (frequency histograms for l_N and d_N are displayed in Figure 3.1C). The hydrodynamic diameter, D_H, quantified in solution via dynamic light scattering, was D_H = 46 nm. All molecular dimensions are summarized in Figure 3.1D. Additionally, the percent conjugation calculated from the molecular weight (M_W) was 83%, the measured polydispersity index PDI obtained from GPC-MALLS was M_w/M_n=1.3, and M_w was 1400 kDa.

We next investigated the effects of mimLUB concentration and incubation conditions on the resulting polymeric network architecture and surface coverage. Three different concentrations (3 mg/ml, 1 mg/ml, and 0.3 mg/ml) and two different incubation protocols were tested: (i) spin coating of mimLUB solutions (2000 rpm) or (ii) incubation of mimLUB solutions for 30 min followed by thorough rinsing with deionized water, both onto freshly cleaved mica substrates. Our AFM imaging indicates that all spin-coated conditions (Figure 3.2, top panels) resulted in a uniform network of densely packed mimLUB molecules, with substrate coverage increasing with increasing concentration. In contrast, incubated mimLUB samples (Figure 3.2, bottom panels) displayed uniformly distributed agglomerates of varied height, with distance between aggregates decreasing with increasing concentration (Figure 3.2, bottom panels). Overall, these results show the mimLUB's capability of self-aggregating and forming various network architectures at surfaces.

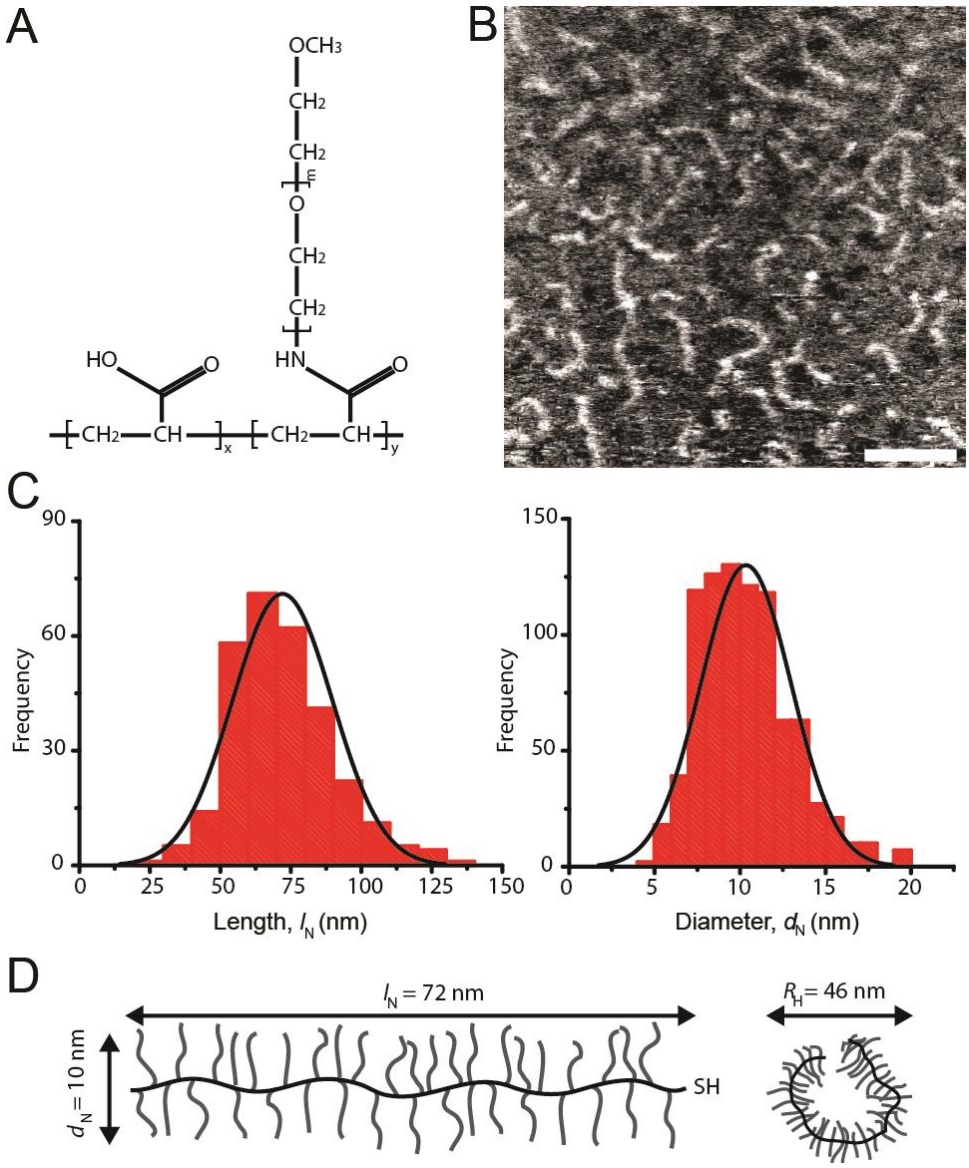

Figure 3.1: **Architecture and dimensions of lubricin-mimetic mimLUB**. (A) Structure of the pAA-g-PEG bottle-brush polymer mimLUB. In our study, x ≈ 185, y ≈ 650, m ≈ 45, and M_W ≈ 1400 kDa. (B) AFM height micrograph of mimLUB chains spin-coated onto freshly cleaved mica, scale bar = 50 nm. (C) Number-average contour length l_N and number-average molecular diameter d_N. (D) Schematic representations of mimLUB with l_N, d_N, and D_H.

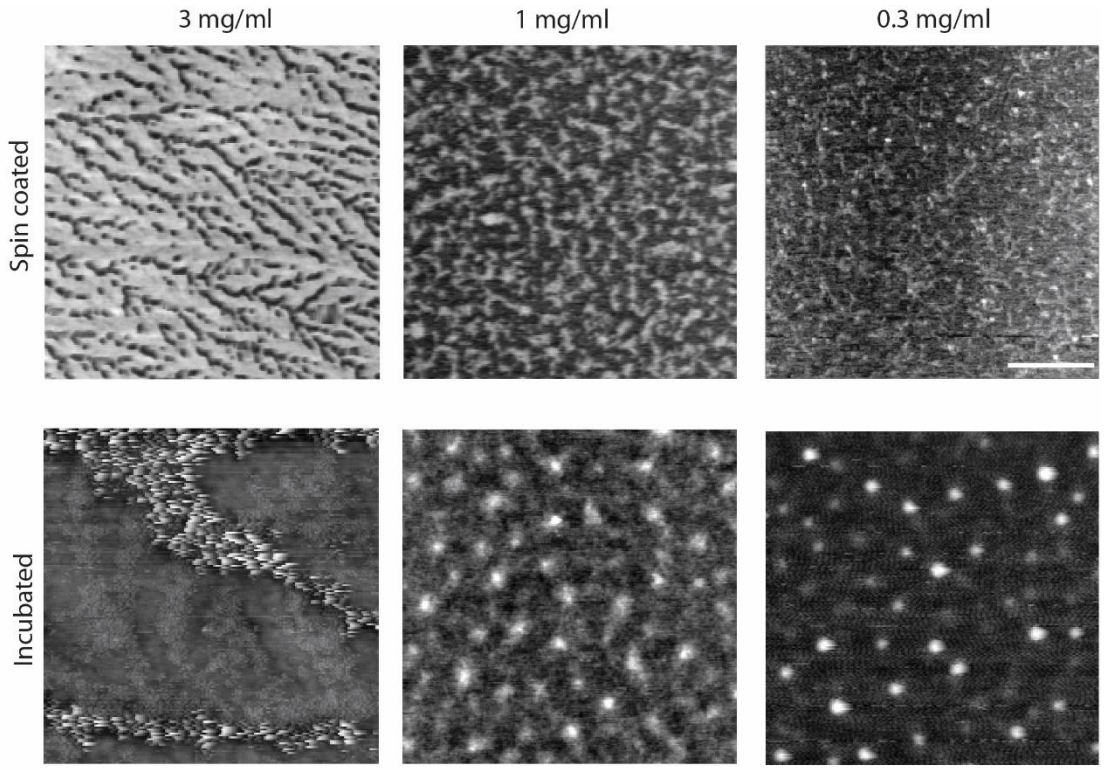

Figure 3.2: **Effect of concentration and incubation protocol on mimLUB network formation.** (Top panels) AFM height micrograph of spin-coated mimLUB indicates the presence of a polymeric network at all concentrations, with coverage that decreases with decreasing concentration, suggesting that mimLUB molecules agglomerate and entangle. (Bottom panels) Incubated samples form polymer agglomerates of varied dimensions. Scale bar = 500 nm.

Role of FN in mediating normal interactions between mimLUB-coated mica surfaces

To determine whether the presence of FN affects the normal interactions between mimLUB brushes, we first used the SFA to perform compressive measurements of mimLUB-coated mica surfaces in presence or absence of an underlying FN layer in PBS at 25 ºC. Figure 3.3A shows the normal interaction forces, reported as $F_{\perp}/R$, $F_{\perp}$ being the normal force and *R* the surface radius of curvature,

between (i) mimLUB films directly adsorbed onto mica surfaces and (ii) mimLUB films adsorbed onto mica previously coated with FN. Interactions measured across FN films alone are also displayed for comparison. Data were fitted with the Alexandre-de Gennes model (AdG), which usually describes the normal interactions between surfaces holding neutral polymer brushes:[36]

$$\frac{F_{\perp}(D)}{R} = \frac{16\pi kTL}{35s^3}\left[7\left(\frac{2L}{D}\right)^{5/4} + 5\left(\frac{D}{2L}\right)^{7/4} - 12\right] \qquad \text{(Eq. 1)}$$

where k is the Boltzmann constant, T is temperature, and L and s are the relaxed brush length and average grafting spacing, respectively, used as fitting parameters for the model. The use of the AdG model to describe the behavior of charged mimLUB chains is justified by the high salinity of the surrounding medium (PBS, 150 mM). Although mimLUB is a polyelectrolyte, the numerous counterions in PBS are expected to screen most of the electrostatic interactions between chains so that mimLUB can be treated as a neutral bottle-brush polymer. We identified both long-ranged (LR) and short-ranged (SR) brush regimes in our mimLUB+FN data. Importantly, by using the AdG model to describe FN (alone), we do not intend to imply that FN layers also possess a well-defined brush structure. Rather, the close agreement between our data and the AdG theory suggests that FN films adsorbed onto mica in PBS can be described as a repulsive "effective brush" layer. In all our measurements, the interactions were reversible: normal forces were purely repulsive, namely, no measurable adhesion and no hysteresis between approach and retraction were observed (data not shown). In absence of FN (mimLUB), a single regime was detected with interaction forces starting at ≈40 nm (corresponding to $2L_{LR}$). In contrast, two regimes were observed in presence of FN

(FN+mimLUB), with long-range interactions starting at ≈ 500 nm ($2L_{LR}$) followed by short-range interactions at ≈ 250 nm ($2L_{SR}$). The existence of two regimes could be explained by a change in conformation of mimLUB, transitioning from a relaxed (collapsed) configuration to a vertical (upright) configuration, in which PEG side brushes contribute to the steric-entropic repulsion. These results are summarized in Figure 3.3A. Average values of onset of interactions, i.e., unperturbed film thicknesses (D_0) are displayed in Figure 3.3B and indicate that FN+mimLUB films are significantly thicker not only than mimLUB or FN films alone but also than the sum of both of them. Average "hardwall" values (*HW*), indicative of film thicknesses under maximum applied load, are shown in Figure 3.3C and confirm that the FN+mimLUB film is thicker than the mimLUB film alone, even under high load. Furthermore, the sum of the HW values of FN alone added to the diameter of mimLUB equal the HW value of FN+mimLUB film, suggesting that upon compression, mimLUB is lying flat against the FN layer. Collectively, our results indicate that FN is able to tether mimLUB to mica in an upright (brush-like) configuration when no compressive load is applied, and that FN-mimLUB interactions are strong enough to retain mimLUB and prevent it from being expelled from the junction when the brush is under compression.

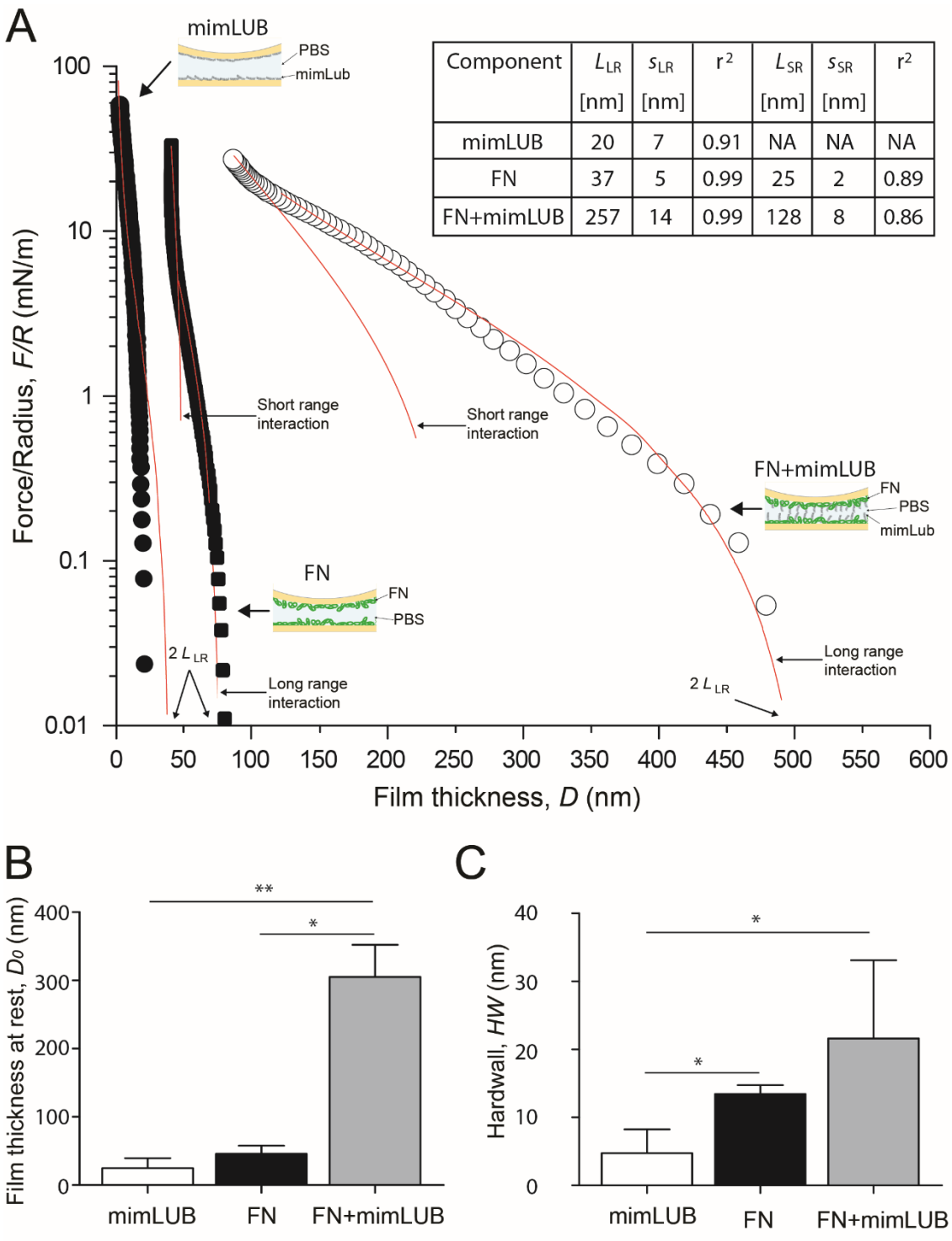

Figure 3.3: **Role of FN in normal interactions between mimLUB-coated surfaces.** (A) Normal force $F_{\perp}$ normalized by the surface radius of curvature *R* between two mica surfaces coated with a mimLUB layer (black circles), coated with a FN layer (black

squares), and coated with a FN+mimLUB layer (gray circles) as a function of total film thickness, *D*. Forces are measured upon approach at a constant velocity of 5 nm/s. (B) Bar charts of average film thicknesses at rest, D_0 and (C) average 'hardwall' thicknesses, *HW* for mimLUB (black), FN (gray), and FN+mimLUB (white) films. Values reported as mean + standard deviation. In all cases, $p < 0.05$ is indicated by a single star and $p < 0.01$ by two stars. All data were fitted using the AdG model (Eq. 1).

Role of FN in mediating lubrication between mimLUB-coated mica surfaces

As FN controls both tethering strength and configuration of mimLUB at the mica surface, we next investigated its role in lubrication and wear protection of mimLUB-coated surfaces upon shearing. This time, the SFA was used to apply shear and measure both the friction forces and the onset of damage between mimLUB-coated mica surfaces in presence or absence of underlying FN. All systems were sheared either in PBS or in dilute mimLUB medium, at 25ºC. Figure 3.4 summarizes the evolution of the interference fringes pattern recorded over a full shearing experiment, from the onset of surface interaction (Figure 3.4A) to the surface flattening observed upon increasing load (Figure 3.4B), which is indicated by a change in shape (flattening) of the fringes, ending in local surface damage when no FN is present at the surface (yellow arrow in Figure 3.4C). At high loads, the contact area, *A*, was directly measured from the fringes' flat region, and the average pressure across the compressed films was calculated as:

$$P = \frac{F_{High}}{A} \qquad \text{(Eq. 2)}$$

where F_{High} is the normal force at high loads, and A is the contact area of the compressed junction. At low load, as surface did not clearly deform (Figure 3.4A), contact pressures, $P(F_{Low})$, were evaluated from:

$$P(F_{Low}) = P(F_{High}) * \left(\frac{F_{Low}}{F_{High}}\right)^{1/3} \quad \text{(Eq. 3)}$$

where F_{Low} is the normal force at low loads.

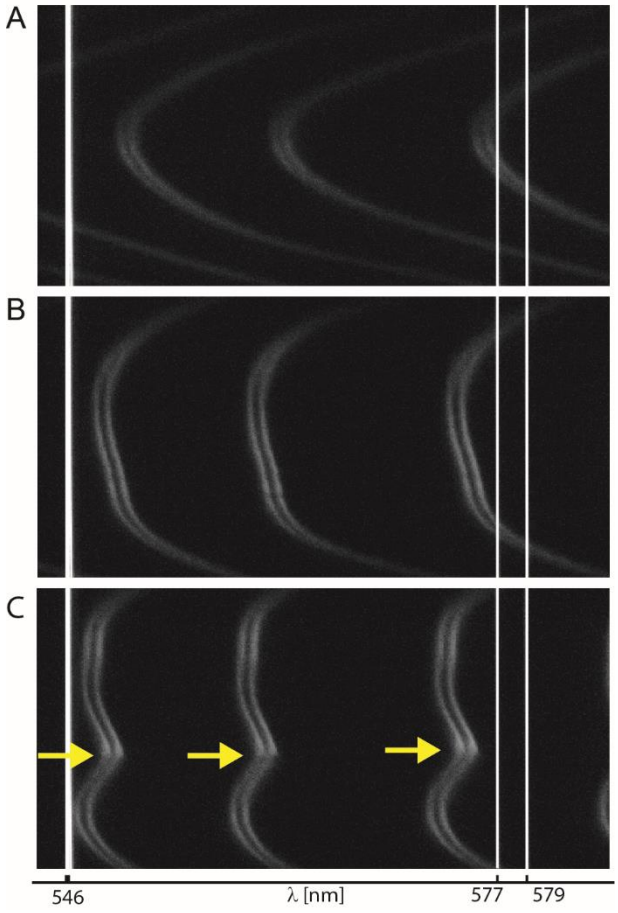

Figure 3.4: Interferometry for monitoring surface damage during shear. Representative interference fringes recorded during surface forces apparatus shearing measurements, as visualized (A) at onset of interaction, (B) at large normal loads deforming contact junction, and (C) at onset of damage, indicated by yellow arrows. Fringes shape and shift (relative to initial mica-mica contact without film, not shown

here) allowed us to monitor surface damage as well as film thickness and size of wear debris.

Figure 3.5 shows the friction force $F_{\parallel}$ as a function of normal force $F_{\perp}$ measured between mimLUB-coated surfaces, in presence or absence of FN coating, when sheared across PBS. Without FN (Figure 3.5A), open symbols, i.e., friction data signaling the presence of wear, indicate that damage between surface occurred almost immediately after shear started, regardless of shearing velocity. Damage was assessed through the irreversible deformation and non-continuous intensity of consecutive (odd and even) interference fringes[11] (representative fringes are shown in Figure 3.4), which further suggests that both the mimLUB film and the underlying mica were affected simultaneously. The resulting damage-associated friction forces $F_{\parallel}$ were nearly independent of shearing velocities and proportional to applied normal load, vanishing at $F_{\perp} = 0$. The average friction coefficient, defined as $\mu = \Delta F_{\parallel}/\Delta F_{\perp}$, was equal to 0.29 ± 0.015. Wear debris were noticed at extremely low loads ($F_{\perp} < 1.5$ mN, equivalent to P = 3 MPa and 1.7 MPa), at low and intermediate speeds, but not at high speeds. These high pressures occurring at low loads are due to the small contact areas encountered during the loading steps.

In contrast, the (higher) friction forces measured in the presence of FN (Figure 3.5B) were sensitive to shearing velocity, did not depend linearly on the applied load $F_{\perp}$, and did not vanish at $F_{\perp} = 0$, particularly at the lowest sliding speed (0.3 μm/s). Interestingly, wearless friction was sustainable up to circa 4 mN (for all speeds), and

damage was triggered only at loads of 3.6 mN and 5 mN (corresponding to pressures of 3 MPa and 1.8 MPa, within the physiological range[37]) at speeds of V = 3 µm/s and 30 µm/s, respectively. However, at low shearing velocities, normal applied loads did not reach high enough values to trigger damage. Overall, our results indicate that FN delays the onset of wear, likely by providing stronger anchorage of the mimLUB molecules to the substrate, which permits shear-induced re-orientation of the film and limited interdigitation upon shearing (as detailed in the Discussion).

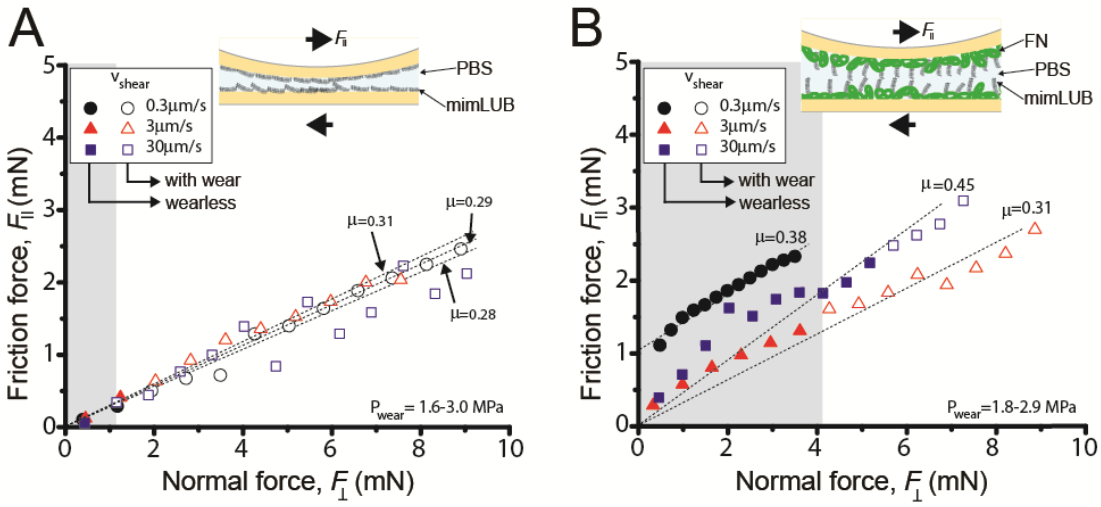

Figure 3.5: **Role of FN in friction and wear of sheared mimLUB-coated surfaces across PBS.** Friction force $F_{\parallel}$ as a function of normal force $F_{\perp}$ measured across PBS between (A) mica surfaces incubated with mimLUB and (B) FN-coated mica surfaces incubated with mimLUB .The surfaces were sheared in PBS at sliding velocities of V = 0.3 µm/s (black circles), V = 3 µm/s (red triangles), and V = 30 µm/s (blue squares). Open symbols indicate measurements after the occurrence of damage in the sheared junction. Gray backgrounds indicate wearless friction regimes.

To better mimic joint lubrication conditions, we next sheared the mimLUB-coated surfaces across a mimLUB solution (Figure 3.6). Here again, the tribological properties of the mimLUB, in particular its resistance to damage, were found to be enhanced in the presence of FN. All friction forces were proportional to applied normal loads and vanished at $F_{\perp} = 0$ but, contrarily to what was observed in PBS, the friction coefficients depended on sliding speed. Figure 3.6A shows that, without FN, systematic surface damage occurred at extremely low loads ($F_{\perp} < 1.5$ mN, equivalent to 1.6 – 2.5 MPa) regardless of sliding conditions. However, damage-associated friction coefficients increased with increasing shearing velocity. In contrast, the presence of FN drastically extended wearless friction and postponed surface damage, which was triggered only at loads $F_{\perp} > 4.5$ mN (and large contact areas), that is, under pressures above 3.4 MPa, 2.4 MPa, and 1 MPa (Figure 3.6B), for slow, intermediate, and fast shearing velocities, respectively. Overall, the presence of mimLUB in the medium (instead of PBS) provides a modest enhancement in the wear protection of the shearing surfaces suggesting that surface-bound mimLUB molecules (rather than free-floating mimLUB molecules from medium) are likely responsible for enhanced lubrication and resistance to damage of the sheared surfaces.

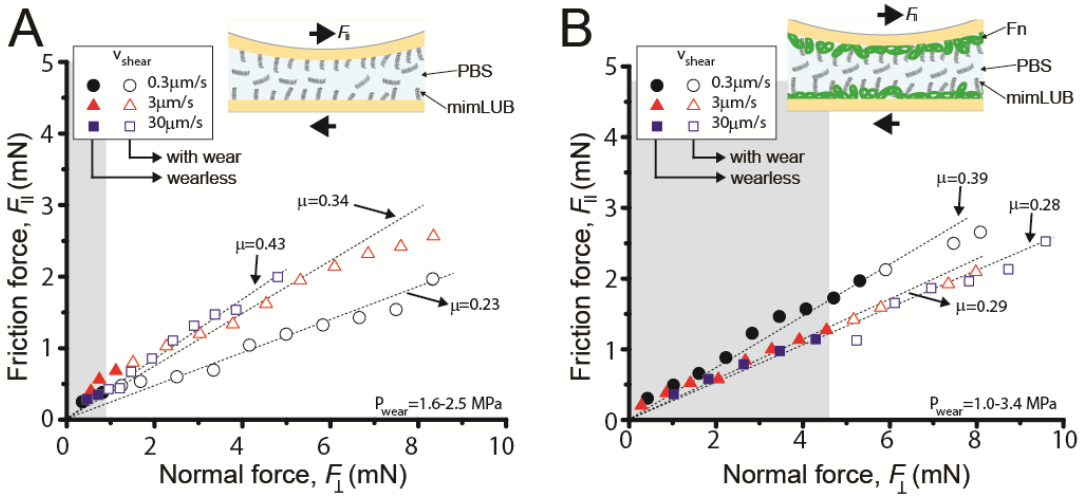

Figure 3.6: Role of FN in friction and wear of sheared mimLUB-coated surfaces across a mimLUB solution. Friction force $F_{\parallel}$ as a function of normal force $F_{\perp}$ measured across mimLUB solution (3mg/ml) between (A) mica surfaces coated with mimLUB and (B) mica surfaces coated with FN+mimLUB). The surfaces were sheared at sliding velocities of V = 0.3 μm/s (black circles), V = 3 μm/s (red triangles), and V = 30 μm/s (blue squares). Open symbols indicate measurements after the surfaces became damaged (with wear). Gray backgrounds indicate wearless friction regimes.

Table 1. Summary of reported pressures. Pressure at onset of interaction (P_{onset}), maximum pressures reached at each condition (P_{max}), and pressures at onset of wear (P_{wear}) measured in our study. Values reported in literature for native LUB are shown for comparison.

Condition	V = 0.3 μm/s			V = 3 μm/s			V = 3 μm/s		
	P_{onset} (MPa)	P_{max} (MPa)	P_{wear} (MPa)	P_{onset} (MPa)	P_{max} (MPa)	P_{wear} (MPa)	P_{onset} (MPa)	P_{max} (MPa)	P_{wear} (MPa)
mimLUB in PBS	1.80	5.08	3.06	1.02	2.85	1.68	1.17	1.62	3.22

mimLUB in mimLUB Solution	1.08	3.09	1.64	1.84	4.54	2.57	1.34	2.33	1.86
FN+mimLUB in PBS	0.414	0.8		1.82	3.78	2.96	0.635	2.2	1.85
FN+mimLUB in mimLUB	1.41	3.78	3.40	0.917	2.80	2.42	0.613	1.38	1.06
LUB[a]						0.4*			
FN+LUB[b]		4			4.5			14	

[a] From ref. [9]. [b] From ref. [11], * at 1 □m/s.

Discussion

This study aimed at characterizing the molecular structure and tribological performance of a lubricin-mimetic pAA-*g*-PEG copolymer (mimLUB) when bound and sheared between model (mica) surfaces. Particular emphasis was placed on the role of FN (present in the superficial zone of cartilage) in mediating the polymer friction/lubrication and ability to protect surfaces against wear during shear.

Overall, our main findings show that FN plays a key role in mediating the lubrication and surface protection of mimLUB-coated model (mica) surfaces during shear. Our normal force characterization combined with AdG theory (Figure 3.3) indicates that FN promotes strong attachment and dense packing of mimLUB onto mica,

which is associated with an upright configuration of the copolymer at the mica surface, as suggested by the long-range reversible brush-mediated repulsive interactions measured upon high surface compression. Additionally, our friction data (Figures 3.5 and 3.6) imply that FN and mimLUB act synergistically to extend wearless friction up to higher pressures (providing improved protection of surfaces upon shear) with respect to mimLUB alone, which weakly binds to surfaces and causes rapid damage as it is easily squeezed out of the shearing junction. Altogether, these findings convey insights not only into the general lubrication mechanisms of synergistic multi-components systems but also into the specific interactions our biomimetic polymer could potentially have with cartilage tissue through the FN layer present into its superficial zone.

Detailed structural imaging via AFM in air revealed that mimLUB molecules possess a worm-like structure (Figure 3.1), similar to what was reported for native LUB.[9] This worm-like structure likely provides flexibility to the polymer when grafted onto mica in high ionic strength solutions, facilitating exposure of its hydrated PEG side chains at the shearing interface to prevent (or at least delay) the interdigitation of opposing brushes. When the sample is incubated at high concentrations, mimLUB forms a layer of evenly distributed agglomerates, as shown in Figure 3.2, providing full surface coverage. Our mimLUB polymer has only one binding domain (thiol moiety), which mimics the hemopexin-like domain located at the C-terminus of native LUB.[7] However, it lacks the heparin and somatomedin-like domains that LUB utilizes for self-aggregation.[7] The mimLUB chains are therefore not capable of self-associating into dimers to form loop-like conformations at the mica surface, as does native LUB.[11] Additionally, mimLUB's contour length is approximately half of that of native LUB.[9]

Collectively, these structural differences between native and mimetic LUB are likely responsible for distinctive binding and assembly mechanisms at the mica surface, which will also cause them to have different tribological properties. Nevertheless, the simplicity of the design of our mimLUB and the high control (pressure, temperature, shear velocity and sheared distance, surface roughness, film thickness, wear debris detection) achieved in our shearing model system allowed us to unravel the role of FN in mediating the resistance to damage of mimLUB-coated surfaces during shear, as schematically summarized in Figure 3.7.

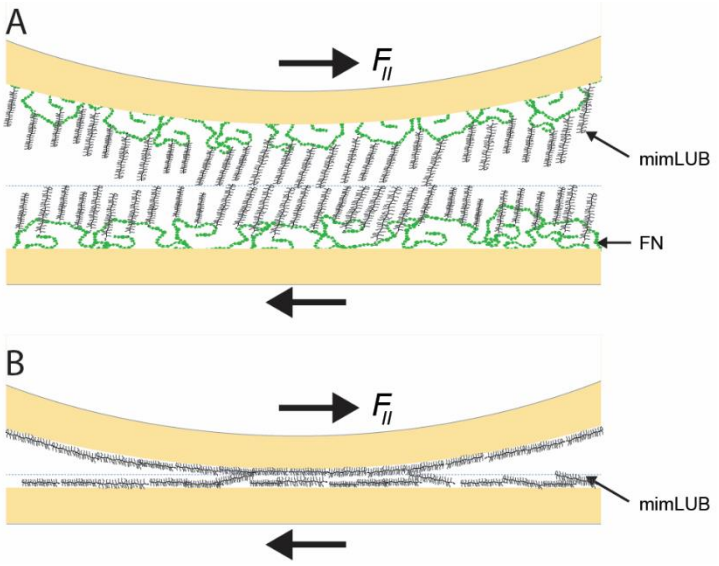

Figure 3.7: Schematics indicating the proposed mimLUB configurations (A) with FN and (B) without underlying FN film.

The fit of our normal forces data using the AdG model (Figure 3.3A) reveals additional interesting molecular details. Analysis of mimLUB alone indicates that the polymer chains are most likely lying down at the mica surface. Although the brush length extracted from the AdG fit is 20 nm, i.e., twice as large as the average molecular

diameter, the raw (unfitted) data shows an onset of repulsion at circa 10 nm, which corresponds to one molecular diameter on each mica surface. In contrast, when mimLUB was incubated onto FN-coated mica, it self-assembled in a densely packed effective brush-like film, as suggested by a brush length of circa 260 nm (long-range interaction) and a grafting spacing of 14 nm. An effective brush length of 260 nm is significantly larger than the combined film thicknesses of mimLUB and FN alone. Such discrepancy could be attributed to the formation of a dense agglomeration of mimLUB (such as those revealed by AFM imaging shown in Figure 3.2) and/or to conformational changes in either FN or mimLUB in the FN+mimLUB film compared to that of FN and mimLUB on bare mica. A grafting spacing of 14 nm is consistent with the average diameter of mimLUB, 10 nm, with an additional 4-nm thick layer of "trapped water" between chains provided by the high hydrophilicity of the PEG side groups, and confirms that the mimLUB polymers adopt an upright conformation on FN prior to pressure or shear application. Under strong compression, the FN+mimLUB system exhibits a second, shorter-range brush behavior, which could be the combination of FN film conformational changes and PEG sidechains interactions with the underlying film while being compressed, *i.e.*, loosing upright configuration.

Surprisingly, the presence of mimLUB in the shearing medium (Figure 3.6) provided only a modest improvement of surface protection against wear with respect to PBS (Figure 3.5) suggesting that surface-bound mimLUB molecules, rather than free-floating mimLUB molecules from medium, are likely responsible for enhanced lubrication and resistance to damage of the sheared surfaces. This finding accentuates the key role of FN in strengthening the anchoring of mimLUB at surfaces during shear.

The intermediate FN layer systematically led to an extension of the wearless friction regime both across PBS (Figure 3.5B) and mimLUB (Figure 3.6B), with increased resistance to surface damage observed up to 5-6 fold more shearing cycles. Despite higher measured friction coefficients (as compared to native LUB), the appearance of wear only at high pressures indicated that mimLUB remained firmly anchored to mica not only under high compression/confinement but also when sheared across large distances (0.7 times the contact area) and over a wide range of velocities. Indeed, the contact pressures we reached here without signs of wear were much higher than those reported for LUB on mica alone[9] (0.4 MPa), and similar to those observed for LUB incubated on FN at low shearing velocities (≈3 MPa).[11] It should be noted that the damage observed when shearing LUB on bare mica[9] was not mica damage, but damage of the LUB film. In this work, however, neither FN+mimLUB film removal nor mica damage was observed at pressures up to 3.4 MPa in specific experimental conditions, which clearly indicates that FN+mimLUB offers better wear protection during shear than native LUB on bare mica and equivalent protection to native LUB on FN-coated mica.

It has been previously reported that strong anchoring of copolymers to shearing surfaces is a key prerequisite for efficient lubrication.[21,26,38–40] Our findings confirm that a boundary lubricant needs to remain tightly bound to surfaces to protect them efficiently, in this case, via FN. Using copolymer brushes, Raviv et al. showed that ultralow friction coefficients could be achieved in synthetic systems.[41] However, the normal forces $F_{\perp}$ and shearing distances Δx investigated in that report were significantly smaller (F_{max}/R < 10 mN/m and Δx = 0.7 μm, respectively)[37] than those explored in our

study (F_{max}/R < 100 mN/m and Δx = 35 μm). Here, we focused on exploring the tribology of *one* mimLUB configuration but is clear that backbone length (pAA molecular weight), side chain length (PEG molecular weight), and grafting distance between PEG side groups are all parameters that can be adjusted to optimize the tribological performance of the synthetic lubricin mimetic. Additionally, the thiol moiety could easily be replaced by a peptide sequence, e.g., a hemopexin-like domain, to attach to underlying substrates. Current work utilizing other copolymer configurations and multiple binding domains that better mimic LUB's tethering to the cartilage tissue surface is in progess in our group.

Finally, it is important to point out that our model system utilizes stiff and nonporous confining surfaces whereas cartilage is compliant and highly porous, which contributes to its capability to carry high loads by distributing pressure to the synovial fluid contained (and circulating) within the pores. This load distribution effectively reduces friction coefficients during locomotion.[42] The use of mica as a model substrate was chosen because it reduces the complexity of the system. As mica is atomically smooth and non-porous, it provides a well-defined model surface ensuring us that all tribological events observed can be attributed to changes in the interfacial polymer caused by phenomena occurring at the junction between surfaces rather than within surfaces.

Conclusions

We report the design and characterization of a synthetic lubricin mimetic (mimLUB) and the role of fibronectin (FN) in mediating the friction and wear between mimLUB-coated mica surfaces upon shear. We found that enhanced surface protection against wear was achieved (up to contact pressures of 3.4MPa) in presence of FN. This effect was attributed to the strong anchoring of mimLUB to mica mediated by FN, which facilitated the formation and retention of a dense (upright) and highly hydrated repulsive brush preventing interdigitation and removal of mimLUB chains when surfaces were sheared, even under high pressures. Our findings provide insights into the (synergistic) lubrication mechanisms of multi-components systems and suggest that our proposed synthetic mimetic could be a potential effective (and affordable) alternative to natural lubricin for the treatment of damaged cartilage surfaces through the FN layer present into its superficial zone.

The functionalization of mimLUB with multiple binding domains to improve its tethering properties to cartilage tissues and prosthetic implants, and the design of other mimetics configurations to yield both enhanced protection and lower friction are currently explored in our group.

REFERENCES

1. Swann, D. a *et al.* Role of hyaluronic acid in joint lubrication. *Ann. Rheum. Dis.* **33**, 318–26 (1974).

2. Roberts, B. J., Unsworth, a & Mian, N. Modes of lubrication in human hip joints. *Ann. Rheum. Dis.* **41**, 217–24 (1982).

3. Jahn, S., Seror, J. & Klein, J. Lubrication of articular cartilage. *Annu. Rev. Biomed. Eng* **18**, 235–258 (2016).

4. Swann, D. a, Slayter, H. S. & Silver, F. H. The molecular structure of lubricating glycoprotein-I, the boundary lubricant for articular cartilage. *J. Biol. Chem.* **256**, 5921–5 (1981).

5. Radin, E. L., Swann, D. A. & Weisser, P. A. Separation of a hyaluronate-free lubricating fraction from synovial fluid. *Nature* **22**, 377–378 (1970).

6. Rhee, D. K. *et al.* The secreted glycoprotein lubricin protects cartilage surfaces and inhibits synovial cell overgrowth. *J. Clin. Invest.* **115**, 622–31 (2005).

7. Jones, A. R. C. *et al.* Binding and localization of recombinant lubricin to articular cartilage surfaces. *J. Orthop. Res.* **25**, 283–292 (2007).

8. Swann, D. A., Silver, F. H., Slayter, H. S., Stafford, W. & Shore, E. The molecular structure and lubricating activity of lubricin isolated from bovine and human synovial fluids. *Biochem. J.* **225**, 195–201 (1985).

9. Zappone, B., Ruths, M., Greene, G. W., Jay, G. D. & Israelachvili, J. N. Adsorption, lubrication, and wear of lubricin on model surfaces: polymer brush-like behavior of a glycoprotein. *Biophys. J.* **92**, 1693–708 (2007).

10. Zappone, B., Greene, G. W., Oroudjev, E., Jay, G. D. & Israelachvili, J. N. Molecular aspects of boundary lubrication by human lubricin: effect of disulfide bonds and enzymatic digestion. *Langmuir* **24**, 1495–1508 (2008).

11. Andresen Eguiluz, R. C. *et al.* Fibronectin mediates enhanced lubrication and wear protection of lubricin. *Biomacromolecules* **16**, 2884–2894 (2015).

12. Chang, D. P., Guilak, F., Jay, G. D. & Zauscher, S. Interaction of lubricin with type II collagen surfaces: Adsorption, friction, and normal forces. *J. Biomech.* **47**, 1–8 (2014).

13. Das, S. *et al.* Synergistic interactions between grafted hyaluronic acid and lubricin provide enhanced wear protection and lubrication. *Biomacromolecules* **14**, 1669–1677 (2013).

14. Elsaid, K. A., Chichester, C. O. & Jay, G. D. Lubricin purified from bovine synovial fluid and from articular cartilage exhibit similar binding affinities to cartilage matrix proteins. *Trans. Orthop. Res. Soc.* **32**, 551 (2007).

15. Balazs, E. The role of hyaluronan in the structure and function of the biomatrix of connective tissues. *Struct. Chem.* **20**, 233–243 (2009).

16. Pettersson, T., Naderi, A., Makuska, R. & Claesson, P. M. Lubrication properties of bottle-brush polyelectrolytes: an AFM study on the effect of side chain and charge density. *Langmuir* **24**, 3336–47 (2008).

17. Krivorotova, T., Makuska, R., Naderi, a., Claesson, P. M. & Dedinaite, a. Synthesis and interfacial properties of novel cationic polyelectrolytes with brush-on-brush structure of poly(ethylene oxide) side chains. *Eur. Polym. J.* **46**, 171–180 (2010).

18. Yan, X. *et al.* Reduction of friction at oxide interfaces upon polymer adsorption from aqueous solutions. *Langmuir* **20**, 423–428 (2004).

19. Perry, S. S. *et al.* Tribological properties of poly(L-lysine)-graft-poly(ethylene glycol) films: influence of polymer architecture and adsorbed conformation. *ACS Appl. Mater. Interfaces* **1**, 1224–1230 (2009).

20. Iruthayaraj, J., Olanya, G. & Claesson, P. M. Viscoelastic properties of adsorbed bottle-brush polymer layers studied by quartz crystal microbalance dissipation measurements. *J. Phys. Chem. A* **112**, 15028–15036 (2008).

21. Banquy, X., Burdyńska, J., Lee, D. W., Matyjaszewski, K. & Israelachvili, J. Bioinspired bottle-brush polymer exhibits low friction and Amontons-like behavior. *J. Am. Chem. Soc.* **136**, 6199–202 (2014).

22. Samaroo, K. J., Tan, M., Putnam, D. & Bonassar, L. J. Binding and lubrication of biomimetic boundary lubricants on articular cartilage. *J. Orthop. Res.* **35**, 548–557 (2016).

23. Lawrence, A. *et al.* Synthesis and characterization of a lubricin mimic (mLub) to reduce friction and adhesion on the articular cartilage surface. *Biomaterials* **73**, 42–50 (2015).

24. Benz, M., Chen, N. & Israelachvili, J. Lubrication and wear properties of grafted polyelectrolytes, hyaluronan and hylan, measured in the surface forces apparatus. *J. Biomed. Mater. Res. Part A* **71**, 6–15 (2004).

25. Lee, S. *et al.* Boundary lubrication of oxide surfaces by poly(L-lysine)-g-poly(ethylene glycol) PLL-g-PEG) in aqueous media. *Tribol. Lett.* **15**, 231–239 (2003).

26. Huang, N. *et al.* Poly(L-lysine)-g-poly (ethylene glycol) layers on metal oxide surfaces: surface-analytical characterization and resistance to serum and fibrinogen adsorption. *Langmuir* **17**, 489–498 (2001).

27. Fan, X., Lin, L. & Messersmith, P. B. Cell fouling resistance of polymer brushes grafted from ti substrates by surface-initiated polymerization: effect of ethylene glycol side chain length. *Biomacromolecules* **7**, 2443–2448 (2006).

28. Heuberger, M., Drobek, T. & Spencer, N. D. Interaction forces and morphology of a protein-resistant poly(ethylene glycol) layer. *Biophys. J.* **88**, 495–504 (2005).

29. Lee, J. H., Kopeckova, P., Kopecek, J. & Andrade, J. D. Surface properties of copolymers of alkyl methacrylates with methoxy (polyethylene oxide) methacrylates and their application as protein-resistant coatings. *Biomaterials* **11**, 455–64 (1990).

30. Chang, D. P. *et al.* Conformational mechanics, adsorption, and normal force interactions of lubricin and hyaluronic acid on model surfaces. *Langmuir* **24**, 1183–1193 (2007).

31. Greene, G. W. *et al.* Adaptive mechanically controlled lubrication mechanism found in articular joints. *Proc. Natl. Acad. Sci. U. S. A.* **108**, 5255–5259 (2011).

32. Yim, E. S. *et al.* Biocompatibility of poly(ethylene glycol)/poly(acrylic acid) interpenetrating polymer network hydrogel particles in RAW 264.7 macrophage and MG-63 osteoblast cell lines. *J. Biomed. Mater. Res. A* **91**, 894–902 (2009).

33. Gourdon, D. *et al.* Mechanical and Structural Properties of BaCrO 4 Nanorod Films under Confinement and Shear. *Adv. Funct. Mater.* **14**, 239–242 (2004).

34. Gourdon, D. & Israelachvili, J. Transitions between smooth and complex stick-slip sliding of surfaces. *Phys. Rev. E* **68**, 1–10 (2003).

35. Banquy, X., Lee, D. W., Das, S., Hogan, J. & Israelachvili, J. N. Shear-induced aggregation of mammalian synovial fluid components under boundary lubrication conditions. *Adv. Funct. Mater.* **24**, 3152–3161 (2014).

36. Israelachvili, J. N. *Intermolecular and Surface Forces*. (Amsterdam: Academic Press and Elsevier, 2011).

37. Morrell, K. C., Hodge, W. A., Krebs, D. E. & Mann, R. W. Corroboration of in vivo cartilage pressures with implications for synovial joint tribology and osteoarthritis causation. *Proc. Natl. Acad. Sci. U. S. A.* **102**, 14819–24 (2005).

38. Mueller, M., Lee, S., Spikes, H. A. & Spencer, N. D. The influence of molecular architecture on the macroscopic lubrication properties of the brush-like co-polyelectrolyte poly (L -lysine)-g-poly (ethylene glycol) (PLL-g-PEG) adsorbed on oxide surfaces. *Tribol. Lett.* **15**, 395–405 (2003).

39. Chawla, K. *et al.* A novel low-friction surface for biomedical applications: modification of poly(dimethylsiloxane) (PDMS) with polyethylene glycol(PEG)-DOPA-lysine. *J. Biomed. Mater. Res. A* **90**, 742–9 (2009).

40. Chen, M., Briscoe, W. H., Armes, S. P. & Klein, J. Lubrication at physiological pressures by polyzwitterionic brushes. *Science* **323**, 1698–701 (2009).

41. Raviv, U. *et al.* Lubrication by charged polymers. *Nature* **425**, 163–5 (2003).

42. Hodge, W. a *et al.* Contact pressures in the human hip joint measured in vivo. *Proc. Natl. Acad. Sci. U. S. A.* **83**, 2879–83 (1986).

CHAPTER 4

Interaction with Cartilage Increases the Viscosity of Hyaluronic Acid Solutions

Abstract

Injection of hyaluronic acid (HA) viscosupplements is a prevalent treatment option for patients suffering from mild to moderate osteoarthritis. The efficacy of these supplements is thought to result from increased synovial fluid viscosity, which leads to improved lubrication and reduced pain. Therefore, viscosity is a key parameter to consider in the development of HA supplements. HA is known to localize at the cartilage surface, resulting in a viscosity gradient with heightened viscosity near the surface. Traditional rheological measurements confine HA between metal fixtures and therefore do not capture the effect of HA localization that occurs on cartilage. In these experiments, we investigate the effect of modifying rheometer fixtures with cartilage surface-coatings on the measured viscosity of HA solutions. Our results demonstrate up to a 20-fold increase in measured viscosity when HA is confined between cartilage surfaces compared to steel surfaces. This "effective" viscosity was found to be dependent on the gap height between the rheometer surfaces for low molecular weight HA, which is consistent with the formation of a viscous boundary film. Together, these results indicate that this method for assessing HA viscosity may be more relevant to lubrication than traditional methods and may provide a more accurate method for predicting the viscosity of HA viscosupplements *in-vivo* where HA is likely to interact with the cartilage surface.

Introduction

Intra-articular injection of viscous hyaluronic acid (HA) solutions is a prevalent therapy for osteoarthritis that has been used clinically for several decades.[1] Global sales of HA viscosupplements exceed $2 billion and are projected to continue rising in coming decades.[2] Despite its prolonged and widespread use, there exists significant controversy over both the mechanism of action and the clinical efficacy of HA viscosupplementation. While some studies and meta-analyses conclude that HA viscosupplementation reduces pain and restores joint function,[3,4,5,6] others report no improvement over placebo controls.[7,8,9] Determining clinical efficacy has proved a challenge due to the variability in symptomatic osteoarthritis which is a multifactorial disease with numerous causes, severities, and manifestations, and in the HA viscosupplements used. A number of HA viscosupplements are available clinically in the US, and they vary in molecular weight (500-6,000kDa), formulation (dilute, semi-dilute, and entangled solution as well as gel forms), modifications, and source--all factors that affect the viscosity of the injections.[10,11]

The mechanism of action of HA viscosupplements is a matter of persistent debate. The FDA classifies current HA injectables as class III medical devices, suggesting that their primary mode of action is mechanical. This assumption is supported by the fact that HA is known to reduce friction ex-vivo and in whole joint studies.[12,13,14] Other proposed mechanisms that mediate the efficacy of these injections include biological effects such as anti-inflammatory, chondroprotective, and analgesic actions. Finally, although HA injection is referred to as “viscosupplementation” because

these high viscosity supplements restore the viscosity in the joint space (which is typically depleted in osteoarthritis), there has been little direct investigation correlating the viscosity of HA injections with clinical efficacy.[15,16]

Interactions between HA and molecules at the cartilage surface have been implicated in mediating joint lubrication. One of the most studied interactions in the literature is between HA and lubricin, a glycoprotein found in the synovial fluid and at the cartilage surface that is attributed with facilitating low-friction boundary lubrication in joints.[17,18,19] HA is localized at the cartilage surface via interaction with surface-bound lubricin, and forms a localized viscous layer that promotes low friction elastoviscous lubrication.[12] Several studies have also reported interactions between HA and other cartilage surface molecules such as phospholipids and albumin. These interactions likewise form a viscous layer at the cartilage surface.[20,21,22,23] The effect of HA molecular weight and chemical modifications on these interactions is not clearly understood which makes it challenging to predict how the various clinically available HA viscosupplements will behave in the joint. Increased HA molecular weight has been linked to improved lubrication in in-vitro lubrication tests, but the correlation between molecular weight and clinical efficacy is less clear.[24,25,26,27,28,29,30] A recent study using a Stribeck framework (a framework developed for engineered bearings to describe the transition between boundary, mixed, and viscous lubrication that has been applied to cartilage)[31] to map the lubrication of HA viscosupplements showed that friction coefficient was a much stronger predictor of clinical efficacy than any rheological properties such as viscosity or storage and loss moduli.[15] Furthermore, the "effective" lubricating viscosities of HA viscosupplements extracted from the Stribeck framework

were different from the viscosity measurements of HA solutions measured using traditional rheological techniques in a commercial rheometer.

These results imply that traditional rheological techniques do not capture the full rheological behavior of HA in the joint. They show that the behavior of HA in these conditions is likely mediated by surface interactions and is hence more complicated than the rheology of isolated HA. Standard rheological techniques for determining HA viscosity confine the HA solution between inert metal surfaces.[11,32,33,34] While this provides a measurement of the bulk viscosity, and other rheological properties of the sample, it does not capture the rheological effects of HA localization at the surface, which is known to contribute to the lubrication of cartilage. This discrepancy may be responsible for the mismatch between the measured viscosity in-vitro and the "effective" lubricating viscosity identified by Stribeck analysis that correlates with in-vivo function. The ability to achieve such surface localization of HA in a commercial rheometer would improve current techniques by capturing not only the bulk viscosity, but also the viscosity of the surface-localized HA layer that forms on cartilage and which likely mediates lubrication.

With this in mind, we developed techniques to functionalize rheometer surfaces with cartilage tissue to determine (i) the effect of this functionalization on the viscosity of HA solutions and (ii) the dependence of this effect on the molecular weight of HA.

Methods

To determine the effect of substrate on HA viscosity measurements, several surface coatings were prepared and used to modify the steel fixtures of a DHR3 rheometer; the surface types prepared were (1) unmodified stainless steel fixtures (2) glass surfaces (3) cartilage slab coatings and (4) pulverized cartilage coatings. To test whether the effect of substrate on HA viscosity was surface-localized, viscosity was measured as a function of gap height for several HAs of different molecular weights. For both types of cartilage coatings, cartilage was harvested from the patellofemoral groove of neonatal bovids.

Cartilage Slab Coatings

Harvested cartilage samples from the patellofemoral groove were stored at -20C until ready to be used. They were then thawed and mounted on a sledge microtome using super glue. The microtome was used to section 500um thick slices of sufficient area to fully cover 25mm round glass coverslips. Acquiring slabs of this size required sectioning into the deep zone s of the cartilage and some vascularization was visible in the tissue. The slices were adhered to 25mm round glass coverslips using super-glue and excess tissue was trimmed with a scalpel so that the tissue exactly covered the coverslip. The cartilage-coated coverslips were affixed to the 25mm stainless steel parallel plate fixture of the rheometer using double-sided tape. After fixing the cartilage to the rheometer, a droplet of phosphate buffered saline (PBS) was added between the plates to allow the cartilage to rehydrate for 10 minutes before running experiments.

Pulverized Cartilage Coatings:

Frozen cartilage samples were thawed, finely minced, and lyophilized. The cartilage was then cryo-pulverized to a fine powder via a manual tissue pulverizer or SPEX cryomill. After pulverization, the average cartilage particle diameter was approximately 220µm, assessed using a microscope with 10x objective and analyzed in ImageJ. The pulverized cartilage was stored frozen at -20C until used. Before fixing to the cartilage coverslips, the pulverized cartilage was rehydrated to a paste-like consistency in PB. This was done to avoid glue absorption when gluing lyophilized tissue to glass coverslips. This paste was spread onto coverslips coated in super-glue or Cargille Meltmount 1.539, a resin with a melting point of 65° C. If using Meltmount, the coverslips were then placed on a hot plate to soften the resin. Moderate pressure was applied to the cartilage to improve adhesion. Pulverized cartilage-coated coverslips were mounted onto the 25mm steel plate rheometer fixture using double-sided tape and rehydrated in PBS before testing.

Surface Roughness Measurements

The surface roughness, R_a, of cartilage slabs and pulverized cartilage-coated surfaces were measured using a laser profilometer (Keyence VK-X260 3D Laser Scanning Confocal Microscope, Osaka Japan). Laser scans were collected at 12 locations on 2

samples for both types of cartilage surfaces and leveled in post-analysis to remove the effect of surface tilt. The R_a reported represents an average from these measurements.

HA Solutions

HA formulations of molecular weight 300-450kDa, 750kDa-1MDa, and >1.8MDa were obtained from Lifecore Biomedical and prepared at a concentration of 10mg/mL in PBS. Solutions were left at room temperature overnight or immersed in a water bath at 37C for 1 hour to promote solubilization of high molecular weight HA. These molecular weights correspond approximately to the range of weights in various HA viscosupplements (e.g. Hyalgan 500-730kDa, Supartz 620-1170 kDa, Orthovisc 1-2.8MDa), although crosslinked HA products exist with molecular weights up to 6MDa.

Rheological Testing

All experiments were conducted on a TA Instruments DHR3 rheometer with 25mm parallel plate geometry. After mounting samples, the gap was zeroed and the geometry inertia, friction, and rotational mapping were recalibrated to compensate for changes in modified geometry height, weight, and moment of inertia. HA samples were then injected into the rheometer and viscosity was recorded for flow sweeps over a range of shear rates ($\sim 10^{-3} - 10^{3} s^{-1}$) to capture the Newtonian plateau and shear-thinning behavior of the tested HAs between cartilage slabs, pulverized cartilage, bare glass coverslips, and stainless-steel surfaces. Untreated stainless-steel rheometer fixture and

bare glass coverslips without cartilage coatings (adhered with double-sided tape in the same way as the cartilage-coated coverslips) were used as controls.

Gap heights ranging from 400μm to 2,00μm were tested for the molecular weight HAs confined between stainless steel fixtures and cartilage slabs. Cartilage slabs were chosen for these experiments because they were more reproducible and provided a lower risk of detachment during shearing than the pulverized cartilage surfaces. Effective viscosity was measured over a range of gap heights to determine whether the effect of surface functionalization increased with decreasing gap height, which would be expected if surface functionalization resulted in a localized boundary layer of HA. Altogether, the tests performed were: 300-450kDa HA confined between cartilage slabs (n=2-4) or stainless steel (n=2-5); 750kDa-1MDa HA confined between cartilage slabs (n=2-4, except n=1 for gap=1,4000μm) or stainless steel (n=2, except n=1 for gap=1,6000μm; HA was expelled at gap=2,000μm at rates above $10s^{-1}$ so this data is not included); 1.8MDa-2MDa HA confined between cartilage slabs (n=3-5 for gap=400-1,000μm; n=1-2 for gap=1,200-2,000μm) or stainless steel (n=3).

Statistical Analysis

A linear mixed model with fixed effects of surface, gap, and rate, with all 2-way and 3-way interactions and a random effect of sample to control for repeated measures was performed. Residual analysis was performed to check model assumptions of normality and homogenous variance. Post-hoc pair-wise comparisons were made using tukey's HSD to control for multiple testing. All analysis in R.

Results

Substrate Affects Viscosity Measurements of HA Solutions

The viscosity of 750 kDa-1MDa HA was measured confined between steel, glass, cartilage slabs, and pulverized cartilage to determine the effect of surface chemistry and surface roughness on measurements of HA viscosity. HA is a shear-thinning non-Newtonian fluid. Flow-sweeps of shear thinning fluids exhibit (1) a high viscosity plateau that occurs at low shear rate (the upper Newtonian plateau), (2) a transitional region in which viscosity drops with increasing shear rate and (3) a low-viscosity plateau (the lower Newtonian plateau). Flow sweeps of HA solutions confined between cartilage-coated surfaces demonstrated notably different behaviors compared to the predicted shear-thinning behavior of HA solutions confined between inert metal or glass surfaces. At low shear rates, the measured viscosity of HA was 10-20 times higher when using cartilage-coated fixtures and decreased continuously without exhibiting a clear upper Newtonian plateau in the range of shear rates tested. In contrast, HA confined between metal and glass surfaces exhibited the shear thinning behavior typical of HA with a stable upper Newtonian plateau. At shear rates $\dot{\gamma}$>1s^{-1} (the start of the transition to the lower Newtonian plateau) the measurements of HA viscosity were less substrate-dependent and the flow sweeps of HA confined between cartilage, glass, and steel surfaces were collapsed onto a single curve (Figure 4.1). The surface roughness of cartilage slabs was $R_a = 2.6 \pm 0.8$μm for cartilage slabs and $R_a = 28 \pm 9$μm for pulverized cartilage surfaces, although the cartilage slabs exhibited spares

pores due to vascularization that were not included in this surface roughness measurement.

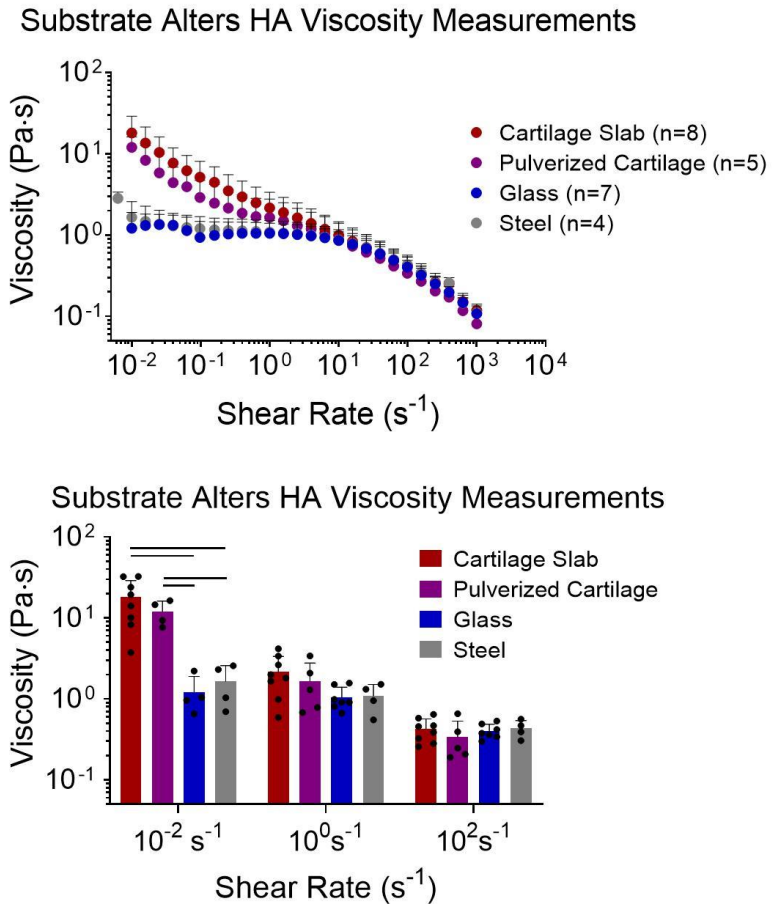

Figure 4.1. (A) Flow sweeps of HA solutions confined between cartilage, glass, or steel surfaces. (B). At a rate of 10^{-2} s^{-1}, HA viscosity between both cartilage coatings were significantly greater than glass or steel surfaces ($p<.001$ indicated by bar). At $1s^{-1}$ and $10^{2}s^{-1}$ there was no statistical difference in HA viscosity measured between any substrates.

Surface-HA Interaction Varies with Molecular Weight and Gap Height

Low-Weight HA: 300-450kDa

The rheological behavior and dependence of viscosity on gap height were measured for three molecular weight HAs. The lowest molecular weight HA (300-450kDa) confined between cartilage slabs exhibited viscosities that were on average 10-20 times greater than stainless steel controls at shear rates below $\dot{\gamma} = 1s^{-1}$ (Figure 4.2 A-B). The effective HA viscosity between cartilage-functionalized surfaces decreased continuously with increasing shear rate, while the steel-confined HA solutions exhibited a stable upper Newtonian plateau. The effect of substrate decreased with increasing shear rate, and at shear rates greater than $1s^{-1}$, HA viscosity became independent of substrate. At low shear rates, a trend was apparent between decreasing gap height and increasing effective viscosity for HA confined between cartilage surfaces (Fig 4.2 C). This trend diminished at high shear rates. For almost all gap heights, the effective viscosity was greater between cartilage than between their stainless-steel counterparts. No trend was observed between gap height and viscosity for HA tested between stainless steel surfaces.

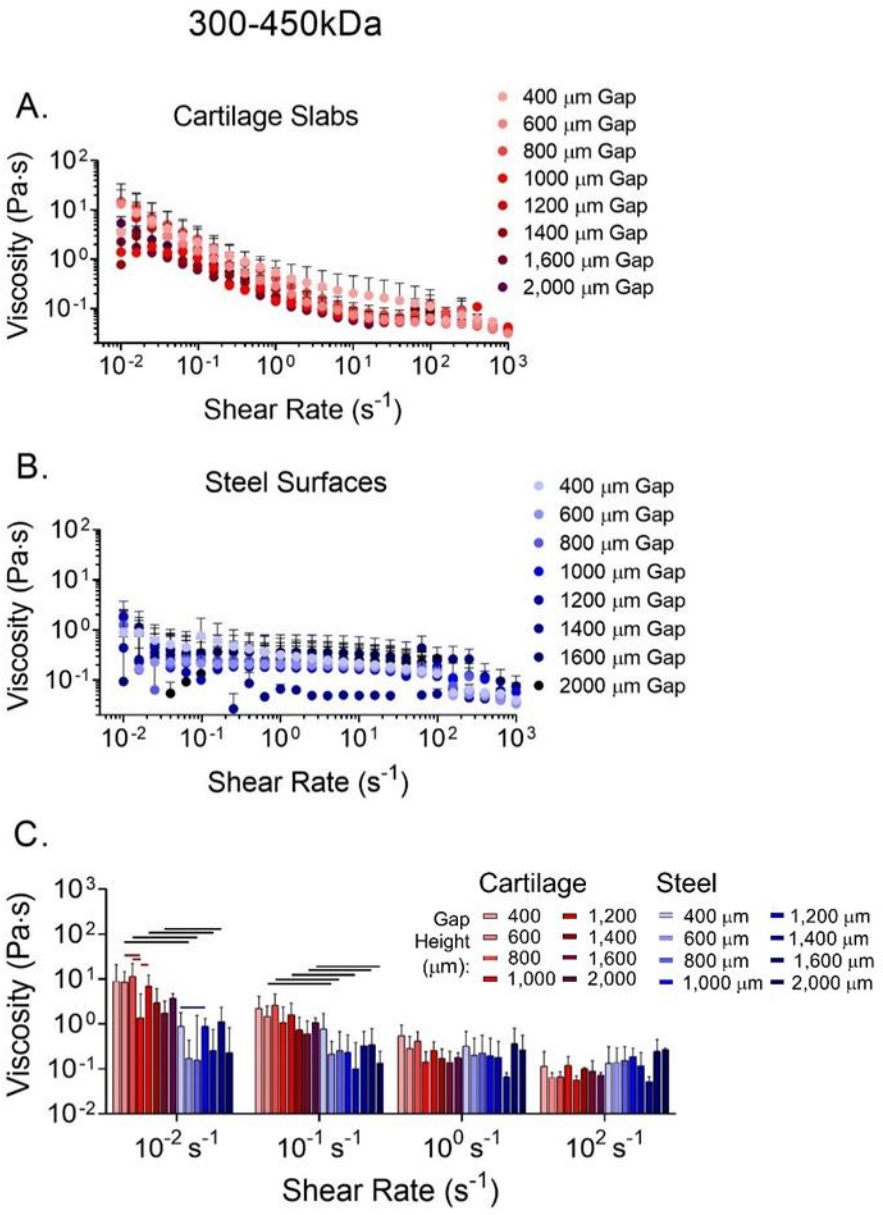

Figure 4.2. Flow sweep of 300-450kDa HA solution confined between (A) cartilage slabs and (B) stainless steel surfaces reveal heightened HA viscosity between cartilage surfaces at slow shear rates. (C) Effective HA viscosity confined between cartilage surfaces is significantly greater than between steel surfaces for nearly all gap heights at shear rates $\dot{\gamma} < 1$s (bar=p<.05). While the effective viscosity of HA confined between cartilage surfaces increased with decreasing gap height, the difference in viscosity with gap height was not statistically significant.

Mid-weight HA: 750kDa-1MDa

The intermediate molecular weight HA (750kDa-1MDa) behaved similarly to the 300-450kDa HA, with a 10-20x increase in effective viscosity at low shear rates that diminished as shear rate increased. (Figure 4.3 A-B). While the viscosity was significantly at a 600μm gap height than for other gap heights tested, no clear trend was apparent between gap height an effective viscosity for cartilage or stainless-steel surfaces. For nearly all gap heights, cartilage coatings significantly increased the effective viscosity compared to stainless-steel controls (Figure 4.3 C).

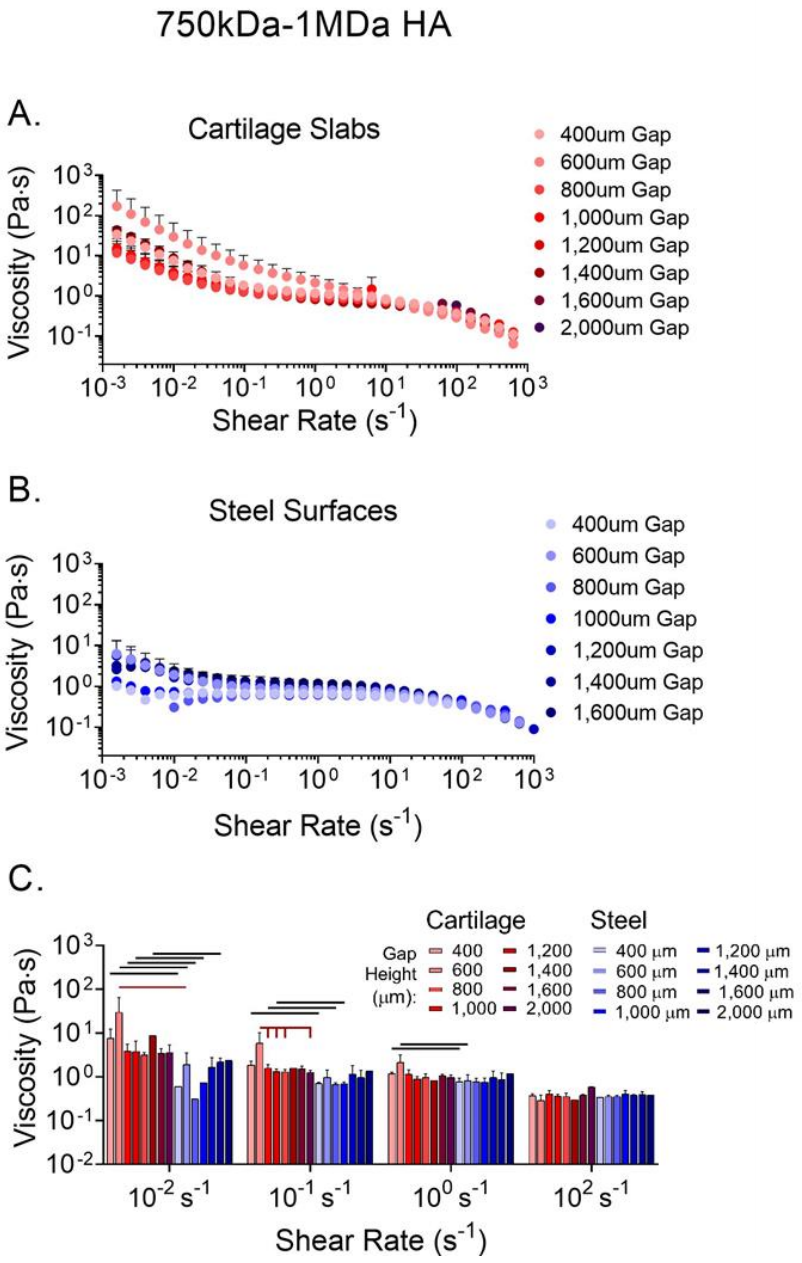

Figure 4.3. The effective viscosity of HA measured between (A) cartilage-functionalized rheometer fixtures is higher at low shear rates compared to (B) stainless-steel surfaces. (C) The increased effective viscosity between cartilage surfaces is significant at nearly all gap heights under shear rates $\dot{\gamma} < 1$s (bar=p<.05). However, the effective viscosity on cartilage did not vary significantly with gap height.

High Molecular Weight HA: 1.8-2MDa

The viscosity of the highest molecular weight HA (1.8-2MDa) was not dependent on the substrate material. Because increasing viscosity shifts the transition from upper to lower Newtonian plateau towards lower shear rates, the flow rate for 2MDa HA was extended to lower shear rates starting at $10^{-3}s^{-1.}$ Both cartilage slabs and stainless-steel substrates resulted in stable upper Newtonian plateaus at low shear rate, followed by a transition to the lower Newtonian plateau at shear rates above 1 s^{-1} (Figure 4.4 A-B). The effective viscosity of HA was not heightened by the presence of cartilage surfaces in the range of shear rates tested. Furthermore, the trend between gap height and effective viscosity between cartilage surfaces that was observed in low molecular weight HA was not apparent (Figure 4.4 C)

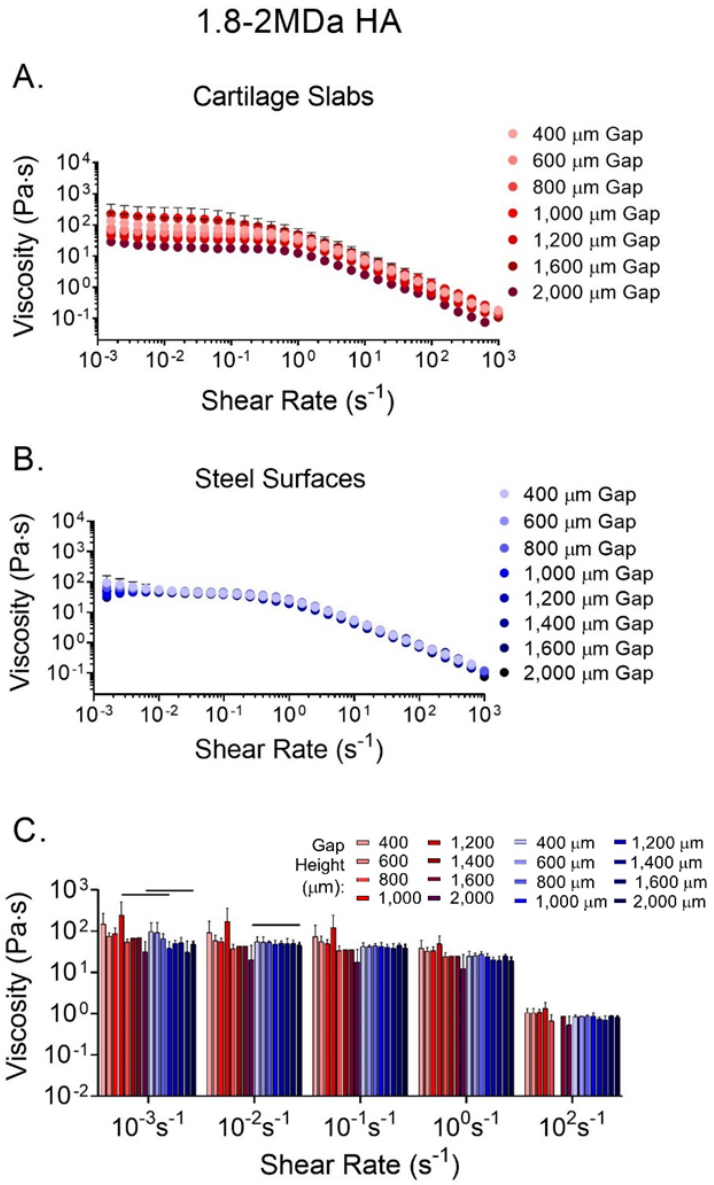

Figure 4.4. No appreciable differences in effective viscosity were observed for HA confined between (A) cartilage slabs and (B) stainless-steel surfaces. (C) The effect of gap height on effective HA viscosity was negligible for both cartilage and stainless-steel surfaces.

Discussion

Our results demonstrate that functionalizing rheometer surfaces with cartilage coatings yields effective viscosities that are greater than those measured using traditional rheological techniques and that this effect was dependent on HA molecular weight. The molecular weights chosen in this study correspond roughly to those of currently available HA viscosupplements (e.g. Hyalgan 500-730kDa, Supartz 620-1170 kDa, Orthovisc 1-2.8MDa), so understanding how molecular weight effects cartilage interaction in this range is clinically relevant. The effect of surface functionalization was most pronounced for low molecular weight HAs under low shear rates, which exhibited a nearly ~20-fold increase in effective viscosity compared to stainless-steel controls. Furthermore, for low molecular weight HA, smaller gap height resulted in higher effective viscosity. These results suggest that a viscous boundary layer forms on the cartilage, increasing the viscosity at the surface (Figure 4.5). The contribution of the viscous surface layer to the "effective" viscosity measurement increases as the gap height decreases because the volume of "bulk" fluid decreases while the boundary layer at the surface remains unchanged. There are multiple possible explanations for why the effect of gap height was only observed for low molecular weight HA. The smaller size and lower steric repulsion may enhance surface attachment, or the small effect of gap height may be simply be below the detection limit of the rheometer for high molecular weight HA which has a significantly higher bulk viscosity; more work is necessary to determine which explanation is correct. The effective viscosity of HA solutions confined between cartilage and stainless-steel converge to a single curve with increasing shear rate. The increased shear stresses that occur at high shear rates may disrupt the

boundary layer of HA, resulting in viscosities that approach bulk values with increasing shear rates.

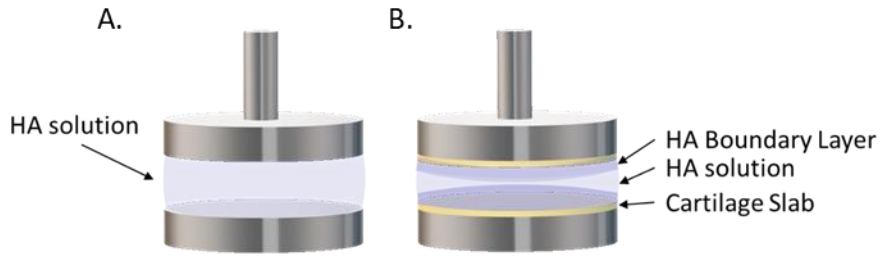

Figure 4.5. Visualization of (A) HA solution confined between stainless steel surfaces and (B) the formation of a viscous boundary layer due to HA localization on rheometer surfaces functionalized with cartilage slabs.

Collectively, these data suggest that interactions between HA and cartilage tissue are critical for mediating the lubricating behavior of viscosupplements. However, the nature of this surface interaction was not investigated. The surface roughness of cartilage slabs was significantly lower than the pulverized cartilage coatings and both resulted in comparable increases in viscosity at slow shear rates, indicating that this is not purely an effect caused by surface roughness. Furthermore, the similarity in the behavior of pulverized and slab cartilage indicates that the HA-cartilage interaction is not dependent on the overall structure of the tissue. Because cartilage slabs were sectioned from the deep zone of the cartilage where lubricin concentrations are negligible,[35,36] it is improbable that the cartilage surface interaction in our experiments was mediated by lubricin. There are several possibilities that could mediate the HA-cartilage interaction: HA can interact with CD44, a glycoprotein on the surface of

cells,[37] and it is known to form aggregates with the proteoglycan aggrecan via interaction with link protein.[38,39] Further investigation into the molecular mechanism of the HA surface localization in our experiments is warranted.

These findings are clinically important because the viscosity of HA viscosupplements measured using traditional rheological techniques is poorly correlated with clinical efficacy[15,16]. In a recent study of six viscosupplements currently in clinical use, it was found that frictional characteristics, but not rheological or viscoelastic properties correlated with WOMAC scores (a self-administered assessment of pain, stiffness, and physical function that is used as a heuristic for treatment efficacy)[15]. High molecular weight HA solutions have been shown to reduce friction in ex-vivo lubrication studies; however, the viscosity of these HA solutions measured using a traditional rheometer differ from the effective lubricating viscosity extracted from the Stribeck curves of the same HA solutions. Together, these results indicate that traditional viscosity measurements, while effective for measuring the bulk rheological properties of HA, do not capture the surface localized viscosity, which is a more relevant parameter for lubrication, and thus likely a better predictor of clinical efficacy.

The proposed existence of a lubrication-mediating, high-viscosity layer of HA on the cartilage is supported by many reports of synergistic interactions between HA and molecules, including lubricin[17,18,40,41,] and phospholipids[20,21,23,42] at the cartilage surface. Lubricin has been reported to entrap HA at the cartilage surface, enhancing lubrication.[12] Removal of lubricin via trypsin digestion resulted in a disruption of both boundary mode friction (mediated by lubricin) and elastoviscous lubrication (mediated

by HA), indicating that not only the presence of HA, but also its entrapment at the surface is critical for effective lubrication.[12] Further compelling evidence of the critical importance of HA surface localization for cartilage lubrication was presented in recent studies on peptide-mediated HA surface localization. A peptide was used to link HA to collagen II, a prevalent structural protein at the cartilage surface. Cartilage with this robustly anchored HA layer yielded equal lubricity when sheared in PBS compared to untreated cartilage sheared in a high concentration bath of HA, and much better lubricity that untreated cartilage sheared in PBS. This confirms that HA at the surface predominantly contributes to successful lubrication without the need for a high concentration of HA in the bulk. HA anchoring was shown to improve not only lubricity, but also residency time in the joint in an in-vivo rabbit model. Our results indicating that cartilage coatings alter local viscosity thus contribute to a building body of evidence suggesting that surface interaction strongly affects the rheological and tribological behaviors of HA viscosupplements and is an important factor to consider in developing HA therapies.

The importance of surface anchoring for effective lubrication by synovial fluid constituents has implications for the design of artificial joints. Metal alloys, ceramics, and ultra-high molecular weight polyethylene (UHMWPE) are used for artificial joint surfaces due to their mechanical properties, biocompatibility, and favorable tribology. A prominent failure mode in artificial joints is the development of wear on the articulating surfaces due to mechanical abrasion (for UHMWPE) or corrosion (for metals) that trigger an adverse biological response.[43,44] As a result, extensive research has been focused on understanding and preventing wear on implant surfaces by

developing improved implant materials and altering implant structure and design to improve mechanics.[45,46,47,48] Some recent studies have focused on the role of globular proteins, which are present in the synovial fluid, in the lubrication of artificial joint implants. These studies suggest that globular proteins form a cushion that improves load distribution between orthopedic surfaces, and others have identified the formation of a metal-protein "tribolayer" at the surface between the joint and the lubricating fluid. Both of these mechanisms of are associated with enhanced resistance to wear.[49,50,51,52,53] The amount of protein adsorption that occurs depends on the chemistry of the surface (UHMWPE, alumina, or metal) and is also influenced by factors such as surface charge and plasma treatment.[54,55,56,57,58] However, while the effect of altering surface chemistry to tune protein adsorption and mediate wear protection has been a topic of increasing interest in recent years, surface modifications to entrap other lubricating components of the synovial fluid have garnered less attention. As demonstrated here and elsewhere, there is mounting evidence that HA localization at the cartilage surface facilitates elastoviscous lubrication by boosting the effective viscosity at the sliding surface. Viscosity is an important factor in elastohydrodynamic lubrication, which is a prominent lubrication mode in artificial joints.[59,60,61] This suggests that modifying implant surfaces to promote the localization of HA at the surface could be an interesting strategy for improving implant design.

There is persistent controversy over the relative contributions of mechanical versus biological roles in the mechanism of action of HA viscosupplements. Much of this stems from the short half-life of these supplements in the joint. While half-lives of HA supplements in the synovial fluid vary from a few hours to over a week (with small

molecular weight HAs exhibiting the shortest half-lives) the efficacy is reported to last for weeks or months.[62,63,64] This mismatch between the short residency time of HA in the joint and the prolonged efficacy of HA injections is typically interpreted as evidence for a therapeutic biological role which outlasts the physical presence of HA in the joint. The results presented here and in other recent studies[12,15,65] hint at another possibility: the HA that contributes the most to lubrication is surface-bound via interactions with cartilage. This HA is therefore not represented in measurements of HA concentration in the synovial fluid, which determines only the concentration of freely floating HA. While there appears to be a correlation between increasing molecular weight and longer residence time in the synovial fluid, there is no corresponding correlation between molecular weight and efficacy. Our results revealed a greater difference between the bulk viscosity and effective viscosity for lower molecular weight HAs, indicating that the smaller HAs tested may localize more readily at the cartilage surface. This could be one reason molecular weight is a poor predictor of lubrication and clinical efficacy of HA supplements.

Conclusions

The results of this study reveal that the local viscosity of HA solutions is significantly increased at low shear rates when confined between cartilage surfaces compared to inert metal or glass surfaces. This supports the growing evidence that interactions between synovial fluid lubricants including HA and the cartilage surface are critical for mediating lubrication. While bulk rheological properties of HA are not correlated with clinical efficacy, frictional characteristics have shown positive

correlations with efficacy. The “effective” viscosity of HA near the cartilage surface measured in this study may be more relevant to lubrication than the bulk viscosity traditionally assessed in rheometer measurements, and therefore may be a better predictor of clinical efficacy. Molecular weight, concentration, and chemical modifications of HA solutions are all factors which can affect the cartilage-surface interactions and therefore impact clinical efficacy in ways that are difficult to predict. However, understanding the effect of these changes on the effective viscosity of the HA solutions on cartilage may be a useful first step in determining their impact on lubrication and efficacy.

REFERENCES

1. Rydell, N. & Balazs, E. A. Effect of Intra-articular Injection of Hyaluronic Acid on the Clinical Symptoms of Osteoarthritis and on Granulation Tissue Formation. *Clin. Orthop. Relat. Res.* **80**, 25–32 (1971).

2. Tiwari, R. Viscosupplementation Market to Hit $2.6 Billion by 2021. *PR Newswire* (2015). Available at: https://www.prnewswire.com/news-releases/viscosupplementation-market-to-hit-26-billion-by-2021-528457891.html. (Accessed: 9th July 2019)

3. Bellamy, N. *et al.* Viscosupplementation for the treatment of osteoarthritis of the knee. *Cochrane Database Syst. Rev.* (2006). doi:10.1002/14651858.CD005321.pub2

4. Migliore, A. & Procopio, S. Effectiveness and utility of hyaluronic acid in osteoarthritis. *Clin. Cases Miner. Bone Metab.* **12**, 31–3 (2015).

5. Reid, M. C. Viscosupplementation for osteoarthritis: a primer for primary care physicians. *Adv. Ther.* **30**, 967–86 (2013).

6. Henrotin, Y. *et al.* Consensus statement on viscosupplementation with hyaluronic acid for the management of osteoarthritis. *Semin. Arthritis Rheum.* **45**, 140–149 (2015).

7. Niemelä, T. M., Tulamo, R. M. & Hielm-Björkman, A. K. A randomised, double-blinded, placebocontrolled clinical study on intra-articular hyaluronan treatment

in equine lameness originating from the metacarpophalangeal joint. *BMC Vet. Res.* **12**, (2016).

8. Jevsevar, D. S. Treatment of osteoarthritis of the knee. *J. Am. Acad. Orthop. Surg.* **21**, 571–576 (2013).

9. Brandt, K. D., Smith, G. N. & Simon, L. S. Intraarticular injection of hyaluronan as treatment for knee osteoarthritis: What is the evidence? *Arthritis Rheum.* **43**, 1192–1203 (2000).

10. Braithwaite, G. J. C., Daley, M. J. & Toledo-Velasquez, D. Rheological and molecular weight comparisons of approved hyaluronic acid products – preliminary standards for establishing class III medical device equivalence. *J. Biomater. Sci. Polym. Ed.* **27**, 235–246 (2016).

11. Nicholls, M., Manjoo, A., Shaw, P., Niazi, F. & Rosen, J. Rheological properties of commercially available hyaluronic acid products in the United States for the treatment of osteoarthritis knee pain. *Clin. Med. Insights. Arthritis Musculoskelet. Disord.* **11**, (2018).

12. Bonnevie, E. D., Galesso, D., Secchieri, C., Cohen, I. & Bonassar, L. J. Elastoviscous transitions of articular cartilage reveal a mechanism of synergy between lubricin and hyaluronic acid. *PLoS One* **10**, (2015).

13. Mori, M. Naito, S. Moriyama, S., Naito, M. & Moriyama, S. Highly viscous sodium hyaluronate and joint lubrication. *Int. Orthop.* **26**, 116–121 (2002).

14. Schmidt, T. A., Gastelum, N. S., Nguyen, Q. T., Schumacher, B. L. & Sah, R. L. Boundary lubrication of articular cartilage: Role of synovial fluid constituents. *Arthritis Rheum.* **56**, 882–891 (2007).

15. Bonnevie, E. D., Galesso, D., Secchieri, C. & Bonassar, L. J. Frictional characterization of injectable hyaluronic acids is more predictive of clinical outcomes than traditional rheological or viscoelastic characterization. *PLoS One* **14**, (2019).

16. Machado, R. C., Capela, S. & Rocha, F. A. C. Polysaccharides as viscosupplementation agents: Structural molecular characteristics but not rheology appear crucial to the therapeutic response. *Front. Med.* **4**, (2017).

17. Das, S. *et al.* Synergistic interactions between grafted hyaluronic acid and lubricin provide enhanced wear protection and lubrication. *Biomacromolecules* **14**, 1669–1677 (2013).

18. Huang, J. *et al.* Probing the molecular interactions and lubrication mechanisms of purified full-length recombinant human proteoglycan 4 (rhPRG4) and hyaluronic acid (HA). *Biomacromolecules* **20**, 1056–1067 (2019).

19. Greene, G. W. *et al.* Adaptive mechanically controlled lubrication mechanism found in articular joints. *Proc. Natl. Acad. Sci. U. S. A.* **108**, 5255–5259 (2011).

20. Jung, S. *et al.* Hyaluronic acid and phospholipid interactions useful for repaired articular cartilage surfaces-a mini review toward tribological surgical adjuvants. *Colloid Polym. Sci.* **295**, 403–412 (2017).

21. Crockett, R. *et al.* Biochemical composition of the superficial layer of articular cartilage. *J. Biomed. Mater. Res. Part A* **82**, 958–964 (2007).

22. Jahn, S., Seror, J. & Klein, J. Lubrication of articular cartilage. *Annu. Rev. Biomed. Eng* **18**, 235–258 (2016).

23. Zhu, L., Seror, J., Day, A. J., Kampf, N. & Klein, J. Ultra-low friction between boundary layers of Hyaluronan-phosphatidylcholine Complexes. *Acta Biomater.* **59**, 283–292 (2017).

24. Maneiro, E., de Andres, M. C., Fernández-Sueiro, J. L., Galdo, F. & Blanco, F. J. The biological action of hyaluronan on human osteoartritic articular chondrocytes: the importance of molecular weight. *Clin. Exp. Rheumatol.* **22**, 307–312 (2004).

25. Kikuchi, T., Yamada, H. & Shimmei, M. Effect of high molecular weight hyaluronan on cartilage degeneration in a rabbit model of osteoarthritis. *Osteoarthr. Cartil.* **4**, 99–110 (1996).

26. Wobig, M. *et al.* The role of elastoviscosity in the efficacy of viscosupplementation for osteoarthritis of the knee: A comparison of Hylan G-F 20 and a lower-molecular-weight hyaluronan. *Clin. Ther.* **21**, 1549–1562 (1999).

27. Bayramoglu, M. *et al.* Comparison of two different viscosupplements in knee osteoarthritis-a pilot study. *Clin Rheomatol* **22**, 118–122 (2003).

28. Ghosh, S. & Abanteriba, S. Status of surface modification techniques for artificial hip implants. *Sci. Technol. Adv. Mater.* **17**, 715–735 (2016).

29. Maheu, E. *et al.* Comparative efficacy and safety of two different molecular weight (MW) hyaluronans F60027 and Hylan G-F20 in symptomatic osteoarthritis of the knee (KOA). Results of a non inferiority, prospective, randomized, controlled trial. *Clin. Exp. Rheumatol.* **29**, 527–35 (2011).

30. Pavelka, K. & Uebelhart, D. Efficacy evaluation of highly purified intra-articular hyaluronic acid (Sinovial®) vs hylan G-F20 (Synvisc®) in the treatment of symptomatic knee osteoarthritis. A double-blind, controlled, randomized, parallel-group non-inferiority study. *Osteoarthr. Cartil.* **19**, 1294–1300 (2011).

31. Gleghorn, J. P. & Bonassar, L. J. Lubrication mode analysis of articular cartilage using Stribeck surfaces. *J. Biomech.* **41**, 1910–1918 (2008).

32. Nicholls, M., Manjoo, A., Shaw, P., Niazi, F. & Rosen, J. A comparison between rheological properties of intra-articular hyaluronic acid preparations and reported human synovial fluid. *Adv. Ther.* **35**, 523–530 (2018).

33. Bhuanantanondh, P., Grecov, D. & Kwok, E. Rheological study of viscosupplements and synovial fluid in patients with osteoarthritis. *J. Med. Biol. Eng.* **32**, 12–16 (2012).

34. Falcone, S. J., Palmeri, D. M. & Berg, R. A. Rheological and cohesive properties of hyaluronic acid. *J. Biomed. Mater. Res. Part A* **76**, 721–728 (2006).

35. Schmidt, T. A., Schumacher, B. L., Klein, T. J., Voegtline, M. S. & Sah, R. L. Synthesis of proteoglycan 4 by chondrocyte subpopulations in cartilage explants,

monolayer cultures, and resurfaced cartilage cultures. *Arthritis Rheum.* **50**, 2849–2857 (2004).

36. A novel proteoglycan synthesized and secreted by chondrocytes of the superficial zone of articular cartilage. *Arch. Biochem. Biophys.* **311**, 144–152 (1994).

37. Lesley, J. & Hyman, R. CD44 can be activated to function as an hyaluronic acid receptor in normal murine T cells. *Eur. J. Immunol.* **22**, 2719–2723 (1992).

38. Hardingham, T. E. & Muir, H. Hyaluronic acid in cartilage and proteoglycan aggregation. *Biochem. J* **139**, 565–581 (1974).

39. Watanabe, H. Cartilage proteoglycan aggregate: structure and function. *Clin. Calcium* **14**, 9–14 (2004).

40. Ludwig, T. E., Hunter, M. M. & Schmidt, T. A. Cartilage boundary lubrication synergism is mediated by hyaluronan concentration and PRG4 concentration and structure. *BMC Musculoskelet. Disord.* **16**, (2015).

41. Zappone, B., Ruths, M., Greene, G. W., Jay, G. D. & Israelachvili, J. N. Adsorption, lubrication, and wear of lubricin on model surfaces: polymer brush-like behavior of a glycoprotein. *Biophys. J.* **92**, 1693–708 (2007).

42. Seror, J., Zhu, L., Goldberg, R., Day, A. J. & Klein, J. Supramolecular synergy in the boundary lubrication of synovial joints. *Nat. Commun.* **6**, (2015).

43. Catelas, I. & Wimmer, M. A. Polyethylene and metal wear particles: characteristics and biological effects. *Semin. Immunopathol.* **33**, 257–271 (2011).

44. Catelas, I. & Wimmer, M. A. New insights into wear and biological effects of metal-on-metal bearings. *J. Bone Joint Surg. Am.* **93**, 76–83 (2011).

45. Ito, H. *et al.* Reduction of polyethylene wear by concave dimples on the frictional surface in artificial hip joints. *J. Arthroplasty* **15**, 332–338 (2000).

46. Auger, D. D., Dowson, D., Fisher, J. & Jin, Z.-M. Friction and lubrication in cushion form bearings for artificial hip joints. *Proc. Inst. Mech. Engeineers* **207**, 25–33 (1993).

47. Jin, Z. M., Dowson, D. & Fisher, J. Analysis of fluid film lubrication in artificial hip joint replacements with surfaces of high elastic modulus. *Proc. Inst. Mech. Eng. Part H* **211**, 247–256 (1997).

48. Wang, W., Ouyang, Y. & Khoon Poh, C. Orthopaedic implant technology: biomaterials from past to future. *Ann. Acad. Med.* **40**, 237–244 (2011).

49. Fan, J., Myant, C., Underwood, R. & Cann, P. Synovial fluid lubrication of artificial joints: protein film formation and composition. *R. Soc. Chem.* **156**, 69–85 (2012).

50. Fan, J., Myant, C. W., Underwood, R., Cann, P. M. & Hart, A. Inlet protein aggregation: a new mechanism for lubricating film formation with model synovial fluids. *Proc. Inst. Mech. Eng. Part H.* **225**, 696–709 (2011).

51. Parkes, M., Myant, C., Cann, P. M. & Wong, J. S. S. Synovial Fluid Lubrication: The Effect of Protein Interactions on Adsorbed and Lubricating Films. *Biotribology* **1**–**2**, 51–60 (2015).

52. Mathew, M. T. *et al.* Tribolayer formation in a metal-on-metal (MoM) hip joint: an electrochemical investigation. *J. Mech. Behav. Biomed. Mater.* **29**, 199–212 (2014).

53. Wimmer, M. A. *et al.* Wear mechanisms in metal-on-metal bearings: The importance of tribochemical reaction layers. *J. Orthop. Res.* **28**, 436–443 (2010).

54. Widmer, M. R., Heuberger, M., Vörös, J. & Spencer, N. D. Influence of polymer surface chemistry on frictional properties under protein-lubrication conditions: implications for hip-implant design. *Tribol. Lett.* **10**, 111–116 (2001).

55. Fröhlich, S. M., Dorrer, V., Archodoulaki, V.-M., Allmaier, G. & Marchetti-Deschmann, M. Synovial fluid protein adsorption on polymer-based artificial hip joint material investigated by MALDI-TOF mass spectrometry imaging. *EuPA Open Proteomics* **4**, 70–80 (2014).

56. Wang, K., Zhou, C., Hong, Y. & Zhang, X. A review of protein adsorption on bioceramics. *Interface Focus* **2**, 259–77 (2012).

57. Yan, Y., Yang, H., Su, Y. & Qiao, L. Albumin adsorption on CoCrMo alloy surfaces. *Sci. Rep.* **5**, (2015).

58. Serro, A. P., Colaço, R. & Saramago, B. Effect of Albumin Adsorption on Biotribological Properties of Artificial Joint Materials. in *Proteins and Interfaces III State of the Art* 497–523 (American Chemical Society, 2012).

59. Mattei, L., Di Puccio, F., Piccigallo, B. & Ciulli, E. Lubrication and wear modelling of artificial hip joints: A review. *Tribol. Int.* **44**, 532–549 (2011).

60. Trotten, G. E. *Handbook of Lubrication and Tibology. Volume I: Application and Maintenance*. (CRC Press, 2006).

61. Gao, L., Wang, F., Yang, P. & Jin, Z. Effect of 3D physiological loading and motion on elastohydrodynamic lubrication of metal-on-metal total hip replacements. *Med. Eng. Phys.* **31**, 720–729 (2009).

62. Jackson, D. W. & Simon, T. M. Intra-articular distribution and residence time of Hylan A and B: a study in the goat knee. *Osteoarthr. Cartil.* **14**, 1248–1257 (2006).

63. McGrath, A. *et al.* A comparison of intra-articular hyaluronic acid competitors in the treatment of mild to moderate knee osteoarthritis. *J. Arthritis* **2**, (2013).

64. Brown, T., Laurent, U. & Fraser. Turnover of hyaluronan in synovial joints: elimination of labelled hyaluronan from the knee joint of the rabbit. *Exp. Physiol.* **76**, 125–134 (1991).

65. Singh, A. *et al.* Enhanced lubrication on tissue and biomaterial surfaces through peptide-mediated binding of hyaluronic acid. *Nat. Mater.* **13**, (2014).

CHAPTER 5

Conclusions and Future Directions

Abstract

In this section, the previous three chapters will be framed in the broader context of their contribution to the field of joint lubrication. Collectively, the original research presented in this dissertation examines the molecular interactions that occur within the synovial fluid and between synovial fluid and the cartilage surface and it investigates the impact of these interactions on lubrication at the molecular and tissue scale. Chapter 2 provides insights into the composition and dynamics of synovial fluid aggregation and draws connections between this phenomenon and a novel "protein aggregation lubrication" mechanism that has been proposed in the context of artificial joints. Chapters 3 and 4 highlight the importance of surface attachment on the function of tribosupplements in both boundary and viscous lubrication. Chapter 3 identifies a synergistic interaction between a lubricin-mimetic polymer and a structural protein (fibronectin) found at the cartilage surface that enhances lubrication and wear resistance at the molecular scale. Chapter 4 investigates the macro-scale effect of hyaluronic acid localization at the cartilage surface on measurements of hyaluronic acid viscosity using a customized commercial rheometer. The difference between the bulk viscosity and the "effective" hyaluronic acid viscosity (which includes both bulk and viscous boundary layer viscosity) may help explain the lack of correlation between in-vitro viscosity characterization and clinical efficacy of hyaluronic acid viscosupplements. Taken together, chapters 2-4 have implications for improving osteoarthritis therapies from tribosupplementation to arthroplasty by considering mechanisms of lubricant

interactions at the shearing surface.

Surface Interactions in Synovial Fluid Lubrication at the Molecular and Tissue Scale

The original work presented in this dissertation emphasizes the importance of substrate choice in the lubrication mechanisms of synovial fluid. The studies in Chapters 2-4 reveal that the mechanical properties and chemical composition of shearing surfaces have a profound effect on the tribology and rheology of synovial fluid components at both the molecular and the tissue scale. Understanding the role of substrate on the molecular interactions that occur in synovial fluid and their resulting macroscopic tribological effects, points to a new approach for developing improved osteoarthritis therapies and artificial implants. Tuning the material properties of the shearing surfaces to facilitate entrapment of lubricating molecules in the synovial fluid can affect the lubrication mechanisms at play and result in macro-scale effects on the tribology of the joint. While previous studies with the Surface Forces Apparatus (SFA) have investigated the molecular interactions between synovial fluid molecules on rigid, nonporous mica substrates from a materials science perspective, and biomedical researchers have studied the tissue-scale lubrication of cartilage using custom tribometers, little research has been conducted that spans the molecular and tissue-scale lubrication and wear protection of synovial fluid as presented in this dissertation.

The studies presented in Chapter 2 probed the dynamics of molecular interactions involved in the aggregation of synovial fluid constituents under shear using the SFA. Our results identified the globular protein albumin as the primary aggregating component. This discovery revealed that the aggregation of synovial fluid is likely a wear-protecting mechanism, since protein aggregation has been associated with reducing wear between artificial joints in-vitro by forming protein cushions that

redistribute load and protect the shearing surfaces. Protein aggregates have been found on the surfaces of retrieved implants in areas of high shear stress, adding further evidence to support the wear-protecting role of protein aggregates in artificial joints.[1,2] While the specific mechanisms of protein aggregation are not fully understood, protein adsorption and subsequent shear-induced unfolding are believed to be critical to the process. Therefore, both the chemical properties (affecting protein adsorption) and mechanical properties (affecting shear stress) of the substrate are important for this mechanism.

Chapter 3 examined the interaction between a lubricin-mimetic polymer and the structural protein fibronectin, which is present in the superficial zone of cartilage. Recent studies suggest that surface attachment is critical for lubricin-mediated cartilage lubrication.[3,4] Natural lubricin binds to fibronectin via its C-terminus[5] and a recent SFA study demonstrated that interaction with fibronectin significantly improved the wear resistance of lubricin films sheared between mica surfaces.[6] The results of this study demonstrate that the wear protection capability of a lubricin-mimetic polymer is also greatly enhanced by interaction with fibronectin. When the mimetic lubricin was confined directly between mica surfaces, damage occurred almost immediately, but when it was anchored to mica by a film of fibronectin, wear only occurred under high loads. Like the results of Chapter 2, this finding emphasizes the importance of substrate on the retention of key lubricating constituents (and their molecular interactions that mediate lubrication) that mediate lubrication.[7]

While Chapters 2 and 3 used the SFA to study lubricating mechanisms at the molecular scale, Chapter 4 investigates the tissue-scale effects of molecular attachment

to the cartilage surface. The results demonstrate that interaction with the cartilage surface increases the effective viscosity of hyaluronic acid solutions. Traditional viscosity measurements confine hyaluronic acid between the metal plates of a rheometer. Because hyaluronic acid does not interact with the metal surfaces, this results in a measurement of the bulk viscosity of free-floating hyaluronic acid molecules in solution. The lack of correlation between these viscosity measurements and the clinical efficacy of hyaluronic acid viscosupplements calls into question the relevance of bulk viscosity measurements of hyaluronic acid. Our results show that when the rheometer plates are functionalized with cartilage slabs, the effective viscosity of hyaluronic acid solutions is up to 20-fold greater than the bulk viscosity. This is attributed to interactions between hyaluronic acid molecules and the cartilage surface, which result in the formation of a highly viscous boundary layer at the surface that affects viscosity measurements. Once again, the choice of substrate had a demonstrable effect on the molecular interactions of important lubricating components in the synovial fluid and was critical for mediating lubrication. Viscosity, a tissue-scale property, was profoundly influenced by choosing a substrate (in this case cartilage) that facilitated molecular interactions with hyaluronic acid.

Implications for Tribosupplementation

Tribosupplementation is the injection of lubricating molecules into the joint space with the aim of improving joint lubrication and restoring joint function. Injection of boundary lubricants, including lubricin and lubricin-mimetic molecules, has been investigated in small animal studies,[8,9,10] and the injection of the viscous lubricant

hyaluronic acid has been used clinically to treat osteoarthritis for decades.[11] Most research on these treatments has focused on the intrinsic lubricating abilities of the molecules involved. However, the results presented in Chapters 3 and 4 reveal that the interaction between tribosupplements and the cartilage surface is also critical for mediating their lubricating abilities. While developing tribosupplements with favorable lubricating properties is important, the interaction between these lubricants and the cartilage surface can also have a profound impact on their success.

The lubricin-mimetic studied in Chapter 3 possessed a highly lubricious mucin-mimicking domain to facilitate low-friction shearing. However, when the molecule did not attach robustly to the shearing surfaces, damage occurred almost instantaneously. Only in the presence of fibronectin, which anchored the lubricin mimetic to the underlying mica surface, was the polymer capable of lubrication under high loads. Fibronectin was chosen because previous studies have identified a strong synergy between natural lubricin and fibronectin.[6] However, while our results reveal that fibronectin-mediated attachment to the surface enabled successful boundary lubrication by the lubricin-mimetic molecule, the specificity of this attachment is likely not critical.

The overall friction performance of lubricin-mimetics can be assessed by macro-scale friction measurements in cartilage-on-glass tribometers,[12,13] but the SFA offers the distinct advantage that it can be used to assess surface attachment and molecular conformation with nanometer resolution while simultaneously measuring the resulting normal and lateral (friction) forces under shear, and monitoring surface wear. SFA surfaces are rigid and non-porous, making them an over-simplified system for capturing the complex mechanical behaviors of cartilage, but their mechanical simplicity allows

for high experimental control and they can be functionalized to chemically mimic aspects of the cartilage surface. The experiments performed in Chapter 2 could be used as a framework to study the interaction between lubricin-mimetics and SFA surfaces functionalized with a range of cartilage proteins, such as collagen II, which is the dominant structural protein in cartilage. Our results suggest that engineering the mechanism of interaction between mimetic lubricins and the cartilage surface could be an important way to tune the overall lubricating and wear-protecting abilities of mimetic lubricin tribosupplements.

While tribosupplementation with boundary lubricants such as lubricin is an emerging area of research, intra-articular injection of hyaluronic acid viscosupplements has been performed clinically for nearly four decades.[11] The efficacy of these supplements is in part attributed to their high viscosity, which promotes low-friction elastoviscous lubrication.[14] However, the lack of a correlation between viscosity and clinical efficacy, paired with recent evidence that hyaluronic acid concentration (and therefore film viscosity) is higher at the cartilage surface than in the bulk synovial fluid, raises questions about the relevance of bulk viscosity measurements of viscosupplements. The results in Chapter 4 emphasize the critical importance of this surface localization by revealing a nearly 20-fold increase in the effective viscosity of hyaluronic acid solutions measured between cartilage substrates compared to stainless steel substrates. These results provide evidence that hyaluronic acid is localized at the cartilage surface, and that this surface localization has significant measurable effects on its viscosity at the tissue-scale.

Hyaluronic acid viscosupplements are intended to restore the viscosity in the

joint when it is depleted in diseases such as osteoarthritis. In order to replicate the synovial fluid viscosity of a healthy joint, both the bulk viscosity and the surface localization of the hyaluronic acid solutions should be considered. However, the chemical and mechanical changes that occur at the cartilage surface in arthritis may affect attachment of hyaluronic acid to the cartilage surface. Developing hyaluronic acid viscosupplements with surface attachment moieties that are robust under various stages of disease progression could significantly enhance the performance of these injections. A recent study of hyaluronic acid modified with a collagen II-binding peptide provides a successful example of such a mechanism.[15]

Taken together, the results from Chapters 3 and 4 emphasize the critical role of surface localization on the function of native and synthetic lubricants. Engineering lubricin-mimetics and hyaluronic acid viscosupplements to promote their entrapment at the cartilage surface is a new and promising approach for enhancing their efficacy as tribosupplements.

Insights for Artificial Joint Design

Mechanically, the rigid, impermeable, non-porous surfaces of artificial joints present a very different tribosystem from the soft, permeable, porous cartilage of natural joints. Because of these differences, artificial and natural joints exhibit some distinct lubricating mechanisms. The research in Chapters 2 and 3 of this dissertation use the SFA to measure the frictional behavior of lubricating films confined between mica surfaces, which are smooth, rigid, and impermeable. While this presents a limitation for certain applications, it also offers some advantages. First, it removes any convoluting

effects of fluid flow into or out of the shearing surfaces so that all phenomena are attributable to the interfacial fluid. Furthermore, the mechanical similarities make the SFA an apt system for investigating the lubricating mechanisms that occur in artificial joints.

In Chapter 2, the molecular dynamics of shear-induced synovial fluid aggregation[16] were investigated using the SFA. The contributions of various synovial fluid molecules to this process were assessed in isolation and in combinations, and the globular protein albumin was identified as the primary component driving this phenomenon. A similar aggregation phenomenon has been reported in macroscale studies of high concentration protein solutions sheared between glass and the surfaces of artificial hip implants, and protein deposits have been observed on the bearing surfaces of recovered metal implants.[17,18] These protein aggregates are hypothesized to play a wear-protecting role in artificial joint lubrication by cushioning the contact and distributing load.[18]

The adsorption of globular proteins on implant surfaces is dependent on the material used (ceramic, metal, or UHMWPE) and is affected by surface characteristics such as hydrophobicity and surface charge.[19,20,21,22] The dependence of this protein-mediating lubrication mechanism on the implant surface chemistry points to the potential to tune lubricating properties by modifying surface chemistry. The formation of wear particles in artificial joints triggers adverse biological responses and is a primary mechanism of implant failure. As such, much research has focused on modifying implant materials, designs, and surface properties to reduce mechanical wear.[23,24] Less attention has been directed towards modifying surface chemistry to enhance lubrication

by the native synovial fluid, which in turn will reduce wear. Engineering interactions between artificial implant surfaces and synovial fluid in order to promote native 'on demand' wear protection mechanisms such as the protein aggregation studied in Chapter 2, rather than modifying surfaces to improve their mechanics independently, is a potential new approach to implant design.

Chapter 3 demonstrated that a mimetic lubricin molecule exhibits favorable friction and wear protection properties when anchored to the underlying shearing surfaces by fibronectin, but results in almost immediate damage when it is sheared between bare mica surfaces. While fibronectin coatings on the mica surfaces were used to mimic the chemistry of the cartilage surface, the mechanics of the system more closely resemble those of artificial implants. The marked improvement of the mimetic lubricin when it was anchored to the rigid mica surfaces via fibronectin indicates that surface attachment is a critical factor to consider in the lubrication of artificial joint implants. For cartilage lubrication, the interaction between the cartilage surface and synthetic lubricants can be tuned by altering the binding properties of the synthetic. For artificial joints, modifying the substrate (metal, ceramic, or UHMWPE) to promote interaction with lubricants provides an additional mechanism for enhancing lubricant attachment.

In Chapter 4, rheometer surfaces were modified with cartilage in order to better mimic the in-vivo conditions of the natural joint. A similar approach may be taken to make SFA measurements even more relevant to artificial joints. Modification of the mica surfaces with metals such as CoCrMo or titanium which are used for joint implants can be achieved via sputtering or thermal evaporation, while UHMWPE surfaces could

be attained with the application of UHMWPE tape to the SFA surfaces. By mimicking the material properties of implant surfaces, the SFA could be used to study the molecular interactions between synovial fluid and implant surfaces under various modifications (surface charge, hydrophobicity, etc). Additionally, modified rheometer experiments using the methodology of Chapter 4 could provide complimentary information on the tissue-scale impact of these molecular interactions on viscosity.

Together, the research presented in Chapters 2-4 of this dissertation demonstrates that lubrication is substrate-dependent. While the mechanics of joint implants are unavoidably different from native cartilage, chemical modifications could promote the entrapment of synovial fluid components that facilitate lubrication. Developing surface modifications that take advantage of the remarkable lubricating mechanisms occurring in natural joints is an interesting and under-studied direction for improvement of implant design.

Friction and Wear in Natural and Artificial Joint Lubrication

The protein-mediated lubrication mechanism in Chapter 2 is associated with a wear-protecting role in artificial joints. However, despite being credited with a lubricating role, the friction coefficient of aggregate films observed in synovial fluid and protein solutions is relatively high compared to the friction coefficients observed for cartilage surfaces lubricated by synovial fluid.[18,16] Lubricin, on the other hand, is another important lubricating component of the synovial fluid and is credited with providing extremely low-friction shearing, but when tested on mica surfaces exhibits poor wear resistance.[25,26] These observations raise the question of the relative

importance of wear protection and friction reduction in the lubrication of artificial and natural joints.

The generation of wear particles is a primary mode of implant failures for metal and UHMWPE joint implants. For both types of surfaces, wear particles result in inflammation and induce an adverse biological response that can result in bone resorption and loosening of the implant, leading to failure.[23,24] Because of these serious negative consequences of wear particles, wear reduction is a primary focus of implant design.[2,27,28] In artificial joints, successful lubrication mechanisms promote wear protection and prevent the cascade of negative effects that result from wear generation. High friction, on the other hand, does not in itself present adverse biological effects in artificial joints. Therefore, despite the relatively high friction measured in the protein-mediated lubrication mechanism of Chapter 2, it presents a promising mechanism for artificial joint lubrication.

Lubricin has been studied widely on cartilage and on mica SFA surfaces. On mica, lubricin exhibits remarkably low friction at low loads, but does not provide wear protection, resulting in damage to the underlying surfaces during shearing even under low loads.[26] When a layer of fibronectin is deposited onto the mica in order to mimic the cartilage surface, the wear resistance of both native lubricin[6] and a lubricin-mimetic polymer (Chapter 3) are greatly enhanced. In ex-vivo experiments, lubricin and lubricin mimetics have been shown to attach to the cartilage surface[3,5,14] and reduce friction.[12,25,29] Together, this evidence suggests that lubricin and lubricin-mimetics are capable of providing low-friction boundary mode lubrication, but that surface attachment (possibly mediated by interaction with fibronectin at the cartilage surface)

is critical for the formation of a robust lubricating film that can protect the shearing surfaces from wear.

Unlike for artificial joints, in which wear protection is the primary concern, high friction has direct adverse effects on cartilage health in natural joints. Recent work has demonstrated that high shear strains at the cartilage surface (a result of high friction) lead to cell death of the chondrocytes in the cartilage.[30] Cells at the surface exhibit an immediate necrotic response while cells in deeper zones experience mitochondrial dysfunction leading to apoptosis. Because of this negative biological response to high friction forces, lubrication mechanisms that maintain relatively low friction coefficients are critical for the health of cartilage and the success of osteoarthritis treatments such as tribosupplementation. Wear protection is also important for cartilage lubrication, since wear can result in pain and increased friction. Lubricin is a successful cartilage lubricant because it can both reduce friction and, when anchored to the cartilage surface, provide sufficient wear protection. Our results in Chapter 3 emphasize the importance of engineering the binding properties of lubricin mimetics to promote strong attachment to the shearing surfaces and consequently prevent wear.

Artificial and natural joints present markedly different tribosystems. The biological differences between these systems result in different requirements for successful lubrication: prevention of wear particles in artificial joints, and robust low-friction shearing in natural joints. Furthermore, the chemical and mechanical differences affect the way synovial fluid and exogenous lubricants interact with the shearing surfaces. However, in both natural and artificial joints, understanding the molecular interactions that occur between lubricating molecules and the shearing surfaces is

critical for developing methods to improve lubrication. The SFA technique used in Chapters 2 and 3 allows for precise measurement of molecular interactions between synovial fluid molecules and the confining mica surfaces. SFA surfaces share mechanical similarities with artificial joint implants and can potentially be modified to chemically mimic implant surfaces as discussed above; as in Chapter 3, they can also be modified with fibronectin or other cartilage matrix proteins to chemically mimic the cartilage surface. While experiments provide insights into molecular mechanisms of lubrication in natural and artificial joints, it is also critical to consider the effects of these molecular interactions at the tissue scale. The study in Chapter 4 presents a framework for measuring the effect of surface interaction on the viscosity of the lubricating fluid. In Chapter 4 the rheometer surfaces were modified with cartilage to investigate the interactions between cartilage and hyaluronic acid; however, the same technique could be used to mimic metal or UHMWPE surfaces used in artificial joints.

Summary

This dissertation explores the molecular interactions that occur within the synovial fluid and between synovial fluid molecules and the shearing surfaces of a joint. Furthermore, it investigates the effect of these interactions on lubrication at the molecular and tissue scale. At these two scales, the results emphasize the critical importance of molecular interactions that entrap lubricating molecules at the joint surface—whether cartilage or implant—on mediating the lubrication necessary for a successful and healthy tribosystem.

Future Directions

The work presented in this dissertation highlights some interesting areas for future research:

(1) Chapter 2 gives insights into the molecular mechanisms of protein aggregation in synovial fluid, which has been associated with a wear protecting role in artificial joints. However, it is unclear whether this mechanism occurs in the lubrication of natural joints. The formation of aggregates both cushions artificial joints and has been hypothesized to alter the frictional regime from sliding to rolling friction. Research into the behavior of protein fluids sheared between soft materials could shed light onto whether this mechanism plays a role in cartilage lubrication.

(2) Lubricin-mimetics offer promise as a potential therapy for osteoarthritis. The mimetic lubricin studied in Chapter 3 demonstrates favorable lubrication and wear resistance in the boundary lubrication regime when anchored to the underlying mica surface with fibronectin. However, in addition to acting as a boundary lubricant, natural lubricin plays an important role in localizing HA near the cartilage surface to promote viscous lubrication. The ability of natural joints to shift between lubricating modes is critical for healthy function. Thus, assessing the ability of this mimetic lubricin to entrap HA is an important future step.

(3) The effect of surface interaction on HA viscosity was investigated in Chapter 4, which demonstrated that HA solutions exhibit a higher effective viscosity when confined between cartilage surface compared to metal or glass surfaces. While this finding has clear implications for the lubricating abilities and clinical efficacy of HA viscosupplements, more research is needed to assess the correlation between these

outcomes. A direct comparison between the effective viscosity of HA measured in a cartilage-functionalized rheometer and the effective viscosity extracted from tribology experiments using the Stribeck framework is a critical next step. A correlation between effective viscosity and frictional behavior is necessary to determine whether this method could be adopted as a reasonable heuristic for viscous lubricating ability.

(4) On cartilage, lubricin is hypothesized to be responsible for localizing HA at the cartilage surface. The cartilage slabs used in Chapter 4 were sectioned from the deep zone of cartilage and likely have negligible quantities of lubricin. Therefore, a different mechanism must be responsible for HA localizations in these experiments. Further investigation into the nature of this interaction could inform the development of modified HAs to enhance surface attachment.

REFERENCES

1. Wimmer, M. A. *et al.* Wear mechanisms in metal-on-metal bearings: The importance of tribochemical reaction layers. *J. Orthop. Res.* **28**, 436–443 (2010).

2. Wimmer, M. A., Sprecher, C., Hauert, R., Täger, G. & Fischer, A. Tribochemical reaction on metal-on-metal hip joint bearings A comparison between in-vitro and in-vivo results. *Wear* **255**, 1007–1014 (2003).

3. Jones, A. R. C. *et al.* Binding and localization of recombinant lubricin to articular cartilage surfaces. *J. Orthop. Res.* **25**, 283–292 (2007).

4. Elsaid, K. A., Chichester, C. O. & Jay, G. D. Lubricin purified from bovine synovial fluid and from articular cartilage exhibit similar binding affinities to cartilage matrix proteins. *Trans. Orthop. Res. Soc.* **32**, 551 (2007).

5. Flowers, S. A. *et al.* Lubricin binds cartilage proteins, cartilage oligomeric matrix protein, fibronectin and collagen II at the cartilage surface. *Sci. Rep.* **7**, (2017).

6. Eguiluz, R. C. A. *et al.* Fibronectin mediates enhanced wear protection of lubricin during shear. *Biomacromolecules* **16**, 2884–2894 (2015).

7. Andresen Eguiluz, R. C. *et al.* Fibronectin mediates enhanced lubrication and wear protection of lubricin. *Biomacromolecules* **16**, 2884–2894 (2015).

8. Teeple, E. *et al.* Effects of supplemental intra-articular lubricin and hyaluronic acid on the progression of posttraumatic arthritis in the anterior cruciate ligament-deficient rat knee. *Am. J. Sports Med.* **39**, 164–72 (2011).

9. Flannery, C. R. *et al.* Prevention of cartilage degeneration in a rat model of osteoarthritis by intraarticular treatment with recombinant lubricin. *Arthritis Rheum.* **60**, 840–847 (2009).

10. Waller, K. A. *et al.* Intra-articular recombinant human proteoglycan 4 mitigates cartilage damage after destabilization of the medial meniscus in the yucatan minipig. *AJSM* **45**, (2017).

11. Rydell, N. & Balazs, E. A. Effect of intra-articular injection of hyaluronic acid on the clinical symptoms of osteoarthritis and on granulation tissue formation. *Clin. Orthop. Relat. Res.* **80**, 25–32 (1971).

12. Samaroo, K. J., Tan, M., Putnam, D. & Bonassar, L. J. Binding and lubrication of biomimetic boundary lubricants on articular cartilage. *J. Orthop. Res.* **35**, 548–557 (2016).

13. Sun, Z. *et al.* Boundary mode lubrication of articular cartilage with a biomimetic diblock copolymer. *Proc. Natl. Acad. Sci.* **116**, 12437–12441 (2019).

14. Bonnevie, E. D., Galesso, D., Secchieri, C., Cohen, I. & Bonassar, L. J. Elastoviscous transitions of articular cartilage reveal a mechanism of synergy between lubricin and hyaluronic acid. *PLoS One* **10**, (2015).

15. Faust, H. J. *et al.* A hyaluronic acid binding peptide-polymer system for treating osteoarthritis. *Biomaterials* **183**, 93–101 (2018).

16. Banquy, X., Lee, D. W., Das, S., Hogan, J. & Israelachvili, J. N. Shear-induced aggregation of mammalian synovial fluid components under boundary lubrication conditions. *Adv. Funct. Mater.* **24**, 3152–3161 (2014).

17. Fan, J., Myant, C. W., Underwood, R., Cann, P. M. & Hart, A. Inlet protein aggregation: a new mechanism for lubricating film formation with model synovial fluids. *Proc. Inst. Mech. Eng. Part H.* **225**, 696–709 (2011).

18. Myant, C. & Cann, P. In contact observation of model synovial fluid lubricating mechanisms. *Tribiology Int.* **63**, 97–104 (2013).

19. Heuberger, M. P., Widmer, M. R., Zobeley, E., Glockshuber, R. & Spencer, N. D. Protein-mediated boundary lubrication in arthroplasty. *Biomaterials* **26**, 1165–1173 (2005).

20. Serro, A. P., Colaço, R. & Saramago, B. Effect of Albumin Adsorption on Biotribological Properties of Artificial Joint Materials. in *Proteins and Interfaces III State of the Art* 497–523 (American Chemical Society, 2012).

21. Yan, Y., Yang, H., Su, Y. & Qiao, L. Albumin adsorption on CoCrMo alloy surfaces. *Sci. Rep.* **5**, (2015).

22. Escudeiro, A., Polcar, T. & Cavaleiro, A. Adsorption of bovine serum albumin on Zr co-sputtered a-C(:H) films: Implication on wear behaviour. *J. Mech. Behav. Biomed. Mater.* **39**, 316–327 (2014).

23. Catelas, I. & Wimmer, M. A. Polyethylene and metal wear particles: characteristics and biological effects. *Semin. Immunopathol.* **33**, 257–271 (2011).

24. Catelas, I. & Wimmer, M. A. New insights into wear and biological effects of metal-on-metal bearings. *J. Bone Joint Surg. Am.* **93**, 76–83 (2011).

25. Gleghorn, J. P., Jones, A. R. C., Flannery, C. R. & Bonassar, L. J. Boundary mode lubrication of articular cartilage by recombinant human lubricin. *J. Orthop. Res.* **27**, 771–777 (2009).

26. Zappone, B., Ruths, M., Greene, G. W., Jay, G. D. & Israelachvili, J. N. Adsorption, lubrication, and wear of lubricin on model surfaces: polymer brush-like behavior of a glycoprotein. *Biophys. J.* **92**, 1693–708 (2007).

27. Ito, H. *et al.* Reduction of polyethylene wear by concave dimples on the frictional surface in artificial hip joints. *J. Arthroplasty* **15**, 332–338 (2000).

28. Büscher, R. *et al.* Subsurface microstructure of metal-on-metal hip joints and its relationship to wear particle generation. *J. Biomed. Mater. Res. Part B Appl. Biomater.* **72B**, 206–214 (2005).

29. Schmidt, T. A., Gastelum, N. S., Nguyen, Q. T., Schumacher, B. L. & Sah, R. L. Boundary lubrication of articular cartilage: Role of synovial fluid constituents. *Arthritis Rheum.* **56**, 882–891 (2007).

30. Bonnevie, E. D. *et al.* Microscale frictional strains determine chondrocyte fate in loaded cartilage. *J. Biomech.* **74**, 72–78 (2018).

APPENDIX A

Effect of Shearing Parameters on the Formation of a Shear-Induced Protein AggregateFilm in Synovial Fluid

Abstract

Synovial fluid is a complex, heterogeneous fluid that lubricates articular joints. Under shear, globular proteins in the synovial fluid form dense aggregates, which have been credited with playing a wear protecting role in the lubrication of artificial joints. However, little is known about the parameters that influence the formation of these protein aggregates. This work investigates the effect of applied load, shear rate, and lubricant bath on the formation and sustainability of protein aggregate films in synovial fluid. We find that slow speeds and low loads are the most conducive to protein film formation, and that shearing in a bath of SF improves the longevity of protein films compared to PBS.

Introduction

Synovial fluid works in conjunction with articular cartilage to provide the remarkable lubrication, of natural joints. The lubricating properties of the synovial fluid are typically attributed to the lubricating molecules lubricin and hyaluronic acid which have well-established boundary and viscous lubricating roles.[1,2,3] Pairings of synovial fluid molecules that work together to synergistically enhance lubrication have also bee identified. Lubricin and hyaluronic have been reported to interact synergistically to form a an effective lubricating film,[4,5] and interactions between

hyaluronic acid and phospholipids have been shown to possess exceptional low-friction properties.[6,7] However, the role of the globular protein albumin, which comprises 90% of the protein content of the synovial fluid, has garnered minimal research.

In 2014, a novel rheological behavior was observed in synovial fluid: under shear the fluid formed dense aggregates, transforming form a homogenous fluid to a heterogeneous mixture of protein and aggregates.[8] The dynamics of this process were characterized, but the composition and lubricating role of the aggregate film was not studied. Meanwhile, researchers of artificial joint lubrication have identified that high-concentration protein fluids formed aggregates when sheared between the rigid surfaces of artificial joints.[9,10,11] Furthermore, these aggregates played a wear protecting role by "cushioning" the contact and distributing load. This lubrication mechanism was termed "protein aggregation lubrication". However, the only studies of this process were done in high-concentration protein films, or in arthritic synovial fluid that exhibited much higher protein content than healthy synovial fluid. In 2019, a study on the shear-induced aggregating behaviors of various synovial fluid molecules revealed that even in healthy synovial fluid, albumin is the primary contributor to the formation of aggregates (Cook et al, submitted to Langmuir 2019).

Despite the potential role of these synovial fluid aggregates in artificial joint lubrication, the effect of shearing parameters on the formation, sustainability, and friction of these aggregates films is largely unstudied. This report studies the effect of

shearing parameters including applied load, shear rate, and lubricant bath on protein aggregation in synovial fluid.

Methods

Surface Forces Apparatus

The Surface Forces Apparatus (SFA) was used to measure friction and normal forces while simultaneously monitoring film thickness and aggregation in the shearing junction. The SFA technique has been fully described elsewhere.[12,13] Briefly, thing homogeneous sections of semi-cylindrical back-silvered mica are adhered onto opposing semi-cylindrical surfaces to form an interferometer. The fluid sample is confined between the surfaces. Load and shear are applied via a motor and piezo bimorph, respectively. A system of double cantilever springs and strain gauges detect forces with high precision, while the interferometer allows highly accurate measurement of surface separation and facilitates direct visualization of the contact junction.

Sample Preparation

For all tests, a layer of fibronectin was first adhered to the mica of the SFA surfaces. This was done to anchor synovial fluid to the underlying mica as it has been shown to prevent expulsion of synovial fluid molecules including hyaluronic acid.[13] Fibronectin was prepared at 0.3mg/mL and incubated on the mica surfaces for 1 hour. The surfaces were then rinsed and synovial fluid was injected into the junction.

For some experiments, the synovial fluid was left to incubate for 1 hour and then shear tests were initiated. In other tests, the synovial fluid was removed after a 1 hour incubation and replaced with PBS. This resulted in the formation of a surface-attached layer of synovial fluid and allowed us to probe the effect of shearing medium (i.e. is surface-bound synovial fluid sufficient for forming a protein film or is a reservoir of synovial fluid necessary?).

Testing Parameters

The effects of load and shear rate were assessed by shearing (1) at low loads (~1mN) or (2) at high loads (~5mN) at shear rates of 3μm/s or 30μm/s. Shear tests were conduced for up to two hours to determine the long-term response under shear.

Results

In all tests, the formation of aggregates occurred nearly instantaneously with the onset of shearing. These aggregates were visible in both the interference fringes from the SFA and through a top-view camera. The index of refraction of the aggregates was greater when the synovial films were sheared in a synovial fluid bath compared to synovial films sheared in PBS (Figure A.1).

At sliding speeds of 3μm/s the effect of applied load was profound for synovial fluid films sheared in both synovial fluid (Figure A.2 A,B) and PBS (Figure A.2 C,D). Under low loads (Figure A.2 A,C), the initial thickening at the onset of shearing was greater, and furthermore, the thickness of the protein aggregate film was more sustainable under prolonged shearing. Under high loads (Figure A.2 B,D), an aggregate film still formed, but it depleted in thickness under prolonged shearing. The

effect of lubricant bath on aggregate film formation and longevity was also apparent. While lubricant bath did not impact the magnitude of the initial increase in film thickness, it did effect longevity. Synovial fluid films sheared in a synovial fluid bath formed more sustainable protein aggregate films.

At faster sliding speeds of 30μm/s, the affect of lubricant bath was negligible. Synovial fluid films sheared in synovial fluid (Figure A.3 A,B) and in PBS (Figure A.3 C,D) exhibited similar evolutions of film thickness under shear. Under high loads (Figure A.3 B,D) the film thickening was smaller and magnitude and more short-lived than under low-loads (Figure A.3 A,C).

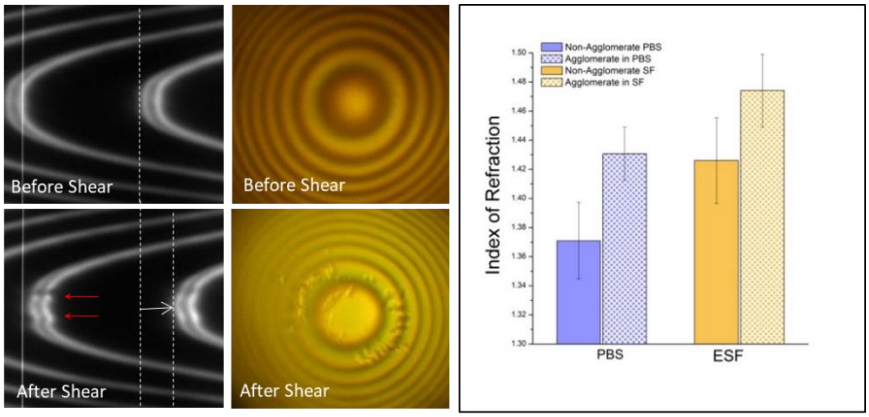

Figure A.1. Aggregates formed in synovial fluid films under shear and were visible both in the SFA interferometer images and through a top-view camera. When synovial fluid films sheared in PBS had a lower index of refraction than those sheared in a synovial fluid bath. Solid bars indicate “bulk” fluid, while textured bars indicate the index of refraction of aggregates.

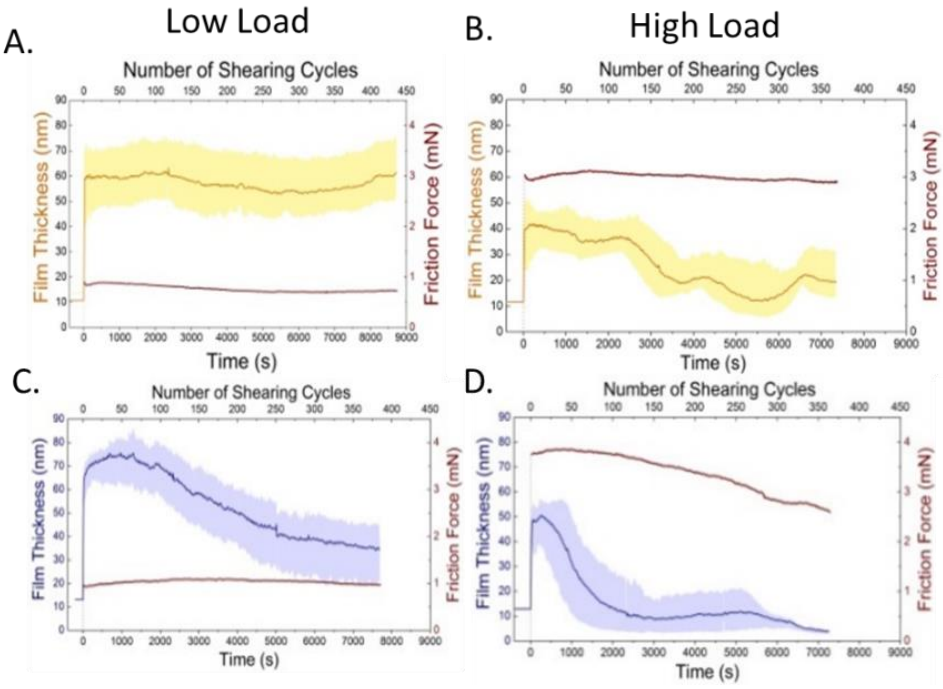

Figure A.2. Film thickness and friction force versus shearing time for FN+SF films sheared at 3μm/s (A) in a synovial fluid bath under low loads (B) in a synovial fluid bath under high loads (C) in a PBS bath under low loads and (D) in a PBS bath under high loads.

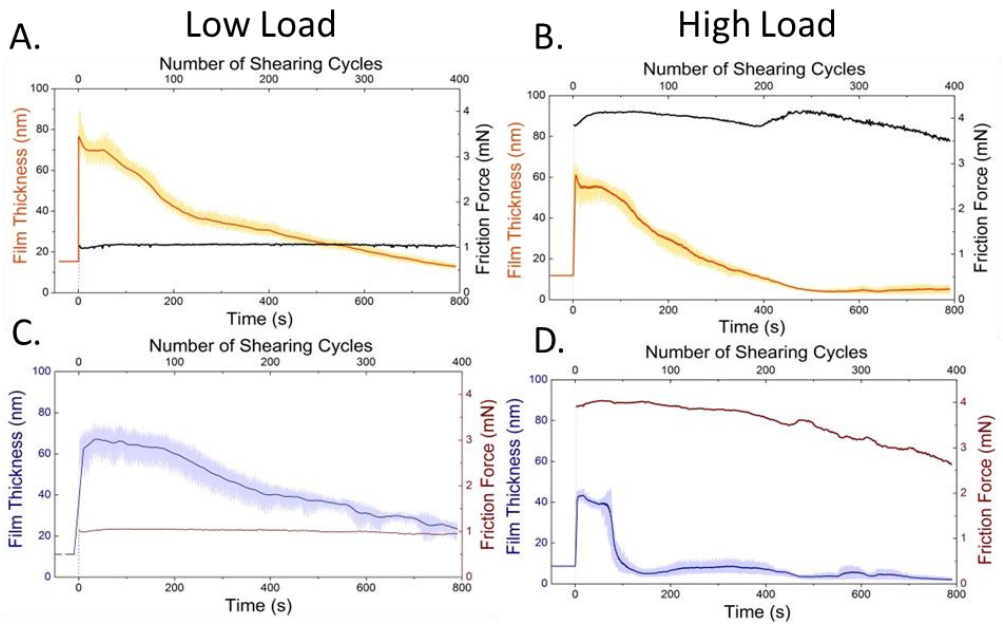

Figure A.3. Film thickness and friction force versus shearing time for FN+SF films sheared at 30μm/s (A) in a synovial fluid bath under low loads (B) in a synovial fluid bath under high loads (C) in a PBS bath under low loads and (D) in a PBS bath under high loads.

Discussion

Our results demonstrate that choice of lubricant bath, applied load, and shear rate are all parameters that affect the thickness and sustainability of shear-induced protein aggregate films. The magnitude of film thickening that occurred with the initial formation of the shear-induced protein film was relatively independent of lubricant bath, indicating that the film is initially formed from surface-bound synovial fluid proteins and not from those in the bath. However, the film thickness was only sustainable when sheared in synovial fluid. This implies that exchange occurs between the lubricant bath and the protein film within the junction, and that this replenishment

is necessary for the formation of a stable aggregate film. Under all conditions, low loads produced thicker and longer-lived aggregate films. The affect of load may be associated with the resulting change in contact area, since the SFA surfaces are not perfectly rigid. Increased contact area under high loads may result in less exchange of material with the reservoir and more time under compression for the aggregate film. Under the faster velocity tested (30μm/s) no sustainable aggregate films were formed, regardless of lubricant bath or applied load. This implies that the rate of aggregate expulsion from the junction exceeded the rate of formation of new aggregates.

Protein aggregation lubrication has been proposed as a mechanism of lubrication in artificial joints.[9] One of the most remarkable features of this novel lubrication mechanism, is the fact that it is adaptive and self-replenishing:[8] Because this transformation of synovial fluid is induced by shearing, more protective protein aggregates are hypothesized to form in areas of greatest shear stress, providing an extra 'cushion' where it is most needed. However, little research has been conducted onto the dynamics of protein aggregate formation in synovial fluid and how they are affected by shearing parameters. Our results indicate that low load, slow shearing environments are in fact more conducive to the formation of protein aggregate films, and that exchange with a synovial fluid reservoir is critical for the sustainability of the films under prolonged shear.

REFERENCES

1. Gleghorn, J. P., Jones, A. R. C., Flannery, C. R. & Bonassar, L. J. Boundary mode lubrication of articular cartilage by recombinant human lubricin. *J. Orthop. Res.* **27**, 771–777 (2009).

2. Balazs, E. A., Watson, D., Duff, I. F. & Roseman, S. Hyaluronic acid in synovial fluid. I. Molecular parameters of hyaluronic acid in normal and arthritic human fluids. *Arthritis Rheum.* **10**, 357–376 (1967).

3. Zappone, B., Ruths, M., Greene, G. W., Jay, G. D. & Israelachvili, J. N. Adsorption, lubrication, and wear of lubricin on model surfaces: polymer brush-like behavior of a glycoprotein. *Biophys. J.* **92**, 1693–708 (2007).

4. Greene, G. W. *et al.* Adaptive mechanically controlled lubrication mechanism found in articular joints. *Proc. Natl. Acad. Sci. U. S. A.* **108**, 5255–9 (2011).

5. Bonnevie, E. D., Galesso, D., Secchieri, C., Cohen, I. & Bonassar, L. J. Elastoviscous Transitions of Articular Cartilage Reveal a Mechanism of Synergy between Lubricin and Hyaluronic Acid. *PLoS One* **10**, (2015).

6. Zhu, L., Seror, J., Day, A. J., Kampf, N. & Klein, J. Ultra-low friction between boundary layers of Hyaluronan-phosphatidylcholine Complexes. *Acta Biomater.* **59**, 283–292 (2017).

7. Jahn, S., Seror, J. & Klein, J. Lubrication of Articular Cartilage. *Annu. Rev. Biomed. Eng* **18**, 235–58 (2016).

8. Banquy, X., Lee, D. W., Das, S., Hogan, J. & Israelachvili, J. N. Shear-Induced

Aggregation of Mammalian Synovial Fluid Components under Boundary Lubrication Conditions. *Adv. Funct. Mater.* **24**, 3152–3161 (2014).

9. Fan, J., Myant, C. W., Underwood, R., Cann, P. M. & Hart, A. Inlet protein aggregation: a new mechanism for lubricating film formation with model synovial fluids. *Proc. Inst. Mech. Eng. Part H.* **225**, 696–709 (2011).

10. Fan, J., Myant, C., Underwood, R. & Cann, P. Synovial fluid lubrication of artificial joints: protein film formation and composition. doi:10.1039/c2fd00129b

11. Myant, C. & Cann, P. In contact observation of model synovial fluid lubricating mechanisms. *Tribiology Int.* **63**, 97–104 (2013).

12. Israelachvili, J. *et al.* Recent advances in the surface forces apparatus (SFA) technique. *Reports Prog. Phys.* **73**, (2010).

13. Eguiluz, R. C. A. *et al.* Fibronectin mediates enhanced wear protection of lubricin during shear. *Biomacromolecules* **16**, 2884–2894 (2015).